HIGH TEMPERATURE MASS SPECTROMETRY: SAMARIUM DICARBIDE AND NEODYMIUM (III) MONOTELLURO OXIDE

Thesis for the Degree of Ph. D.
MICHIGAN STATE UNIVERSITY
Philip A. Pilato
1968

This is to certify that the

thesis entitled

HIGH TEMPERATURE MASS SPECTROMETRY:
SAMARIUM DICARBIDE AND
NEODYMIUM(III) MONOTELLURO OXIDE

presented by

Philip A. Pilato

has been accepted towards fulfillment
of the requirements for

Ph. D. degree in Chemistry

Harry A. Eick
Major professor

Date February 22, 1968

ABSTRACT

HIGH TEMPERATURE MASS SPECTROMETRY:
SAMARIUM DICARBIDE AND NEODYMIUM(III) MONOTELLURO OXIDE

by Philip A. Pilato

I. Samarium Dicarbide

Samarium dicarbide was prepared from stoichiometric mixtures of samarium metal and graphite powder by heating in a sealed tantalum bomb. Analysis on three different preparations gave the following mole percentages: samarium, 32.72 ± 0.57% (calc., 33.33%); bound carbon, 67.28 ± 0.57% (calc., 66.67%). In a separate analysis 99.53% of the total sample weight was accounted for. X-ray powder diffraction analysis gave the tetragonal lattice parameters: $a_0 = 3.77_6 \pm 0.004$ Å; $c_0 = 6.31_9 \pm 0.008$ Å. The lattice parameters did not change detectably after a portion of the sample had been vaporized.

The mode of vaporization of SmC_2, investigated over the temperature range 1431-2058°K using both graphite-lined molybdenum and tungsten Knudsen effusion cells, was found to be

$$SmC_2(s) \longrightarrow Sm(g) + 2C(gr). \qquad (a)$$

Absolute pressures of Sm(g) in equilibrium with $SmC_2(s)$ were obtained by calibrating the mass spectrometer with: (1) the vapor pressure of samarium metal or with, (2) the loss in weight of $SmC_2(s)$ at a fixed temperature for a given time. This equilibrium vapor pressure is described as a

fun

equa

Therm

58.6

dynam

with

and ΔS

for re

functi

combin

data y

ΔS^0_{298},

deg.

II. Ne

Th

vapor

98.3 a

der di

indica

quioxi

indicat

Te(g) a

function of temperature by the empirical least squares equation:

$$2.303R \log P_{Sm} = \left(\frac{-58,600 \pm 2,100}{T}\right) + 13.7 \pm 1.8 \quad \text{(b)}$$

Thermodynamic data calculated for reaction (a) are ΔH^0_{1745} = 58.6 ± 2.1 kcal/gfw and ΔS^0_{1745} = 13.7 ± 1.8 cal/gfw-deg.

These data were reduced to 298°K by use of the thermodynamic data of CaC_2, corrected for replacement of calcium with samarium, and resulted in ΔH^0_{298} = 64.2 ± 2.6 kcal/gfw and ΔS^0_{298} = 22.1 ± 2.3 cal/gfw-deg. The third law enthalpy for reaction (a) calculated with an estimated free energy function for SmC_2(s) is ΔH^0_{298} = 66.9 ± 1.7 kcal/gfw. A combination of the average enthalpy value with literature data yielded for SmC_2(s): $\Delta H^0_{298,f}$ = -14.6 ± 2.8 kcal/gfw, $\Delta S^0_{298,f}$ = 5.0 ± 2.8 cal/gfw-deg, S^0_{298} = 24.4 ± 2.4 cal/gfw-deg.

II. Neodymium(III) Monotelluro Oxide

The purity of samples prepared by passing tellurium vapor over Nd_2O_3 using hydrogen as the carrier gas was 99.6, 98.3 and 100.3% according to mass uptake data. X-ray powder diffraction analyses of the residues after vaporization indicated the compound vaporized incongruently to the sesquioxide. Mass spectrometric analysis of the effusing vapor indicated that (1) the vaporization species are Nd(g), NdO(g), Te(g) and that O(g) is also a product at higher temperature;

and (2) the ratio of partial pressures of NdO(g) to Nd(g) is temperature dependent changing from less than to greater than unity at about 2150^0K.

These observations are consistent with the hypothesis that several simultaneous equilibria are occurring in the vaporization of Nd_2O_2Te. The probable reactions are:

$$Nd_2O_2Te(s) \longrightarrow 2/3\ Nd_2O_3(s) + 2/3\ Nd(g) + Te(g) \quad (c)$$

$$Nd_2O_2Te(s) + O(g) \longrightarrow Nd_2O_3(s) + Te(g) \quad (d)$$

$$Nd_2O_3(s) \longrightarrow 2NdO(g) + O(g) \quad (e)$$

$$Nd_2O_2Te(s) \longrightarrow 2NdO(g) + Te(g) \quad (f)$$

Reaction (c) is postulated to predominate at lower temperature while reactions (e) and (f) become favorable at higher temperatures and this temperature dependence is consistent with calculated equilibria constants for the reactions in which the free energy function and standard enthalpy of formation of $Nd_2O_2Te(s)$ were estimated.

HIGH TEMPERATURE MASS SPECTROMETRY:

SAMARIUM DICARBIDE AND NEODYMIUM(III) MONOTELLURO OXIDE

By

Philip A. Pilato

A THESIS

Submitted to
Michigan State University
in partial fulfillment of the requirements
for the degree of

DOCTOR OF PHILOSOPHY

Department of Chemistry

1968

ACKNOWLEDGMENTS

The author wishes to express his sincere appreciation to Dr. Harry A. Eick for the suggestions, encouragement and friendship which he generously extended throughout the course of this investigation.

Thanks are also due to my colleague, Mr. John Haschke, for many helpful and lively discussions during the course of this work.

The help extended by Mr. Russel Geyer who constructed some of the effusion cells and by Mr. James Grumblatt for aiding the author in re-wiring the mass spectrometer is acknowledged.

A lasting sense of gratitude and appreciation is extended to the author's wife, Fran, and daughter, Paulette, for their patience, understanding and unselfishness which they expressed throughout this study.

Financial support from the Atomic Energy Commission under Contract AT(11-1)-716 is gratefully noted.

TABLE OF CONTENTS

TABLE OF CONTENTS (Cont.)

TABLE OF CONTENTS (Cont.)

TABLE

I.

II.

III.

IV.

V.

VI.

VII.

VIII.

IX.

X.

XI.

XII.

LIST OF TABLES

LIST OF FIGURES

LIST OF APPENDICES

CHAPTER I

INTRODUCTION

Research efforts into the field of high temperature thermodynamics hardly need justification in this age in which two of the most significant technological advances of man--atomic energy and space travel--were derived largely from this very field. The practical need to develop new refractory building metals and alloys which possess such combinations of properties as high tensile strength, oxidative resistance, low density, and malleability requires thermal data which may guide the scientist in his synthetic work. This need alone would be sufficient to justify a project whose aim was to obtain high temperature thermodynamic data. But aside from this reason, another is the elucidation, clarification and formulation of ideas in chemical bonding and structure. As stated by Ackermann and Thorn (1): "The rapid accumulation of high temperature properties makes it possible to begin a synthesis of the systematic behavior of ··· phases in order to discover the fundamental concepts which determine the strength of bonding ···"

The general plan of work for this thesis was to characterize both qualitatively and quantitatively the vaporization process of samarium dicarbide (SmC_2) and neodymium(III) monotelluro oxide (Nd_2O_2Te). The principal procedure was

to use Knudsen effusion-mass spectrometry. Using this method the enthalpy of vaporization was obtained directly from the ion intensity-temperature data, and the entropy of vaporization was derived from absolute pressures obtained by calibration of the mass spectrometer. The choice of these compounds was based partially on the fact that samarium dicarbide may be a potential core moderator material since samarium has a high neutron capture cross-section and that Nd_2O_2Te is the homologue of neodymium sesquioxide --thus comparisons of thermodynamic data could be correlated to the effect of a one atom substitution. Furthermore in the dicarbide, samarium is believed to be in the +2 oxidation state and this study would allow a comparison of its thermal properties with ytterbium and europium dicarbide and with the various alkaline earth dicarbides to which it might be similar.

CHAPTER II

HISTORICAL

2.1. Reported Work on the Lanthanon-Dicarbide Systems

2.1.1. Preparation and Characterization

In the past seventeen years there has been a widespread and intensified interest in the lanthanide and actinide carbides. Various techniques have been developed for their preparation. DeVillelume (2) reduced lanthanum sesquioxide with carbon at 2000^0 and obtained the dicarbide. In 1958, Chupka and coworkers (3) first prepared lanthanum dicarbide *in situ* in a mass spectrometer by reaction of lanthanum metal with the graphite liner of a Knudsen cell, then examined the vapor effusing from the cell.

In 1958, Spedding, Gschneidner and Daane (4) studied the lanthanon-carbon systems extensively, reporting carbides of three generalized types: Ln_3C, Ln_2C_3, LnC_2. They also reported lattice parameters for the various phases including all the lanthanon dicarbides except promethium. Their preparative technique depended on the volatility of the lanthanon metal. Thus, for those lanthanon metals with a boiling point in excess of 2000^0 mixed powders of the element and graphite were pressed into pellets and arc melted under an atmosphere of helium or argon, while for the metals whose boiling point is less than 2000^0 (Sm, Tm, Yb) the reaction between the elements was constrained in a tantalum bomb.

Subsequent to the work of Spedding, et al.(4) a series of articles by Vikery, Sedlacek and Ruben was published in which the preparation of a series of lanthanon carbides (5) and both their magneto-chemistry (6) and their X-ray absorption characteristics (7) were presented. In their work the authors prepared all the lanthanon dicarbides, except those of europium, promethium, lutetium and thulium by the reduction of the sesquioxide with carbon under a low pressure of argon. In their second paper the authors conclude that both samarium and ytterbium are in the +2 oxidation state in the dicarbide because their experimentally observed values of the Bohr magneton numbers differ from the values calculated for the +3 oxidation states of the respective ions.

Pollard, et al. (8) also prepared a number of the dicarbides using the method described by Vikery (5) but at the maximum temperature of their equipment, 1900°, they were unable to prepare samarium dicarbide. They noted that at this temperature dysprosium dicarbide formed very slowly. Other work on the hydrolysis of lanthanon dicarbides has been performed by Palenik and Warf (9) and DeVillelume (2). In addition, the hydrolysis products of lanthanon sesquicarbides as well as the dicarbides have been characterized by Svec, et al. (10), Greenwood and Osborn (11) and by Spedding and coworkers (4) who in addition studied the hydrolysis products of the tri-lanthanon carbides. Svec, et al. (10), who hydrolyzed many of the

ca

12.

pro

acid

12.

port

oxida

is si

Hoffm

tion

differ

for th

1288 x

x 10^{-6}

Greenw

not be

formed

stoich

vated

proced

contar

bide,

parame

carbide samples which had been examined by Gschneidner (4, 12,13), indicated that the three principal hydrolysis products obtained with samarium dicarbide in 1M hydrochloric acid were ethyne (62.2%), hydrogen (16.6%) and ethene (12.5%)--no methane was observed. Their observation supports Vikery's (6) conclusion that samarium is in the +2 oxidation state in the dicarbide and that this dicarbide is similar to the alkaline earth dicarbides in its behavior.

However, this theme has been challenged by Jensen and Hoffman (14) who also prepared the compound by the reduction of the sesquioxide with graphite. The most significant difference between the two studies is the values obtained for the room temperature paramagnetic susceptibility: 1288 x 10^{-6} emu/mole obtained by Jensen and Hoffman; 2306 x 10^{-6} emu/mole by Vikery and coworkers.

The lanthanon dicarbide preparatory procedure used by Greenwood and Osborn (11), although a standard method, had not been used previously for lanthanum dicarbide. They formed lanthanum dihydride first and then reacted it with stoichiometric amounts of graphite under vacuum at elevated temperatures. This is probably the best preparative procedure for lanthanon dicarbides which are low in oxygen contamination and free of excess graphite.

In 1964 the previously missing phase, europium dicarbide, was prepared by Gebelt and Eick (15) and its lattice parameters and some physical properties characterized.

The crystal structures of the lanthanon dicarbides have been characterized reproducibly many times. Spedding, et al. (4) using both Debye-Scherrer diffraction and symmetrical focusing back reflection cameras report the lattice parameters for most of the lanthanon dicarbides, as well as the sesquicarbides. The values they obtained are probably the best reported to date since they used specially prepared, highly purified metals. Atojii, et al. (12) performed room temperature neutron diffraction studies on lanthanum di- and sesqui-carbides while Atojii (16) undertook a similar study on the dicarbides of lanthanum, cerium, terbium, yttrium, ytterbium and lutetium, as well as those of calcium and uranium. He found all of them to exhibit the I4/mmm calcium dicarbide structure with all metals, except Ca(+2), Yb (possible +2.8) and U (possible +4), in the +3 oxidation state. Recently Atojii and Williams (17) determined the magnetic and crystal structures of five lanthanon dicarbides at low temperatures (to $2^{0}K$). The sesquicarbides of four selected lanthanon metals have also been studied by neutron diffraction at room temperature (18).

In 1967, a high temperature neutron diffraction study of lanthanum and yttrium dicarbides was undertaken by Bowman, et al. (19). These authors reported tetragonal lattice parameters which are in agreement with the room temperature data of Atojii (16) and, in addition they observed the tetragonal to cubic transition temperatures to be in agreement

with

for Y

lanth

tetra

1150°

F

carbon

severa

and to

2.

The

have pr

dicated

cording

Chupka,

Various

1 and

at 2500°

However,

lantha

using a

workers

phased

with the previously reported values (1060^0 for LaC_2; 1320^0 for YC_2) observed in thermal analysis studies. For lanthanum dicarbide the lattice parameters obtained were: tetragonal at 900^0, $a_0 = 4.00$ Å and $c_0 = 6.58$ Å; cubic at 1150^0, $a_0 = 6.02$ Å.

For a knowledge of the work done on the lanthanon-carbon systems prior to 1950 the reader is referred to several reviews (20,21), to the references contained in (5) and to Gebelt (22).

2.1.2. Vaporization Studies

The species which vaporize from lanthanon dicarbides have proven to be unusual and varied. Previous work indicated that lanthanon dicarbide vaporizations occur according to one or more of the following modes

$$MC_2(s) \longrightarrow M(g) + 2C(s) \qquad (1)$$

$$MC_2(s) \longrightarrow MC_2(g) \qquad (2)$$

$$MC_2(s) + 2C(s) \longrightarrow MC_4(g) \qquad (3).$$

Chupka, et al. (3), in their mass spectrometric study of various dicarbides, observed for lanthanum dicarbide modes (1) and (2). They measured the LaC_2/La pressure ratio and at 2500^0K they calculated the value of the ratio to be 16. However, Jackson and co-workers (23) obtained, for lanthanum dicarbide, a LaC_2^+/La^+ ratio of 0.45 at 2500^0K using a Langmuir vaporization technique. The latter workers also studied the vaporization behavior of cerium, praseodymium, gadolinium and lutetium dicarbides. They

observed (23) that the ion intensity ratio LaC_2^+/La^+ increased from 0.17 to 0.45 as the temperature was increased --this observation appears to be an example of Brewer's law (24) that at higher temperatures the formation of the less dominant species (usually polymeric or more complex) will be favored in a vaporization process.

The vaporization pressure of holmium dicarbide was measured using the Knudsen effusion weight loss method by Wakefield, Daane and Spedding (25). Gadolinium dicarbide has been studied by Jackson, et al. (26) with a mass spectrometer. They found $GdC_2(g)$ and Gd(g) to be the minor and major species, respectively. The minor component varied from 1% of the gas at 2000^0K to 5.8% at 2422^0K.

DeMaria and co-workers at the University of Rome have studied the vaporization of a series of lanthanon-carbon systems (27-29). An unexpected result of their studies was vaporization according to mode (3), and observation of the tetracarbide species, HoC_4 and CeC_4, in the effusate. Additionally, the PrC_4 molecule was identified tentatively. In all these studies the carbides were prepared in situ. Various data such as relative intensities of the various species, their dissociation energies and heat of reaction are also presented (27). Both the yttrium-carbon (28) and the neodymium-carbon system (29) were observed to vaporize according to both mode (1) and (2). A tabulated comparison of the enthalpies of vaporization will be made in Chapter VII, page 95.

The vapor pressure of europium dicarbide was studied both by target collection and a mass spectrometric technique (30). The principal mode of vaporization was according to equation (1).

Since lanthanon-dicarbides are often compared to the alkaline earth dicarbides, two recent alkaline earth dicarbide studies will be mentioned. Flowers and Rauh (31) studied the vaporization of strontium and barium dicarbides by both target collection and mass spectrometry. They used extreme precautions to obtain pure specimens. Diffusion effects were experimentally determined and minimized by variation of orifice sizes. Flowers and coworkers (32) also studied the vaporization of calcium dicarbide. They used target collection to sample the effusing beam and analyzed the deposits with an integrating flame photometer. Their absolute accuracy is quoted to be within 10%.

The vaporization energy for graphite may be needed if one wishes to undertake energy calculations of the Born-Haber cycle type on equations (1), (2) or (3). Both Hoch, et al. (33), using Langmuir vaporization, and Chupka and Inghram (34), using a mass spectrometer, determined the heat of sublimation of graphite to the monomeric species and agree on the value of 171 kcal/mole. Graphite has been found to vaporize in more than one mode giving C_2, C_3 and C_4 molecules in the effusate, and a dissociation energy of 150 kcal/mole has been calculated for the C_2 species (34).

A generalized conclusion concerning the vaporization of the lanthanon dicarbides was made by Wakefield, et al. (25) who state that "the stability of the rare earth dicarbides is related to the volatility of the metals, in that the more volatile rare earths have the less stable dicarbides."

In the course of the writing of this thesis the author became aware from the references in an article by Avery, et al. (96) that others were working on the samarium carbon system. These references have appeared in the literature (105, 106, 107). A tabulation of the results obtained is shown in Table I. The first column lists the literature reference and the second column lists the vapor pressure equation in the form such that the first number is ΔS_T^0 and the second number is ΔH_T^0 for the vaporization process: $SmC_{2(s)} \longrightarrow Sm_{(g)} + 2C_{(gr)}$ evaluated at the midpoint of the temperature range shown in column three. The general method used by Avery and coworkers (105) and by Cuthbert, et al. (106) to study the SmC_2 vaporization was mass spectrometric while Faircloth, et al. (107) used Knudsen effusion collection techniques.

Table I. The samarium - carbon system

Ref	$2.303R \log P_{(atm)}$	Range, ^0K
105	18.7 - 65,200/T	1300-2051
106	15.5 - 61,500/T	1400-2000
107	16.5 - 63,300/T	1400-2080

absol

inten

previo

sectio

measur

convert

ratio o

Stevens

calcula

samariu

$$\frac{dw}{dt}$$

n which

molecula

in ergs-

The calc

actual m

factor w

multipli

losses i

0.171 i

times hig

error qu

Cut

of samar

trometer

The calibration procedure employed by Avery to obtain absolute pressures of samarium from the mass spectrometric intensity data consisted of a method which had been used previously (96). This method utilizes an effective cross-section for samarium vapor, which is calculated from a measured sensitivity of the instrument for argon gas and converts this sensitivity to that for samarium using the ratio of ionization cross-sections as derived by Otvos and Stevenson (69). For a series of experiments, using the calculated absolute pressures, the total weight loss of samarium, w, was computed by integrating the expression

$$\left(\frac{dw}{dt}\right)_T = \frac{\pi d^2}{4} \quad \frac{1000M}{22400} \quad \frac{273}{T}\left(\frac{8RT}{\pi M}\right)^{1/2} \quad \frac{P}{4} \quad \text{mg sec}^{-1}$$

in which d is the orifice diameter in cm, M is the molecular weight of the effusate, R is the gas constant in ergs-deg/deg-mole, and P is the pressure in atmospheres. The calculated total weight loss was then compared with the actual measured weight loss and for each sample a correction factor was obtained by which all calculated pressures were multiplied to bring the calculated and measured weight losses in agreement. The factors thus obtained (0.183 and 0.171) indicate their calculated pressures were about 5.7 times higher than the pressures based on weight loss. The error quoted by these authors is "of a factor of about 5."

Cuthbert, et al. (106) determined the vapor pressure of samarium dicarbide using both a magnetic sector spectrometer and the target collection technique. They performed

twen

tungs

ture

press

loss

and th

be ±30

F

lanthar

reasure

2400°K

targets

γ-ray sp

reproduc

2.2. Re
Sy

2.2

In

lanthanu

gently i

powder d

La_2O_2S,

rivable

substitu

In 1958,

lanthano

twenty-one experiments on two samples of the dicarbide using tungsten cells with 0.025 cm diameter orifices. The temperature range covered in any one experiments was 400^0. Absolute pressures of Sm(g) were calculated from the measured weight loss of material which left the cell during an entire run, and the uncertainty in absolute pressures is estimated to be ±30%.

Faircloth, et al. (107) studied the dicarbides of lanthanum, cerium, neodynium, samarium and europium and measured their vapor pressures in the temperature range 1300-2400^0K using target collection effusion techniques. Exposed targets were analyzed by neutron activation analysis and γ-ray spectrometry. The measured pressures are said to be reproducible to within ±10%.

2.2. Reported Work on the Lanthanon Oxide Chalcogenide Systems

2.2.1. Preparation and Characterization

In 1949 Zachariasen (35) prepared an impure sample of lanthanum oxide sulfide (mixed with 30% La_2S_3) by heating gently in air lanthanum sesquisulfide. From an X-ray powder diffraction study he determined the structures of La_2O_2S, Ce_2O_2S and Pu_2O_2S. These structures were derivable from those of the corresponding sesquioxide by substitution of a sulfur atom for a unique oxygen atom. In 1958, Eick (36) reported the preparation of thirteen lanthanon mono-thio oxides (Ce, Pm excepted) and determined

their l

prepara

oxide us

impuriti

The mono

prepared

hydrogen

the latt

The meth

most of t

that used

crystal s

has been

One

of a new

type Ln_2C

pared by

mixture c

three pha

meters (i

$a_0 = 4.12$

2.2.2

The a

ization be

unpublishe

by Jacobs

Both of th

their lattice parameters. The basic procedure used in the preparation was to convert the sesquioxides to the monothio oxide using carbon disulfide, and then to remove the solvent impurities by heating in an atmosphere of flowing hydrogen. The monoseleno oxide phases of some of the lanthanons were prepared by a solid-vapor reaction of the sesquioxide with hydrogen selenide gas diluted by hydrogen and helium (37); the lattice parameters and structure were also determined. The method of preparation used by Kent and Eick (38) for most of the lanthanon monotelluro oxides was analogous to that used in preparing the monoseleno oxides. Recently the crystal structure of the neodymium (III) monotelluro oxide has been determined (39).

One report on the preparation and crystal structure of a new series of lanthanon oxide-chalcogenides of the type $Ln_2O_2S_2$ was reported (40). These compounds were prepared by reaction of sulfur vapor with Ln_2O_2S or with a mixture of $2Ln_2O_3 + Ln_2S_3$. The crystal symmetry of the three phases prepared was tetragonal and the lattice parameters (in Å units) were: La, $a_0 = 4.197$, $c_0 = 13.28$; Pr, $a_0 = 4.127$, $c_0 = 12.88$; Nd, $a_0 = 4.11$, $c_0 = 12.80$.

2.2.2. Vaporization Studies

The author knows of no published studies on the vaporization behavior of any lanthanon oxide chalcogenide. Two unpublished investigations are known, however. These are by Jacobs on Nd_2O_2S (41) and by Wiedemeier on Ce_2O_2S (42). Both of these studies used mass spectrometers and each

system was observed to produce MO and S as the volatile species.

The vaporization behavior of the lanthanon sesquioxides has been studied extensively and only a few selected references are listed. White, et al. (43,44) studied the vaporization of five lanthanon sesquioxides and yttrium sesquioxide as well as the thermodynamics of certain exchange reactions of the type

$$LnO_{(g)} + Ln'_{(g)} \longrightarrow Ln'O_{(g)} + Ln_{(g)}.$$

These studies permit calculation of the dissociation energies of gaseous molecules of the type LnO. Panish has also studied the vaporization of almost all the lanthanon sesquioxides (45,46) and he points out several trends: (1) the vaporization process shifts from one giving MO(g) and O(g) to one giving M(g) + O(g) with increasing atomic number of the metal; (2) the vaporization behavior may be subdivided into two groups which are the same as the cerium and yttrium groups, and (3) within each group the trend indicated previously is followed.

CHAPTER III

THEORETICAL CONSIDERATIONS

3.1. General Introduction

Several gross prerequisites must be observed if reliable thermodynamic data are to be obtained by monitoring, with a mass spectrometer as a function of temperature, the vapor effusing from a Knudsen crucible containing a refractory phase. These restrictions are: Gibbs' Phase Rule, existence of equilibrium between the condensed refractory and its vapor, a means of sampling the equilibrium vapor with the mass spectrometer and, if absolute pressures are to be computed, a means of standardizing (calibrating) the sensitivity of the mass spectrometer with regard to the particular species in question.

These restrictions will be illustrated further in this section. According to Gibbs' Phase Rule, (eq. 4)

$$V = C - P + 2 \qquad (4)$$

where V is the variance (degrees of freedom) of the system --the number of variables which must be fixed to define uniquely the state of the system; C is the number of components (smallest number of independent variable constituents participating in an equilibrium process); and P is the number of phases (homogeneous, distinct and mechanically separable portions). The plausibility of this form of the

Phase
are ba
phase
tempera
a pure
specifi
two pha
librium
pressur
pure su
tem is
and pres
paramete
App
the type

which ha
variance
that the
function
the syst
other th
tion of
meaningf
a functi

Phase Rule may be seen from the following examples which are based on the usual case that the state of a single phase of a pure substance is specified by two variables, temperature and pressure. For a one component system of a pure substance the temperature and the pressure must be specified in order to determine (fix) a single phase; for two phases of such a substance constrained to be in equilibrium the state of the system is specified if either the pressure or temperature is defined; for three phases of a pure substance in mutual equilibrium the state of the system is uniquely determined at only one set of temperature and pressure parameters and no variation from these parameters is possible, i.e. the system is invariant.

Applying the Phase Rule to a vaporization process of the type

$$AB_y(s) \longrightarrow A(g) + yB(s) \qquad (5)$$

which has three phases and two components, results in a variance of one for the equilibrium system. This means that the equilibrium vapor pressure of A(g) is a unique function of temperature, i.e. at a specific temperature the system is invariant with respect to pressure (or any other thermodynamic variable) providing that the composition of AB_y is also invariant. Thus, for such a system meaningful vapor pressure measurements may be obtained as a function of temperature.

Fu

the var

only on

vaporiz

measure

Th

establis

ray and

tion rer

maining

equilib

spectro

imply wi

3.2 The

3.2

Let

If this

exists t

and

Combinin

equation

For a phase vaporizing congruently as

$$AB_y(s) \longrightarrow AB_y(g) \qquad (5a)$$

the variance is also unity since there are two phases with only one component. Hence, when one component systems vaporize congruently, unique equilibrium vapor pressure measurements may be made as a function of temperature.

The question of congruence of vaporization must be established by performing appropriate analyses, e.g. X-ray and chemical analyses, to confirm that the composition remains invariant as vaporization proceeds. The remaining two general prerequisites previously mentioned, equilibrium and sampling of the effusing beam with the mass spectrometer, as well as others which these restrictions imply will be discussed subsequently in this Chapter.

3.2 Thermodynamic Relationships in Vaporization Studies

3.2.1. Second Law Relationships

Let us consider in more detail equation (5)

$$AB_y(s) \longrightarrow A(g) + yB(s) \qquad (5).$$

If this reaction is constrained such that equilibrium exists then at any specified temperature T

$$\Delta G^0_T = \Delta H^0_T - T\Delta S^0_T \qquad (6)$$

and

$$\Delta G^0_T = -RT\ln K_p \qquad (7).$$

Combining equations (6) and (7) with the value of K_p gives for equation (5)

where

cal deg

rigorou

approxi

phases

species

reactio

tempera

extent

experim

AB_y's

B's the

deviatio

method w

mination

trometer

measure

sumption

conditio

1000-250

these co

viding t

the vap

B's and

be justi

$$\ln P_{A(g)} = \frac{-\Delta H_T^0}{RT} + \frac{\Delta S_T^0}{R} \qquad (8)$$

where R, the universal gas constant, is in units of cal/deg/mole. The last three equations are obtained from rigorously derived thermodynamic functions by making the approximations (a) that the activities of all the solid phases are unity, (b) that the fugacity of the gaseous species equals its vapor pressure, and (c) that ΔC_p^0 for reaction (5) is approximately zero over the experimental temperature range. The first assumption (a) is good to the extent that Raoult's Law holds for $AB_y(s)$ in the actual experiment: for pure $AB_y(s)$ the activity is unity but for $AB_y(s)$ in a solid solution with another substance such as B(s the activity will deviate from unity, though this deviation may be very small. Recently, an experimental method was described by Belton and Fruehan (47) for determination of activities of molten systems in a mass spectrometer. This method may be used, in certain cases, to measure the activities of solid systems. The second assumption (b) is almost always valid under the experimental conditions of temperature and pressure in the range of $1000\text{-}2500^0$ and 10^{-8} to 10^{-3} torr, respectively--since under these conditions the vapor behaves as an ideal gas. Providing that there is no composition change in $AB_y(s)$ during the vaporization process and that the mutual solubility of B(s) and $AB_y(s)$ is negligible, the third assumption (c) may be justified sometimes <u>a posteriori</u> by observing a linear

plot of ln P_j

Curvat

ther proce

sumed negli

are occurri

reaction no

A_2 g , A_3 g

vaporizatio

is evident

to perform

non-zero ΔC

capacity da

reactants a

as a functi

But if ΔC_p^0

only one te

substituted

to give equ

ΔH

where ΔH_I^0

results by

and then i

plot of $\ln P_A$ *vs* $1/T$.

Curvature in a Clausius-Clapeyron plot indicates that other processes which were either unaccounted for or assumed negligible in deriving the Clausius-Clapeyron equation are occurring. These processes may arise from ΔC_p^0 of the reaction not being negligible, from polymer formation (e.g. $A_2(g)$, $A_3(g)$) or from stoichiometric variation in AB_y with vaporization or as a function of temperature. If curvature is evident in the Clausius-Clapeyron graph it is necessary to perform a "Σ-plot" in order to take into account the non-zero ΔC_p^0 term. To undertake such a treatment heat capacity data or estimates of them are necessary for all reactants and products. Hopefully, ΔC_p^0 may be expressed as a function of temperature by an equation of the form

$$\Delta C_p^0 = \Delta a + \Delta bT + \Delta cT^{-2} \qquad (9)$$

But if ΔC_p^0 is a constant, equation (9) would simplify to only one term, (the Δa term). The heat capacity may be substituted into equation (10) which then may be integrated to give equation (11)

$$\Delta H^0 = \int \Delta C_p^0 \, dT \qquad (10)$$

$$\Delta H^0 = \Delta H_I^0 + \Delta aT + \frac{\Delta b}{2} T^2 - \frac{\Delta c}{T} \qquad (11)$$

where ΔH_I^0 is the constant of integration. Equation (13) results by substituting equation (11) into equation (12) and then integrating (12) and combining the result with (7)

In this

senting

equation

which sh

against

may be c

Thus, th

over whi

obtained

from equ

vised [

namic va

explicit

term [

Since

It is ap

$$\frac{\partial\left(\frac{\Delta G^0}{T}\right)}{\partial T} = \frac{-\Delta H^0}{T^2} \qquad (12)$$

$$\frac{\Delta H_I^0}{T} + \Phi = -R \ln K_p + \Delta a \ln T - \frac{\Delta b}{2} T + \frac{\Delta c}{2} T^{-2} \qquad (13)$$

In this equation Φ is the integration constant. Representing the right hand terms of (13) by Σ produces the equation

$$\Sigma = \frac{\Delta H_I^0}{T} + \Phi \qquad (14)$$

which should produce a straight line when "Σ" is graphed against 1/T. The two integration constants ΔH_I^0 and Φ may be obtained from the slope and intercept, respectively. Thus, the value of ΔH^0 at any temperature in the interval over which the heat capacity equations are valid may be obtained from equation (11), ΔG_T^0 using (13) and then ΔS_T^0 from equation (6). Cubicciotti (48) has presented a revised Σ-plot treatment which utilizes tablular thermodynamic values to give the entropy and enthalpy change explicitly at the reference temperature. In his method the term Σ' is defined according to equation (15)

$$\Sigma' \equiv -R \ln K - \frac{\Delta(H_T^0 - H_{298}^0)}{T} + \Delta(S_T^0 - S_{298}^0) \qquad (15)$$

Since

$$\frac{\Delta G_T^0}{T} = \frac{\Delta H_{298}^0}{T} + \frac{\Delta(H_T^0 - H_{298}^0)}{T} - \Delta S_{298}^0 - \Delta(S_T^0 - S_{298}^0) \qquad (16)$$

it is apparent that

This t

transi

in the

I

was ach

effusat

either

mass spe

vapor pr

case the

P_i is re

ionizati

T_i by th

The prop

tivity o

Methods

Com

ing rela

of reacti

This equa

signated

reaction

against

$$\Sigma' = \frac{\Delta H^0_{298}}{T} - \Delta S^0_{298} \qquad (17)$$

This technique has the advantage of linearity even if a transition state (e.g. melting, polymorphic change) occurs in the experimental temperature range.

In this work experimental utilization of equation (8) was achieved by obtaining pressure in one of two ways. The effusate, A(g), which vaporized from a Knudsen cell was either collected (cf. Section 3.3) or monitored with a mass spectrometer, and from these data the equilibrium vapor pressure was calculated. In the mass spectrometric case the partial pressure of the specific vapor species, P, is related to the ion current intensity, I, produced by ionization of the i species and the absolute temperature, T, by the equation

$$P = kIT \qquad (18)$$

The proportionality constant, k, is related to the sensitivity of the spectrometer to the species being examined. Methods for evaluating it are discussed in Section 3.4.

Combining equations (8) and (18) produces the following relationship between ln IT and the enthalpy and entropy of reaction

$$\ln IT = \frac{-\Delta H^0_T}{RT} + \frac{\Delta S^0_T}{R} - \ln k \qquad (19)$$

This equation (which is linear only if the conditions designated previously are satisfied) permits the enthalpy of reaction to be obtained when the product ln IT is graphed against 1/T. From such a plot ΔH^0_T may be obtained directly

for react

the sensi

a ΔH^0_T obta

a "Second

In c

temperatu

where Q

the refere

be 298.16°

zation pro

or ΔS^0_{298} b

equal eit

function c

which one

it is very

over the t

eral, C^0_p f

phases. T

is a consta

and

Finally, i

for reaction (5), but the entropy, ΔS_T^0, is a function of the sensitivity $\underline{k}$ and the intercept as follows

$$\Delta S_T^0 = R(a + \ln k) \qquad (20)$$

A ΔH_T^0 obtained in this manner is commonly referred to as a "Second Law Enthalpy".

In order to relate ΔH_T^0 and ΔS_T^0 to a standard reference temperature use is made of the relationship

$$\Delta Q_T^0 = \Delta Q_\theta + \int_\theta^T \left(\frac{\partial \Delta Q}{\partial T}\right)_P dT \qquad (21)$$

where Q may be any thermodynamic state property, and θ is the reference temperature which in this work is chosen to be 298.16°K. Equation (21) implies that ΔC_p^0 for the vaporization process be either known or estimated so that ΔH_{298}^0 or ΔS_{298}^0 be obtained. In the range 298°K to T°K ΔC_p may equal either zero or a non-zero constant, or may be a function of temperature. For a vaporization process, in which one or more products is always in the gaseous state, it is very improbable, if not impossible, that ΔC_p^0 be zero over the temperature interval 298°K to T°K since, in general, C_p^0 for gases are quite different from C_p^0 for solid phases. Thus this possibility will be ignored. When ΔC_p^0 is a constant integration of equation (21) produces

$$\Delta H_T^0 = \Delta H_{298}^0 + \Delta C_p^0 (T - 298) \qquad (22)$$

and

$$\Delta S_T^0 = \Delta S_{298}^0 + \Delta C_p^0 \ln\left(\frac{T}{298}\right) \qquad (23)$$

Finally, if ΔC_p^0 is a known function of temperature, the

appropri

will res

Nec

majority

unavailab

tropy cha

22° and

ity estim

was one o

CaC_2 s

pound of

to equati

expressio

entropy f

ΔQ^0_{298}

This expre

sing equa

3.2.2

A vis

errors in

errors in

ship. The

because o

based on

appropriate substitution and integration of equation (21) will result in a ΔH^0_{298} and ΔS^0_{298}.

Necessarily for most new compounds, and for the vast majority of refractory materials, heat capacity data are unavailable. Consequently, reduction of enthalpy and entropy changes to standard conditions utilizing equations (22) and (23) is formally impossible. However, heat capacity estimates may be made--the method employed in this work was one of analogy. A similar compound of known C^0_p ($CaC_2(s)$) was used to estimate the C^0_p value for the compound of interest ($SmC_2(s)$). $SmC_2(s)$ vaporizes according to equation (5) with y being equal to two. Thus, the expression used to correct both changes in enthalpy and entropy for this reaction to 298°K was

$$\Delta Q^0_{298} = \Delta Q^0_T - [(Q^0_T - Q^0_{298})Ca(g) + 2(Q^0_T - Q^0_{298})C(gr) - (Q^0_T - Q^0_{298})CaC_2(s)] \qquad (24)$$

This expression is noted to be an alternate way of expressing equations (22) and (23).

3.2.2. Third Law Relationships

A visual inspection of equation (19) indicates that errors in T, (and to a lesser extent in I), produce large errors in ΔH^0_T and ΔS^0_T because of the logarithmic relationship. The Third Law method of calculating ΔH^0_{298}, so-called because of its use of absolute heat capacities which are based on the fact that for a pure crystalline substance

$S_0^0 = 0$ (the Third Law), utilizes the free energy function, fef. The ΔH_{298}^0 values calculated by this technique are rather insensitive to temperature errors. Use of this method provides a check on the ΔH_{298}^0 value obtained from the Second Law method. In addition it points out determinate errors associated with temperature since an independent value of ΔH_{298}^0 is calculated for every pair of pressure-temperature values. The free energy function, fef, is defined as

$$\text{fef} \equiv \frac{(G_T^0 - H_{298}^0)}{T} = \frac{(H_T^0 - H_{298}^0)}{T} - S_T^0 \qquad (25)$$

From equation (25) the Δfef of a reaction may be determined provided sufficient thermodynamic information is obtainable for all products and reactants. The Δfef of reaction (5) may be used to obtain ΔH_{298}^0 by using equation (26) which results by combining equation (7) and the equation for Δfef obtainable from equation (25)

$$\Delta H_{298}^0 = -T[\Delta\text{fef} + R \ln P_{A(g)}] \qquad (26)$$

By substituting equation (18) into (26) the following is obtained for the mass spectrometric vaporization of samarium dicarbide

$$\Delta H_{298}^0 = -T[\Delta\text{fef} + R(\ln IT + \ln k)] \qquad (27)$$

3.3. The K

3.3.1.

Knudse

is utilized

vapor press

49-51 . H

have been v

have been r

53 . The

which is to

small orifi

tainer is h

an equilibri

vapor. The

measuring t

caping thro

ditions of

experiment

cooled targ

sure is ob

P

in which w

A is the o

fusing bea

probabilit

3.3. The Knudsen Effusion Method

3.3.1. General Introduction

Knudsen developed the general effusion equation which is utilized in this work for determination of equilibrium vapor pressures in a series of papers published in 1909 (49-51). His basic equation and its requisite conditions have been verified by numerous experiments and recently have been re-examined critically by Carlson (52) and Ward (53). The method consists of confining the condensed phase which is to be studied in a sealed container in which a small orifice has been machined. When the charged container is heated (under conditions discussed subsequently) an equilibrium is established between the solid and its vapor. The equilibrium vapor pressure is determined by measuring the rate of mass flow of the vapor species escaping through the orifice in the cell. Under ideal conditions (cf. next Section) for a Knudsen-type vaporization experiment in which the effusing vapor is collected on a cooled target and then assayed, the equilibrium vapor pressure is obtained from equation (28)

$$P^*_{eq} = \frac{w}{At\epsilon}\left(\frac{2\pi RT}{M}\right)^{1/2}\left(\frac{r^2 + d^2}{r^2}\right) \qquad (28)$$

in which w is the mass of the volatile species collected, A is the orifice area, t is the time of exposure of the effusing beam to the collection plate, ϵ is the transmission probability term of the orifice or "Clausing correction",

R is the

T is the

of the ef

collectio

to the co

assumes a

in equati

g^{1} ^{2} cm^{2} s

it is appa

given by

P_{eq}

For Knudse

are collec

the geome

and e assu

e assumes

appears.

3.3.2

It wa

derived fo

ideality w

Non-ideali

can be cla

R is the universal gas constant expressed in ergs/deg-mole, T is the absolute temperature, M is the molecular weight of the effusing species, r is the radius of the exposed collection disc and d is the distance from the orifice to the collection disc. For collection work, ϵ normally assumes a value of unity. Use of the CGS system of units in equation (28) results in P^*_{eq} having the units of $ergs^{1/2}$ $g^{1/2}/cm^2$ sec. Recalling that 1 atm = 1,013,250 dynes/cm^2 it is apparent that the pressure in atmosphers, P_{eq}, is given by

$$P_{eq} = \frac{P^*_{eq}}{1013250} = .022561 \frac{w}{At\epsilon}\left(\frac{T}{M}\right)^{1/2}\left(\frac{r^2 + d^2}{r^2}\right) \quad (29)$$

For Knudsen vaporizations in which temperature-weight data are collected pair-wise (e.g. mass-vacuum balance work) the geometry factor term $\left(\frac{r^2 + d^2}{r^2}\right)$ drops from equation (29), and ϵ assumes non-unity values. In mass spectrometer work ϵ assumes unity values, and the geometry factor term disappears.

3.3.2. Restrictions and Constraints

It was mentioned that equations (28) and (29) were derived for ideal conditions. The extent of deviation from ideality will determine how these equations are altered. Non-ideality factors in a Knudsen vaporization experiment can be classed into three categories.

3.3.

lation.-

tions in

be infini

external

tions are

normally

However,

varying d

orifice c

and a tab

ities, fo

ratios ha

Edwards a

probabili

57

treat

noted tha

collector

the orific

through th

walls of

for the t

spectrome

lar requir

are unnece

lection, c

have to i

3.3.2.1. Limitations Arising from Mathematical Formulation.- Knudsen had to make certain necessary approximations in the derivation of his equations. The orifice must be infinitesimally thin, the vapor must be ideal and the external pressure must be negligible. The last two restrictions are usually satisfied, since the experiments are normally conducted at high temperatures and low pressures. However, a knife-edged orifice can be fabricated only with varying degrees of success. The "channeling" effect of an orifice of finite thickness was considered by Clausing (54) and a table of Clausing factors, or transmission probabilities, for cylindrical orifices of various length to radius ratios have been calculated by Dushman (55). More recently Edwards and Gilles (56) have calculated the transmission probability for spherical orifices, and Freeman and Edwards (57) treated the conical shaped orifice case. It must be noted that in any type of effusion experiment in which the collector (or sampler) is located in a plane parallel to the orifice and directly above it, the molecules must pass through the orifice without collision with the channel walls of the orifice. Under such conditions the correction for the transmission coefficient will be unity. The mass spectrometer ionization sampling system satisfies this angular requirement of the beam and thus Clausing corrections are unnecessary. Experiments employing total sample collection, or total mass loss, however, would most certainly have to include the transmission probability coefficient.

Hence, it

brated by

while mea

the trans

sure calc

3.3.2

difficult

with the s

zation coe

measuremer

surface of

leaving th

equal the

is defined

adhering t

Deviation

in a measu

than the eq

58 treat

logy of ir

problem mat

and

in which a e

Hence, it follows that when the mass spectrometer is calibrated by determining the total weight loss of the sample while measuring the ion intensity at constant temperature, the transmission coefficient must be included in the pressure calculations.

3.3.2.2. Limitations Arising from the Sample.- Most difficult to correct are some of the limitations associated with the sample. The most troublesome is a non-ideal vaporization coefficient. For an equilibrium vapor pressure measurement to be meaningful equilibrium must exist at the surface of the sample. Hence the total number of particles leaving the surface by evaporation, or by reflection, must equal the number condensing. The condensation coefficient is defined as the ratio of the number of grams of particles adhering to the surface to the number hitting the surface. Deviation of the condensation coefficient from unity results in a measured pressure using equations (28) or (29) of less than the equilibrium pressure. Ackermann, Thorn and Winslow (58) treat the subject of vaporization within the phenomenology of irreversible thermodynamics and formulate the problem mathematically. They derive the equations

$$J_m = \alpha_e G_s - \alpha_c G_i \qquad (30)$$

and

$$G_s = \frac{P_s}{(2\pi m k T_s)^{1/2}} \qquad (31)$$

in which α_e is the vaporization coefficient (ratio of the

rates of

for a Lan

face in a

coefficien

of particle

which is de

per cm^2 of s

rate flow of

of equation

ferring to s

a Langmuir-t

j_s using a

one obtains

quantities

periment and

known values

superficial

condensation

in general,

particular,

The exp

countered,

ficient are

(59) on grap

(58) point

surface temp

ates in the

rates of particles leaving the sample surface per unit area for a Langmuir-type vaporization to those leaving an orifice in a Knudsen-type vaporization), α_c is the condensation coefficient as defined previously, G_i is the total number of particles impinging on the surface of the sample; G_s, which is defined by equation (31), is the particle rate flow per cm^2 of surface area at equilibrium, and J_m is the net rate flow of particles away from the surface; the symbols of equation (31) have their usual significance with s referring to saturation (equilibrium) values. By performing a Langmuir-type vaporization ($G_i = 0$) and by calculating G_s using a P_s value determined a priori for a specific T one obtains the value of α_e (using equation (30)). The quantities G_i and J_m may be measured in a separate experiment and the value of α_c may be obtained using the known values of $\alpha_e G_s$. It must be noted, at least in a superficial way, that at the present time the role the condensation coefficient plays in a vaporization process in general, and in an equilibrium vaporization process in particular, is not easily determined experimentally.

The experimental methods, as well as the problems encountered, in obtaining values for the vaporization coefficient are illustrated in the work of Thorn and Winslow (59) on graphite. Commenting on this work Ackermann, et al. (58) point out one inherent difficulty in trying to measure surface temperatue--most of the thermal radiation originates in the interior of the sample and not at the outermost

atomic layer

gest tempera

velocity dis

described by

Another

work is that

maintain the

this necessit

small so that

is easily ach

proximate a c

In practice t

sure measurem

in which all

stant. When

temperature i

sures are ass

ollary deduci

izing species

Three ot

must be chose

under molecul

this conditio

that the mean

at least ten

action betwee

should occur.

atomic layer (from which evaporation occurs); they suggest temperature should be determined by measuring the velocity distribution of all the particles in the manner described by McFee, et al. (60).

Another condition required of the sample for Knudsen work is that the vaporization rate must be sufficient to maintain the equilibrium vapor pressure above the solid. This necessitates that the orifice area be sufficiently small so that replenishment of the lost or reacted vapor is easily achieved, i.e. the experimental conditions approximate a closed system containing the solid and vapor. In practice this condition is verified by performing pressure measurements on a series of vaporization experiments in which all parameters except orifice size are held constant. When the absolute pressure measured at a given temperature is independent of orifice area equilibrium pressures are assumed for the particular system studied. A corollary deducible from this is that the area of the vaporizing species should be much greater than the orifice area.

Three other restraints remain. First, temperatures must be chosen such that the vapor species will effuse under molecular rather than hydrodynamic flow. Although this condition is somewhat hazy, Carlson (52) indicates that the mean free path of the vapor particles should be at least ten times the orifice diameter. Second, no interaction between the vaporizing system and the container should occur. Third, the vapor pressure measured must

neither be af

formed in the

any small con

reactant duri

3.3.2.3

First Knudsen

re-examined t

flux through

which is tang

as long as ef

conclusion is

bution for Kn

but certain a

tribution abo

to be caused

fusion cells

law may be fo

where dN is t

area at some

flux of parti

tween the nor

section of un

be seen that

total flux wh

results as a

neither be affected by any solid residue product being formed in the vaporization process nor must it vary with any small composition change which may occur in the solid reactant during the course of the experiment.

3.3.2.3. Limitations Arising from External Geometry.- First Knudsen (49-51) and subsequently Carlson (52), who re-examined the subject, concluded that the rate of particle flux through a unit area situated on the surface of a sphere which is tangent to an orifice plane is everywhere equal as long as effusion flow limits are not exceeded. This conclusion is known as the cosine law of particle distribution for Knudsen effusion. Recently, Ward (53) pointed out certain apparent anamolies occur in the cosine distribution above effusion cells. These effects were found to be caused by the internal geometric design of the effusion cells and are a consequence of the law. The cosine law may be formulated as

$$dN = \left(\frac{1}{\pi}\right) N_0 \cos\theta \, d\omega \qquad (32)$$

where dN is the equilibrium flux of particles per unit area at some distance from the orifice, N_0 is the total flux of particles through the orifice, θ is the angle between the normal of the unit area plane and the conical section of unit area of the solid angle $d\omega$. Thus, it may be seen that $\left(\frac{1}{\pi}\right) \cos\theta \, d\omega$ is the fractional part of the total flux which has a specified direction. The $\left(\frac{1}{\pi}\right)$ term results as a normalizing factor for total integration over

the hemisp

When integ

32 it is

This integ

solid angl

sin θ dθ d

to give

which upon

result.

It is

from the po

rigorous ma

cosine law

references

effect of re

rates and pr

When th

the collecti

and a correc

does not adh

must be prov

pendence on

Finally

of the exper

tion made wh

the hemisphere of space above the plane of the orifice. When integration over all space is performed on equation (32) it is apparent that the total flux is indeed N_0. This integration may be effected by first expressing the solid angle in spherical coordinates such that $d\omega = \sin\theta\, d\theta\, d\Phi$ with subsequent integration of Φ from 0 to π to give

$$dN = N_0\left(\frac{1}{\pi}\right)(\pi)\sin\theta\cos\theta\, d\theta \qquad (33)$$

which upon integration of θ from 0 to $\frac{\pi}{2}$ gives the desired result.

It is apparent that the Knudsen equation is derivable from the postulates of the kinetic theory of gases and a rigorous mathematical derivation and/or analysis of the cosine law from this viewpoint may be found in a number of references (52,53). Rosenblatt (61) analyzes further the effect of restrictions of molecular flow on vaporization rates and pressures.

When the effusing vapor is condensed on cold targets, the collection efficiency of the targets must be determined and a correction applied for the fractional amount which does not adhere. Additionally, the collection efficiency must be proven to be temperature independent or its dependence on temperature measured.

Finally, the expansion of the crucible during the course of the experiment must be considered and the proper correction made when necessary.

3.4. Measurement of Partial Pressures With a Mass Spectrometer

3.4.1. General Introduction

The utilization of the coupled Knudsen effusion-mass spectrometer experiment in the study of refractory phase vaporizations is now an established technique (62). Some of the reasons for its widespread use are its advantages of high sensitivity, a wide dynamic range of measuring pressures, and the ability to identify uniquely all vapor species emanating from the cell. Basically, the procedure consists of performing Knudsen effusion vaporization experiments and measuring the intensity of the effusing vapor beam mass spectrometrically. The vapor beam is collimated critically by a double slit system so that only those species which have straight-through flight from the cell (i.e. no collisions with the orifice wall) are sampled by the instrument. The intensity of the fractional part of the vapor beam which is sampled is determined as a function of temperature. The relative intensities described in this manner may be converted to absolute pressures when the mass spectrometer has been calibrated in a manner similar to that discussed in the following Section.

3.4.2. Absolute Pressures With a Mass Spectrometer

The proportionality constant relating the absolute pressure of a species to its ion intensity-temperature

product is a function of a number of parameters which may be classified into two broad categories: (1) instrumental parameters and (2) ionization cross-section efficiency. Instrumental parameters arise from the variation of the sensitivity of the ion detector with effective mass and from the physical and electromagnetic dimensions of the ion source and flight tube. Hence k, the proportionality constant for the element (or molecule) as obtained for a specific isotope of the element (equation (18)) is related to σ, the ionization cross-section, by the equation

$$k = [\beta\delta r\sigma]^{-1} \qquad (34)$$

The variable δ is the effective multiplier gain, r is the isotopic abundance factor and β is the effect of any other machine parameters. Since no Faraday cup is designed into the time-of-flight mass spectrometer, the effective multiplier gain is difficult to determine and conventionally is assigned the value of unity. The ionization cross-section for a single ionization process (as differentiated from the total ionization cross-section) is not readily obtainable by ordinary methods in a mass spectrometer since the concentrations of the species being ionized are not usually measurable. Although many theoretical methods for calculation of ionization cross-sections have been published (e.g. 63-68), the number of experimentally determined data are considerably fewer (e.g. 69-73). Many of the theoretical approaches require a knowledge of various parameters which

for many sub

elements are

the experime

by Lampe, et

units of cm^2

relation

where a is t

in units of

cross-sectio

have been us

that one of

viz. the addi

molecule may

each constit

values report

do not agree

and 11.4 x 10

tively the a

quite arbitra

if the mass s

vapor e.g. c

ratio of cros

of interest t

the individua

are being det

tained using

for many substances, and especially for the lanthanon elements are either not known or not readily available to the experimentalist. As an example, the method employed by Lampe, et al. (71) calculates the cross-section, σ, in units of cm^2 with the theoretically-justified empirical relation

$$\sigma = (1.80 \times 10^8)\alpha \qquad (35)$$

where α is the polarizability of the neutral vapor species in units of cm^3. For most of the past decade the ionization cross-section values calculated by Otvos and Stevenson (69) have been used even though Lampe, et al. (71) pointed out that one of the main postulates on which the work was based, viz. the additivity principle that the cross-section of a molecule may be obtained by summing the cross-sections of each constituent atom, was in error. Since, even the values reported in the two most recent articles (67,68) do not agree (e.g. for Ag, σ is given as 5.44×10^{-16} cm^2 and 11.4×10^{-16} cm^2 in references (68) and (67), respectively) the actual choice of ionization cross-sections seems quite arbitrary. It should be pointed out, however, that if the mass spectrometer is calibrated with another metal vapor (e.g. copper or samarium) it is the error in the ratio of cross-sections between the standard and the species of interest that is significant and not absolute errors in the individual cross-sections. In general, when elements are being detected in the mass spectrometer and it is calibrated using a metal other than the one that is present in

the effusate

whether they

ly determine

not to intro

effusing spe

problem becon

A proce

eliminate th

volves calib

as that obse

the absolute

as a functio

general equa

of mass spec

rate of effu

tive intensi

that this me

species are g

To summa

calibrate a m

sures above a

measurements.

method, or th

solute pressu

these two gro

substance whi

While in meth

the effusate the only requisite is that any set of σ, whether they be theoretically calculated or experimentally determined, must be internally consistent in order not to introduce errors into the calibration. When the effusing species is a molecule, however, the cross-section problem becomes more complicated.

A procedure which may be employed in certain cases to eliminate the whole ionization cross-section question involves calibrating the instrument with the same species as that observed in the vaporization experiment provided the absolute vapor pressure of the metal itself is known as a function of temperature. Cater and Thorn (74) derive general equations and give two procedures for calibration of mass spectrometric partial pressures using the total rate of effusion as a function of temperature and the relative intensities of the individual species. They indicate that this method is applicable when two or more vapor species are present in the effusate.

To summarize, two basic methods may be employed to calibrate a mass spectrometer so that absolute partial pressures above a compound may be obtained from relative measurements. These are: (1) the Knudsen vaporization method, or the integration method (75); (2) explicit absolute pressure method. The distinguishing feature of these two groupings is that in method (1) one may use a substance which differs from the effusate being calibrated while in method (2) the calibrating substance is the same

as the effus

perimentally

forward proc

pressure is

spectrometer

to that to k

the same cel

temperature

tion derive

the absolute

culated at a

perature ran

Substituting

and the rela

tial pressur

intensity of

chart record

ture s . Th

related to t

$$\frac{1}{x}$$

in which all

Question and

is the molec

is the weigh

as the effusate. The first method may be implemented experimentally in two ways. In the first and most straightforward procedure a known mass of the compound whose vapor pressure is to be calibrated is vaporized in the mass spectrometer from an effusion cell of geometry identical to that to be used for the experiments (or, preferably, the same cell) for a definite period of time at a fixed temperature. Using the following form of the Knudsen equation (derived from equation (29))

$$P_{eq} = \frac{0.022561\ w}{At\epsilon} \left(\frac{T}{M}\right)^{1/2} \qquad (36)$$

the absolute partial pressure, in atmospheres, may be calculated at a fixed temperature preferably within the temperature range of the experiment and near its midpoint. Substituting P_{eq} into equation (18), $\underline{k}$ may be calculated and the relative intensities converted into absolute partial pressures. In the integration method (75) the ion intensity of a particular species is monitored on a strip chart recorder as a function of time at (a) fixed temperature(s). The mass of material vaporized from the cell is related to the constant k^* by the equation

$$\frac{1}{k^*} = \left(\frac{M}{2\pi R}\right)^{1/2} \left(\frac{A}{G}\right) \sum_j I_j T_j^{1/2} \Delta t_j \qquad (37)$$

in which all quantities refer to the particular ion in question and the units are in the CGS system. The term, M is the molecular weight, A is the area of the orifice, G is the weight loss, Δt_j is the time interval over which the

intensity I_j (nanoamperes) and the temperature (^0K) have been measured, and the other symbols have their usual significance. A dimensional analysis of equation (37) shows that $\underline{k}$ is related to $\underline{k}^*$ by the expression

$$k = (9.9344 \times 10^{-4})k^* \qquad (38)$$

in which $\underline{k}$ is defined by equation (18) in units of atm/nA/^0K.

The second method consists basically of graphing the the absolute pressure of the calibrating substance (obtained for the literature from the experimental temperature) against IT for the substance. This is a graph of equation (18) and the slope of this graph gives $\underline{k}$ directly for the calibrating substance. As an example, for the calibration of Sm(g) over SmC_2(s) elemental samarium would be vaporized at a series of temperatures and the IT product would be recorded at each temperature. The pressure of the element recorded in the literature (76) would be graphed against IT, and the value of k_{Sm} would be determined. This value would be used subsequently to calibrate the Clausius-Clapeyron line for SmC_2 vaporization by substitution into equation (19) for a specific pair of ln IT and 1/T values.

Should a method employ for calibration a metal other than the one being standardized, conversion of the proportionality constants will have to be effected using ionization cross-sections (77)

3.4.3

In co
work, geome
respect to
in the cali
position of
and the vap
These two p
the k_i of e
periment wi
ality const
ment.

The Kn
the mass spe
fice size is
The truth of
tion of the
odified for
metric-depe
it has been
achine para
temperature
so calibrate
temperature-

$$k_A = k_B\left(\frac{\sigma_B}{\sigma_A}\right) \qquad (39)$$

3.4.3. Geometry Considerations in Calibration

In contrast to target collection Knudsen effusion work, geometry variables, such as crucible position with respect to the ionizing electron beam, are not critical in the calibration procedure. Rather it is the relative position of the crucible during the calibration experiment and the vaporization experiment which is of importance. These two positions should be as close as possible so that the k_i of equation (18) determined in the calibration experiment will be numerically identical to the proportionality constant for species i in the vaporization experiment.

The Knudsen effusion weight loss method of calibrating the mass spectometer is both geometry-independent (orifice size is corrected) and has no machine parameter errors. The truth of this statement may be demonstrated by inspection of the Knudsen equation (29). When this equation is modified for mass spectrometric work it contains no geometric-dependent variables (orifice size is excluded since it has been considered) nor do the variables depend on any machine parameters per se. They are only a function of the temperature and thus a series of vaporization experiments so calibrated are all referenced to the same absolute, temperature-dependent value.

In an

that once

kept fixed

tative dat

stant for

ant from ex

factor is t

3.5. Tempe

The me

eter in Knud

transmissio

the emitted

which the ho

on Wien's la

where J_{λ},T

length λ ra

and C_2 are

spectively.

through an in

where T_a is

through the f

In any mass spectometric experiment it is necessary that once machine parameters have been maximized they be kept fixed throughout the experiments in which quantitative data are being taken. In addition to being constant for one experiment, these parameters must be invariant from experiment to experiment if the same calibration factor is to be used.

3.5. Temperature Corrections

The measurement of temperatures using an optical pyrometer in Knudsen effusion experiments requires that certain transmission corrections be made for partial absorption of the emitted radiation by various windows and/or prisms through which the hot object is viewed. These corrections are based on Wien's law of radiation (95):

$$J_{\lambda,T} = C_1 \lambda^{-5} \exp\left(\frac{-C_2}{\lambda T}\right) \qquad (40a)$$

where $J_{\lambda,T}$ is the energy flux per unit area at a wavelength λ radiated by an object at a temperature T; C_1 and C_2 are the first and second radiation constants, respectively. The diminuation of the energy flux in passing through an intervening filter is given by

$$J_{\lambda,T_a} = J_{\lambda,T} \exp(-kx) \qquad (40b)$$

where T_a is the apparent object temperature as observed through the filter, T is the true temperature, k is the

absorption c

path length

results in

from which t

The term

the intensity

ished by the

law of radiat

substance is

of this term

where T_f is

the pyrometer

perature of t

K_1 and K_1

ature is then

to give

absorption coefficient in cm^{-1} and x is the absorbing path length in cm. Combining the two previous equations results in

$$C_1\lambda^{-5}e^{-C_2/\lambda T_a} = e^{-kx}\, C_1\, \lambda^{-5}\, e^{-C_2/\lambda T} \quad (40c)$$

from which the two following equations result

$$\frac{-C_2}{\lambda T_a} = -kx - \frac{C_2}{\lambda T} \quad (41a)$$

$$\frac{1}{T} - \frac{1}{T_a} = \frac{-kx\lambda}{C_2} \quad (41b)$$

The term $\frac{kx\lambda}{C_2}$ may be evaluated by measuring how much the intensity of light radiated by a hot object is diminished by the filter (prism and/or window). Since Wien's law of radiation states that the energy radiated by a given substance is proportional to its temperature the magnitude of this term is obtained by

$$K_i = (\frac{1}{T_f} - \frac{1}{T_L}) \quad (41c)$$

where T_f is the temperature of a standard lamp read with the pyrometer sighted through the filter, T_L is the temperature of the standard lamp read with the pyrometer directly, and K_i is defined by equation (41c). The true temperature is then obtained by using equations (41b) and (41c) to give

$$\frac{1}{T} = \frac{1}{T_a} - K_i \; . \quad (41d)$$

E

4.1. General

The four
pressure stud
the mass spect
age electron
sembly and ne
2) the vacuu
erator; and
used for fabr
products.

4.2. Detaile

4.2.1.

The instr
mass spectrome
with a Model 1
multiplier. F
instrument and
where 78,79).
laboratory fr
fied considera
ionization kit

CHAPTER IV

EXPERIMENTAL EQUIPMENT AND MATERIALS

4.1. General Description of Experimental Equipment

The four major pieces of equipment used for vapor pressure studies in the course of this work were: (1) the mass spectrometer with its associated d.c. high voltage electron bombardment power supply and furnace assembly and necessary read-out oscilloscope and recorder; (2) the vacuum preparation system; (3) the induction generator; and (4) the glove box. Various materials were used for fabricating crucibles and for the synthesis of products.

4.2. Detailed Description of the Apparatus

4.2.1. The High Temperature Mass Spectrometer

The instrument used was a Model 12, Bendix T.O.F. mass spectrometer fitted with a 167-cm long flight tube, with a Model 107 ion source and with a M-105-G6 electron multiplier. Figure 1 illustrates the basic design of the instrument and a detailed description may be found elsewhere (78,79). This instrument had been assembled in this laboratory from commercial components and has been modified considerably as described below: (1) a continuous ionization kit, purchased from the Bendix Corporation, was


+150 Vd.c.

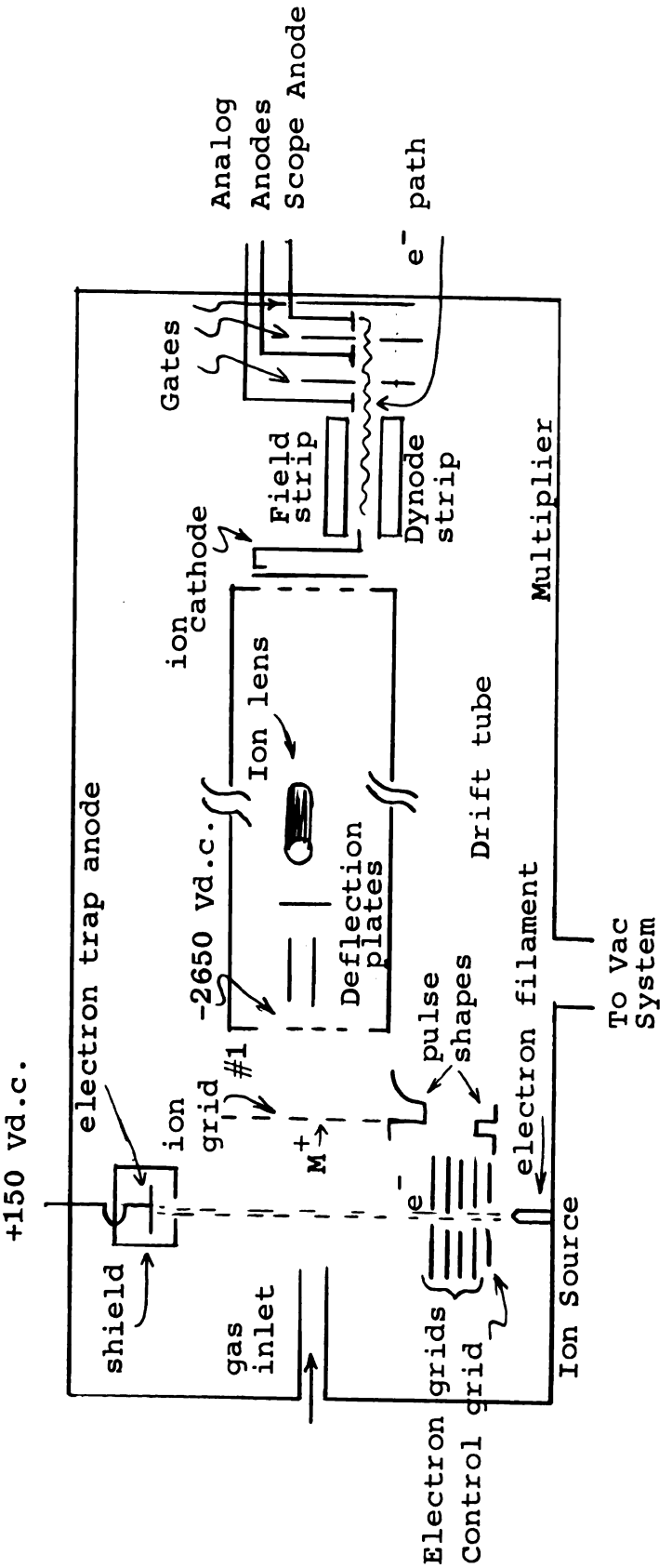

Figure 1. Schematic: Time-of-flight mass spectrometer.

added to permit the electron gun of the ion source to be operated in either normal pulsed (10KHz) or in continuous duty mode. Operation of the electron gun in continuous mode increased the sensitivity by a factor of about 100. Changes were made in the ion source such that one of the electron grids may be either grounded or have -150 V DC impressed on it. This alteration prevents the electron beam from traversing the ion source and thereby turns off the spectrum without necessitating any alteration of adjustable instrument parameters. Such a feature prevents contamination of the multiplier between measurements and also permits the detection of and correction for residual ionization processes which do not result from the electron beam (e.g. thermal, potential).

(2) A 3.0 volt battery was connected to the electron gun filament (negative terminal of battery) and to one of the electron grids (positive side) so that the trap current would be increased in the ion source by dissipating the charge cloud of emission electrons on one side of the electron gun filament.

(3) A small steel plate was spot welded behind the filament and maintained at the same potential as the filament thereby retarding electron emission in the "reverse" direction.

(4) The anode shield was connected to a switch which either connected it to the trap anode or to electrical ground. Use of this switch permits critical alignment of

the ion source magnets thereby insuring that the electron beam traverses the electron gun filament-trap anode region in a linear rather than spiral trajectory.

(5) All the nickel mesh grids in the ion source and in the electron multiplier were replaced with molybdenum mesh grids which have a higher transparency for ions and which interact less with potential fields than do the nickel grids.

(6) A 50 liter/sec titanium sublimation gettering pump, Varian Associates Model 922-0032, was inserted between the Knudsen cell furnace housing and the 15 liter/sec Vac Ion pump.

(7) A new Knudsen cell furnace assembly was designed and constructed. The improvements incorporated in the new design as compared to the previous one were: (a) a smaller heat zone which thereby minimized temperature gradients and (b) quartz discs to replace the boron nitride ones which out-gassed excessively after they had been exposed to the atmosphere. A more complete description of the furance assembly is given by Rauh, et al. (80).

(8) The analog scanner circuit was fitted with a pulse transformer which increased the gate pulse on the electron multiplier from about 60 nsec to 360 nsec. This alteration allowed monitoring the sum of the integrated peak intensities of up to four isotopes instead of just one peak, thereby increasing the sensitivity of the instrument. The pulse transformer set was purchased from Polyphase Instrument Co., Bridgeport, Pa.

As is indicated in reference (22), the spectrum was observed on a Tektronix Model 545A oscilloscope fitted with a CA dual channel pre-amplifier and was recorded using a Bausch and Lomb Model V.O.M.-5 strip chart recorder.

The power supply used to heat the cell in the spectrometer is a well regulated electron bombardment unit and has been described elsewhere (22). In this system the cell is grounded and the filament assumes a negative potential. Temperatures were measured using a Leeds and Northrup disappearing-filament type optical pyrometer, serial no. 1619073 calibrated previously against the 1948 International Scale of Temperature at the National Bureau of Standards and by sighting through a prism and optical window into the cell orifice. The calibration data for the pyrometer are presented in Appendix D.

4.2.2. The Vacuum Preparation System

Either of two vacuum systems was used for the preparation or vaporization of samples. One was an all glass system (81) while the other was a fast pumping station employing a current concentrator designed for maximizing the current flow through the crucible material (82). The fast pumping station which employed a 45 ft^3/min (1274 liters/min) forepump and a three-stage 500 liter/sec diffusion pump was used in conjunction with the current concentrator. The induction generator was a 20 Kw, 250-450 KHz Thermonic brand unit manufactured by Induction Heating

Corporation, whose input voltage was stabilized by a General Electric Inductrol Voltage Regulator and whose current was controlled by a saturable core reactor.

4.3. Chemical Materials

The purity and source of the materials used in the experiment were: (1) samarium metal, 99.9%, from Lunex Corp., Pleasant Valley, Iowa; (2) graphite powder, Acheson Grade #38, Fisher Scientific Co., Fair Lawn, N.J.; (3) tellurium metal chips, 99.999%, Fairmount Chemical Co., Newark, N.J.; (4) neodymium sesquioxide, 99.9%, Michigan Chemical Corp., St. Louis, Mo.; (5) hydrogen gas, 99.95%, The Matheson Co., Chicago, Ill.; (6) thin-wall, seamless tantalum tubing from Fansteel Metallurgical Corp., North Chicago, Ill.; (7) molybdenum stock from the Kulite Tungsten Co., Ridgefield, N.J.; and (8) sintered tungsten rod from Sylvania Co., Towanda, Pa..

4.4. Knudsen Cell Design

Effusion cells used for vapor pressure experiments were of the basic design illustrated in Figure 2. Those cells which were made of molybdenum and were used for the samarium dicarbide study were fitted with a graphite cup liner while those fabricated from tungsten metal were used without any liner. The effusion cells were each converted to a one piece assembly by heating them to such a temperature that the halves of the cells fused together.

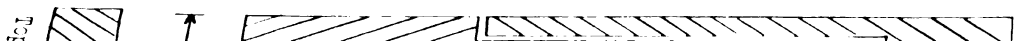

Figure 2. Effusion cell

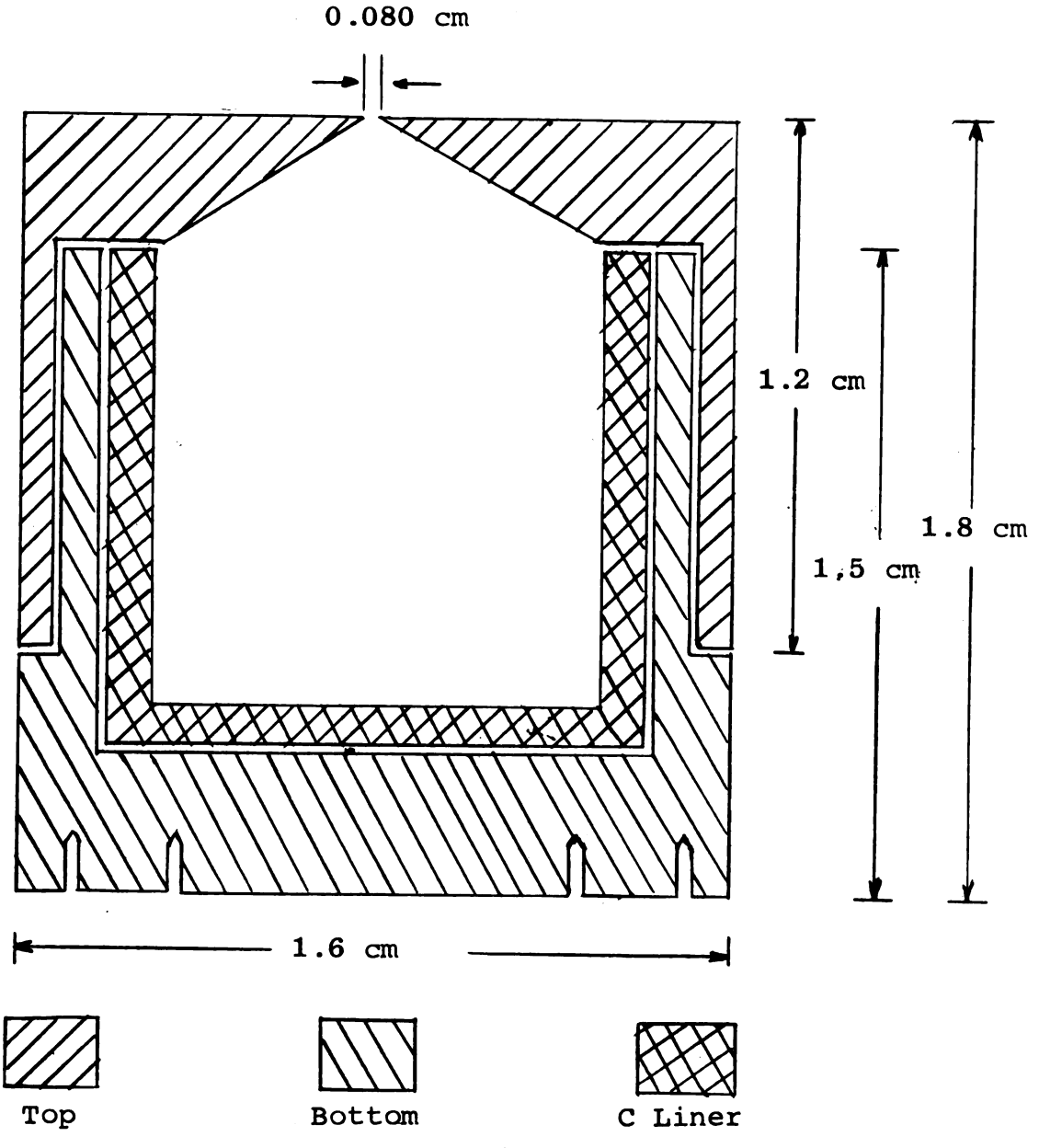

4.5. Heliarc Apparatus

An evacuable heliarc welding apparatus was constructed to seal small tantalum bombs charged with samarium metal and graphite powder. This assembly is illustrated in Figure 3. The apparatus consists of a glass tube 18 in (45.6 cm) long, 7 in (17.8 cm) in diameter, with 1/8 in (0.32 cm) wall thickness whose ends are beaded to be 1/4 in (0.63 cm) wide; and two 1/2 in (1.25 cm) thick bakelite blocks for capping the ends of the glass tube. Each bakelite block has an 1/8 in (0.32 cm) groove into which a rubber gasket is fitted. Electrical feedthroughs in the bakelite consist of Swagelok connectors, which serve also as gas ports. Torr-Seal epoxy resin (Varian Associates, Palo Alto, Calif.) was used to vacuum seal the metal feedthroughs to the bakelite blocks. Polyethylene tubing (an insulator), was used to connect the Swagelok fittings to the copper tubing valve system. Entry and manipulations inside the apparatus were executed with a rubber glove. The two bakelite blocks were necessary to allow simultaneous evacuation (or pressurizing) on both sides of the glove. Hoke valves (type 309A) were situated on the copper tubing leading from the apparatus to a mechanical pump so that the system could either be filled with helium (or any purging gas) or be evacuated. An oil bubbler permitted the equalizing of pressures when manipulations were performed with the rubber glove. Four symmetrically-spaced springs applied cohesive

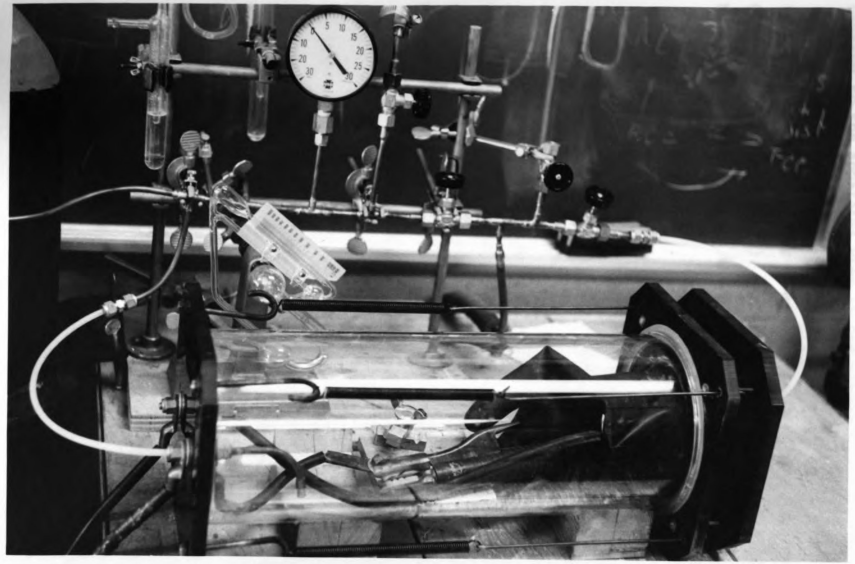

Figure 3. Evacuable heliarc apparatus.

tension to the apparatus when it had atmospheric, or higher, internal pressure. The pressure was monitored by an aneroid-type pressure gauge and by a McLeod mercury manometer (Kontes Glass Co., Vineland, N.J.). An Airco Welding Products, Union, N.J., arc welder provided the D.C. current.

CHAPTER V

EXPERIMENTAL METHODS

5.1. Preparation of Samples

5.1.1. Samarium Dicarbide

The preparative technique was an adaptation of Spedding, et al. (4). Tared amounts of samarium metal chips, scraped free of oxide coating, were inserted into a 6.5 mm diameter (about 3.5 in (8.5 cm) long) seamless tantalum tube which had been outgassed at an observed temperature of 2000^0 for about 10 hours. A stoichiometric amount of graphite which had been outgassed at 2000^0 for about 5 hours was added to the samarium metal. The ends of the tantalum tube were crimped tightly and were sealed by heliarcing (Cf. Section 4.5) after the tube had been evacuated to a pressure of 0.06 torr or less and flushed with helium gas several times. This procedure reduced the possibility of oxygen contamination. Subsequently the tantalum was suspended in a Vycor vacuum system and heated inductively at an observed surface temperature of 1500^0 to 1700^0 for 6 to 10 hours. Since samarium dicarbide hydrolyzes in air, the bomb was opened in a helium-filled glove box (hereafter called "glove-box") and all subsequent manipulations were performed in this box; the samples were stored in a vacuum desiccator.

5.1.2. Neodymium Monotelluro Oxide

Samples of this phase were prepared according to the vapor transport procedure employed by Kent and Eick (38). Calcined neodymium sesquioxide and tellurium chips were placed in separate, adjacent quartz boats enclosed in an open-ended Vycor tube which was located in a tube furnace. A 1.5 mole excess of tellurium was provided to assure complete conversion of the oxide. The temperature, measured with a chromel-alumel thermocouple and potentiometer was increased slowly to about 700^0 and maintained there for about 5 hours while hydrogen gas was swept through the tube, thereby transporting the tellurium vapor over the sesquioxide.

5.2. Methods of Analysis

5.2.1. Samarium Dicarbide

Chemical analyses were performed using the oxalate precipitation method. Tared samples were dissolved in 6 M hydrochloric acid, digested on a hot plate for about 4 hours, and filtered to remove free carbon which was dried and weighed. The pH was adjusted to 4-5 using bromcresol green indicator, and the samarium was then precipitated as the oxalate. The precipitate was calcined to the sesquioxide by heating overnight at 900^0 in a muffle furnace and weighed after it had cooled. Samarium content was calculated from the weight of the converted sesquioxide; bound carbon was calculated from the difference between the original weight of the sample and the sum of the free carbon and samarium

weights. Duplicate analyses for carbon and samarium content were performed on one sample by Galbraith Laboratories, Knoxville, Tennessee.

X-ray powder diffraction photographs of the various preparations were taken with 114.59 mm diameter Debye-Scherrer cameras. Lattice parameters for three preparations were determined using the Nelson-Riley least squares extrapolation techniques which is part of a larger computer program (83).

5.2.2. Neodymium Monotelluro Oxide

Three preparations of this compound were made. The mass increase which resulted from substitution of a tellurium atom for an oxygen atom was used as a basis for calculating the purity of the product as well as for indicating completeness of reaction. The preparation was then heated for several hours in a dynamic hydrogen atmosphere to purge it of any free tellurium. The purity of the olive green product, as well as its identification was proven further by its characteristic X-ray powder diffraction pattern.

5.3. Temperature Measurements

A chromel-alumel thermocouple was used for the Nd_2O_2Te preparatory procedure since accurate temperature measurements were not required. The optical pyrometer described previously was used for all effusion work. To reduce random errors, each temperature value reported in this thesis is an average of three independent readings.

Temperatures measured by optical pyrometry must be corrected for absorption due to the material of the viewing port window-prism assembly. To effect this correction, the transmissivity term, K_A, was determined for the window and prism assembly after every experiment by measuring first the temperature of a tungsten strip lamp whose input voltage was regulated carefully, and then by measuring the apparent temperature through the window-prism assembly. The window and prism were then cleaned to remove any film deposit which may have formed during the vaporization experiment, and the apparent temperature of the lamp was re-measured. Subsequently the temperature of the lamp was measured directly. For each of these temperature measurements five independent readings were taken and the average of each set was used. Since the transmissivity may change over the course of an experiment as a result of deposit formation on the optical window, the average transmissivity of the "clean" and "dirty" optical assembly, K_A, was used. This value was obtained from the relation

$$K_A = \frac{2}{T_C + T_D} - \frac{1}{T_L} \qquad (42)$$

where T_C and T_D are the observed average apparent temperatures of the lamp through the "clean" and "dirty" optical assembly, respectively, and T_L is the observed average temperature of the lamp measured directly. The true temperature is obtained from the observed experimental value, T_a, using equation (43)

$$\frac{1}{T} = \frac{1}{T_a} - K_A \quad . \qquad (43)$$

In all correction determinations of this type a tungsten lamp temperature of about 1500^0 was chosen since this is the most accurate scale region of the pyrometer. It must be noted that the pyrometer correction listed in Appendix D was applied first to the observed pyrometer readings and the corrected values were used in equations (42) and (43).

5.4. Vaporization Experiment Procedure

Samples of Nd_2O_2Te were manipulated in air while those of SmC_2 were handled only in the glove box. In both cases samples were pulverized and were loaded into the effusion cells through the orifice. Transfer of the effusion cell from the glove box on to the Knudsen cell furnace assembly and insertion of the assembly into the mass spectrometer were performed as quickly as possible and, in general, required no more than two minutes. The mass spectrometer was evacuated immediately and the pressure decreased rapidly to 5×10^{-5} torr or less. The effusion cell was then heated slowly so that the pressure did not exceed 5×10^{-5} torr until a heater filament current of 11 amperes (about 1000^0) was reached. A negative D.C. voltage was then applied to the filament, and the cell was heated to higher temperatures by electron bombardment since the effusion crucible was at ground potential. Although an induction period of about one

minute is required for the cell temperature to equilibrate in this system after a new power setting is chosen (84), a five minute interval was always allowed before measurements were initiated. Temperatures were usually incremented systematically until a maximum value was reached and then decreased in like fashion. The viewing window for temperature measurement was protected from undue coating by the effusate with an externally operated, magnetic shutter. A similar shutter positioned between the ion source and the effusion cell was used to demonstrate that the effusing species did, indeed, originate from the cell and was also used to correct for background contributions to the measured intensities. The integrated intensities were recorded in both pulsed and continuous ionization modes by scanning all the isotopes and/or monitoring and recording the intensity of the most abundant isotope.

5.5. Congruency Tests on Neodymium(III) Monotelluro Oxide

To ascertain whether Nd_2O_2Te vaporized congruently, preliminary vaporization experiments were performed using tungsten and molybdenum effusion cells. These effusion cells were outgassed to constant rate weight loss to be certain that they were clean. The outgassing data are shown as Table H-I in Appendix H. Subsequently a series of eleven vaporization experiments were performed using the molybdenum cell over a temperature range of 1505-1848^0, and from 7-81% of the sample vaporized in each run. Three other vaporizations

were performed using tungsten cells. After each experiment the residue was examined by X-ray powder diffraction analysis. The results are shown in Table H-II of Appendix H and are discussed in Section 6.8.

5.6. Calibration of the Mass Spectrometer for Samarium Dicarbide

5.6.1. Transmission Coefficient

Knudsen effusion crucibles used in this work were machined from molybdenum and tungsten bar stock. The orifice of each cell was machined in the following manner. A tapered drill of the correct size was cut into the crucible top inside section until 5-10 mils of metal remained. The orifice was then formed by machining the top face until the correct diameter hole remained. Since all the orifices were made in this fashion, they should have comparable dimensions. An attempt was made to determine the channel thickness of one of these orifices by a "depth of field" type measurement with an 100X magnification microscope. This procedure failed, however, and the top was cleaved along a cross-section of the orifice and mounted on edge so that the field of vision in the microscope was along the channel width of the orifice. Although in this position it was impossible to focus on the entire "channel width", continual variation of the focus moved the field of vision along portions of the "channel". Clay impressions of the cleaved cross-section were also made.

5.6.2. Calibration with Elemental Samarium

Two techniques involving samarium vapor were used to calibrate the mass spectrometer. In the first procedure a tared Knudsen effusion cell of the same design and orifice size as the cell used in the vaporization experiment being calibrated was loaded with 1-2 grams of samarium metal cleaned by abrasion to remove the oxide coating. The charged cell was then placed into the mass spectrometer and the system evacuated. The samarium was then vaporized and temperature and ion current intensity data were collected as described previously. After the experiment the cell was reweighed to confirm that metal still remained in it and the window-prism transmissivity was checked. Then, at each corrected temperature the value of the total samarium vapor pressure, P (obtained from Habermann and Daane(76)), was graphed against I_iT, in which I_i is the normalized intensity of samarium obtained from isotope i. Such a graph results in a line whose slope is k_i, the proportionality constant obtained from isotope i. Since reference (76) expresses the pressure in a logarithmic form, equation (18) was used in the form

$$\log k_i = \log P - \log I_iT - 2.8808 \qquad (44)$$

where the reference states for k and P are in atmospheres and torr, respectively, and the number 2.8808 arises from conversion of torr to atmospheres.

The second procedure was the integration method (*cf.* Section 3.4.2). In calibration experiment II 63 a tared effusion cell was loaded with about 1-2 grams of cleaned samarium metal and weighed accurately. After evacuation, the temperature was elevated quickly to a pre-determined power setting and the intensity of one isotope of samarium was monitored as a function of time at constant temperature. At various times background intensity readings were determined by stopping the effusing beam with the shutter. The sample was heated for a time sufficient to cause a significant weight loss (*e.g.* one hour at 1100^0K causing loss of 0.1 to 0.2 gram), and the temperature was monitored periodically. Heating was then terminated suddenly, the time recorded and the cell re-weighed after it had cooled. From equation (37) a sensitivity was calculated for which k was found using equation (38). The orifice diameter was corrected for thermal expansion at the weighted mean temperature of the calibration experiment using Krikorian's data (85).

5.6.3. Calibration with Elemental Silver

In this procedure a small, known weight of silver metal (about 10 mg) was placed into the effusion cell containing samarium dicarbide powder and the metal was vaporized at a fixed temperature while the intensity of the ^{107}Ag isotope was monitored as described in Section 5.6.2 for samarium metal. The time required for the intensity of the silver

peaks to fall to the background level was recorded as the end time of the calibration. The temperature was then elevated and vaporization of samarium dicarbide was started using instrumental conditions identical to those used for the silver calibration. In a fashion analogous to that described previously, the calculations of the integration method were performed on the silver data. Conversion of the proportionality constant, k, from silver to samarium was effected using equation (39).

5.6.4. Calibration with Samarium Dicarbide

Calibration experiment IV 3 utilized the pressure calculated above samarium dicarbide as obtained in a Knudsen vaporization experiment to obtain absolute pressures. An effusion cell to be used subsequently for vaporization experiments (after calibration) was loaded with samarium dicarbide and weighed in the glove box. After the spectrometer had reached a sufficiently low pressure (5×10^{-5} torr), the cell was heated to a pre-selected temperature which was in the range of the planned vaporization experiments and the ion current intensity was monitored. The temperature was measured at regular intervals and the total time of the vaporization was recorded. The cell was then removed and weighed. Applied corrections included: background intensity, transmittance effects of the optical assembly on temperature, and orifice diameter expansion (85). The calculated Knudsen pressure (Cf. equation (29) without

geometric term) at the weighted mean temperature, $\overline{T}$, of the calibration experiment was then used to obtain $\underline{k}$ for (Sm-152 and Sm-154) by using equation (18) and obtaining the value of IT at $\overline{T}$ from the Clausius-Clapeyron least squares line of the vaporization experiment being calibrated.

In this calibration experiment the 360 nsec gate pulse transformer was used. This alteration allowed simultaneous measurement of the sum of the ion current intensities of the two most abundant isotopes. In the subsequent vaporization experiments for which this calibration was used the intensity data were collected in the same manner.

5.7. Appearance Potential Measurements

The appearance potential of an ion is defined as the minimum energy required to produce that ion (and any co-appearing neutral fragments) from a given species (ion, atom, or molecule). For an ion produced from a neutral species and resulting in only the ion and two electrons the appearance potential is the same as the ionization potential, viz., the energy required to remove an electron from the species.

Ionization efficiency data were collected on various vapor species in the mass spectrometer with two objects in mind: (1) to show whether these were primary species coming directly from the effusion cell or secondary species produced by rupture of a bond and subsequent ionization; (2) to further identify any species coming from the effusion

cell by its ionization potential. The instrument used is not adequately equipped for highly accurate ionization potential work, but it suffices for the two aforementioned objectives. Because of its simplicity and its sufficiency the linear extrapolation method was employed. A general discussion and appraisal of the experimental techniques used to obtain appearance potentials may be found elsewhere (91). The principal feature of the linear extrapolation method is that in the ionization efficiency plot of ion current vs electron energy the linear portion of the curve is extrapolated to zero ion current intensity. Another substance, ideally isoelectronic with the first, whose ionization potential is well known, is used to calibrate the energy axis and thereby correct for machine parameters. The calibrating substances are usually the noble gases; krypton and xenon were used in this work.

5.8. Treatment of the Vaporization Data

All mass spectrometer data were reduced by a computer least squares program whose logic is listed in Appendix E. This program corrected observed intensities for background contributions, normalized isotopic intensities using the isotopic abundance data found in reference (91), corrected observed temperatures for window-prism transmissivity and applied to temperatures a pyrometer correction taken from the table in Appendix D.

The computer program had a rejection criterion such that any experimental point which varied by greater than three standard deviations of that least squares calculated value would be rejected and a new least squares value calculated. This criterion guards against gross erratic errors but is not very reliable for small sets (10-20 points) of data. After each computer least squares analysis the output data were graphed and if a point was found to exhibit a large deviation from the others in the set another rejection criterion was applied.

This second criterion was that developed by Grubbs (92) for small sets of data. His rejection criterion for the largest member of a set of size $n(2 < n \leq 25)$ uses the statistic

$$\frac{S_n^2}{S^2} = \frac{\sum_{i=1}^{n-1} (x_i - \bar{x}_n)^2}{\sum_{i=1}^{n} (x_i - \bar{x})^2} \qquad (44a)$$

where x_n is the largest member; $\bar{x}_n$ and $\bar{x}$ are the arithmetic averages of the set with x_n excluded and x_n included, respectively, and n is the initial number of points. Basically, the criterion of equation (44a) is the comparison of the variances of the two sets--one with the suspect rejected and one with it included, see equation (44b)

$$\frac{S_n^2}{S^2} = \frac{\sigma_{n-1}^2}{\sigma_n^2} \left(\frac{n-2}{n-1}\right) \qquad (44b)$$

If the calculated statistic described was found to have $\leq$ 5% significance ($\geq$ 95% confidence that the point does not belong to the set) using the percentage points tables (92) it was rejected. An equation similar to (44a) was used for testing the smallest observation. Of a total of 446 points 29 were rejected by this scheme.

[illegible]

th

as

0.

65

di

sa

12.

ana

in

[illegible]

[illegible]

[illegible]

[illegible]

[illegible]

Tab

[illegible]

[illegible]

[illegible]

[illegible]

CHAPTER VI

RESULTS

6.1. Analysis on Samarium Dicarbide

From seven analyses on three different preparations the following mole percentages and uncertainties expressed as standard deviations were determined: samarium, 32.7 ± 0.6% (calc., 33.3%); bound carbon, 67.3 ± 0.6% (calc., 66.7%). The Galbraith Laboratories' analysis of samarium dicarbide accounted for 99.53% of the sample weight with samarium 86.81 weight % (theoretical 86.22%) and carbon 12.72 weight % (theoretical 13.78%). The weight percent analysis indicates that little oxygen contamination can be in the samples.

The lattice parameters calculated for two preparations are shown in Table II. They agree within experimental error with those reported by Spedding et al. (4) for samarium dicarbide: a_0 = 3.770 Å, c_0 = 6.331 Å. For preparation III 1 it may be seen that the lattice parameters of SmC_2 are the same before and after a vaporization experiment.

Table II. Lattice parameters for samarium dicarbide

Prep. No.	Film No.	$a_0 \pm \sigma$, (Å)	$c_0 \pm \sigma$, (Å)
I 57	A-1854II 4	3.776 ± 0.004	6.319 ± 0.008
III 1	A-1901III 3	3.767 ± 0.003	6.312 ± 0.014
III 1*	A-1933III 17	3.769 ± 0.002	6.318 ± 0.009

*After vaporization experiment.

6.2. Analysis on Neodymium(III) Monotelluro Oxide

From the mass increase data resulting from converting the sesquioxide to the monotelluro oxide, the purity of three preparations was calculated to be 99.6%, 98.3% and 100.3%. The interplanar d-spacings obtained from X-ray powder diffraction photographs agree with those reported in the literature (38).

6.3. Vaporization Mode of Samarium Dicarbide

The sublimation of samarium dicarbide was observed to occur according to equation (45) in the temperature range 1431-2058^{0}K

$$SmC_2(s) \longrightarrow Sm(g) + 2C(gr) \qquad (45)^*$$

Neither $SmC_2(g)$ nor SmC (g) species was observed in the vapor above the dicarbide samples studied in the mass spectrometer. In each vaporization experiment the mass region 154-250 amu was examined occasionally and no peaks other than background were noticed. A vaporization experiment was performed at a low ionization energy of 10.0 volts and the same vapor species were observed. That samarium was the vapor species observed was confirmed by its isotopic abundance distribution and by its ionization potential.

---

*That carbon is in the graphite allotrope is based on the fact that heating amorphous carbon at high temperatures (> 1500^0) in vacuo causes it to convert to the graphite form and also on the fact that in the X-ray powder diffraction photograph of the residue obtained from vaporization of SmC_2 strong lines attributable to graphite were present.

Typical spectra for the samarium isotopes obtained from samarium dicarbide and those from samarium metal are presented in Figure 4.

6.4. Vaporization Mode of Neodymium(III) Monotelluro Oxide

The ions observed in the mass spectrum for the vaporization of Nd_2O_2Te were Nd^+, NdO^+, Te^+ and O^+ and these (excluding O^+) are shown in Figure 5. These ions were identified in the manner described previously except for O^+ whose low intensity prevented measuring its ionization potential. That O^+ was originating from the effusion cell was shown by its disappearance from the spectrum upon tilting the molecular beam out of the path of the ionizing electron beam. The four vapor species observed in the spectrum cannot be described by a single equilibrium process. (Cf. Section 7.2).

The temperature for which the O^+ was determined to be coming from the cell was about 2300^0K. It was also observed that the ratio of p_{NdO}/p_{Nd} increased with temperature and from a plot of $[(IT)_{NdO}/(IT)_{Nd}]$ vs $1/T$ (using experiments III 61 and III 46) the inversion of the ratio at unity occurred at about 2160^0K.

6.5. Transmission Coefficient of the Effusion Cell

Attempts to measure the channel thickness of the Knudsen cell's orifice indicated the depth to be immeasurably thin, i.e., the orifice was knife-edged within the limits of detection. Furthermore, since it was impossible to focus

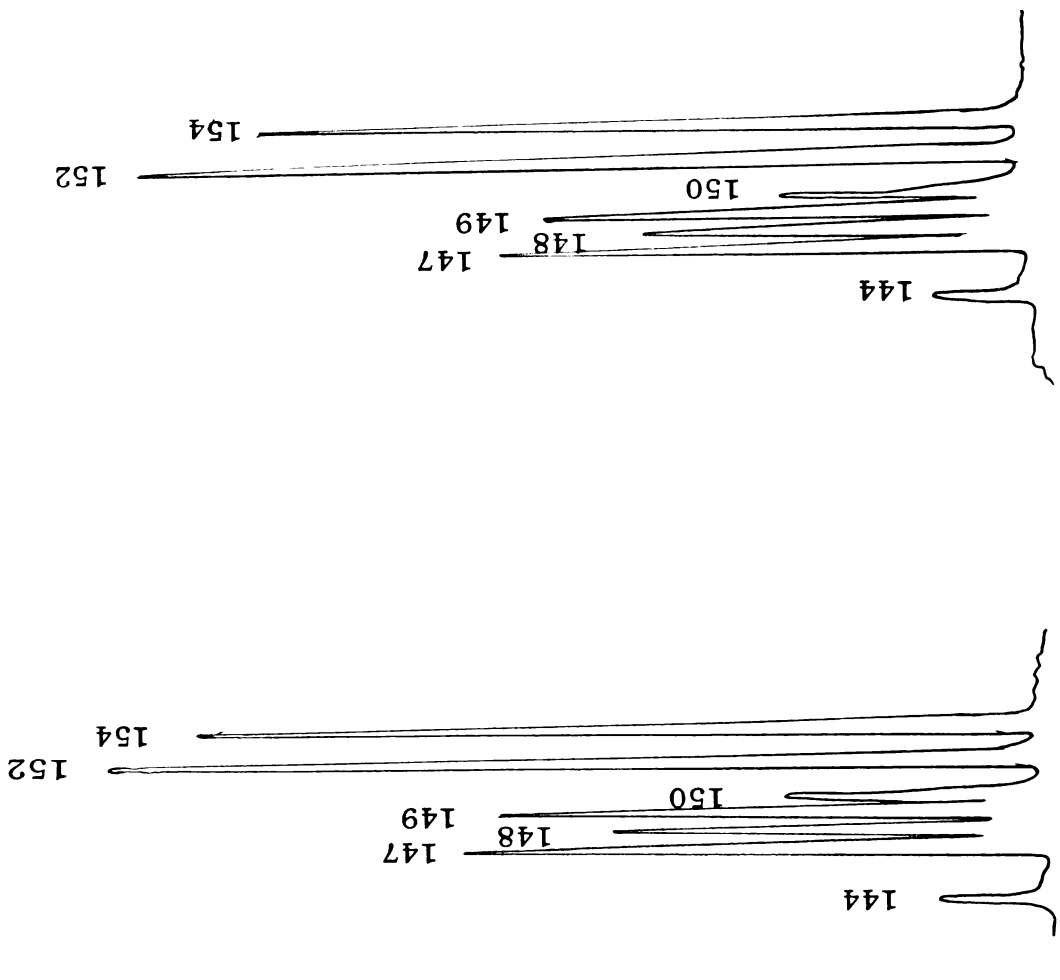

Figure 4. Mass spectrum of Sm^+.

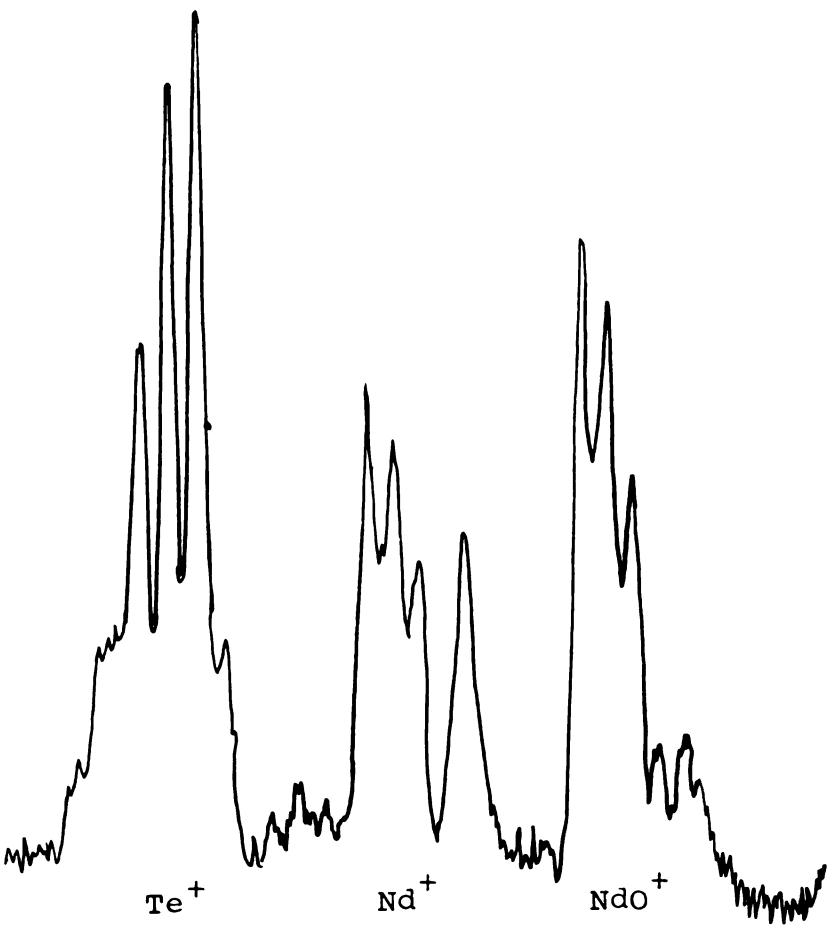

Figure 5. Ions from neodymium(III) monotelluro oxide vaporization.

the microscope on the entire channel "width" and since changing the focus continuously moved the field of vision along portions of the channel it was concluded that the orifice "channel" was really a conical section and that no perceptible cylindrical channel was present. Clay impressions taken along the cross-section of the orifice channel also indicated no perceptible width. Therefore, a value of unity was used for the transmissivity correction (Clausing factor) in the Knudsen equation of pressure, e.g., the weight-loss calibration procedure.

It should be mentioned that the effusion cells were not machined with the specific purpose of attaining knife-edges, but that they resulted from the machining procedure (described in Section 5.6.1). Cells with finite, measurable channel depths are suitable for absolute pressure measurements since corrections for this type of geometry are very accurately known quantities.

6.6. Calibration of the Spectrometer for Absolute Pressure

Values of the proportionality constant between the partial pressure and the ion current-temperature product for the various samarium isotopes, as well as the method employed to obtain each value, are listed in Table III. Equation (18) may be obtained in the form

$$\log P = \log k + \log IT + \log 760 \qquad (44)$$

where the reference state for P and k are torr and atm, respectively. A graph of equation (44) for the calibration

Table III. Proportionality Constant of $P = kIT$.

Vaporization Expt.	Isotope	Calibrating Expt.	Type of Calibration	-ln k
II 27	147	II 27	Ag integration method	12.67
II 27	152	II 27	Ag integration method	12.67
II 27	154	II 27	Ag integration method	12.67
II 41, II 43	147	II 62	Sm vapor pressure	12.33
II 41, II 43	149	II 62	Sm vapor pressure	12.42
II 41, II 43	152	II 62, II 63	Sm v.p. and Sm integr.	12.86
II 41, II 43	154	II 62, II 63	Sm v.p. and Sm integr.	1276
III 63	2-4	IV 3	SmC_2 Knudsen vap.	15.56
III 701	2-4	IV 3	SmC_2 Knudsen vap.	15.21
III 701	2-4	IV 3	SmC_2 Knudsen vap.	15.04
III 702	2-4	IV 3	SmC_2 Knudsen vap.	14.30

experiment II 62 is shown in Figure 6. Inspection of this equation shows that at log P = 0 the value of k is obtained from the corresponding value of IT at this point.

6.7. Thermodynamics of Vaporization for Samarium Dicarbide

6.7.1. Enthalpy of Reaction

The results of the ten vaporization experiments of samarium dicarbide are listed in Tables IV and V. Individual data points for the experiments are presented in Appendices A and G. The value of ΔH^0_{298} was obtained using the assumption that the heat content of SmC_2 was equal to that of CaC_2 and that the two compounds have identical phase transition enthalpies and entropies in the tetragonal to cubic phase changes. The average value obtained for the Second Law ΔH^0_{298} for reaction (45) was 64.2 ± 2.1 kcal/gfw and the total number of experimental points was 417. The uncertainty in ΔH^0_{298} is the weighted average of $R\sigma_b$ (R is the gas constant, σ_b is the standard deviation in the slope of the least squares line) for the individual experiments as listed in Table V. A typical graph of the vapor pressure of samarium in equilibrium with SmC_2 is shown in Figure 7. A Σ-plot treatment of the data was not performed since no curvature was evident in the Clausius-Clapeyron graph of the vapor pressure and the absence of curvature in the temperature range 1561-2030°K may be seen from Figure 7.

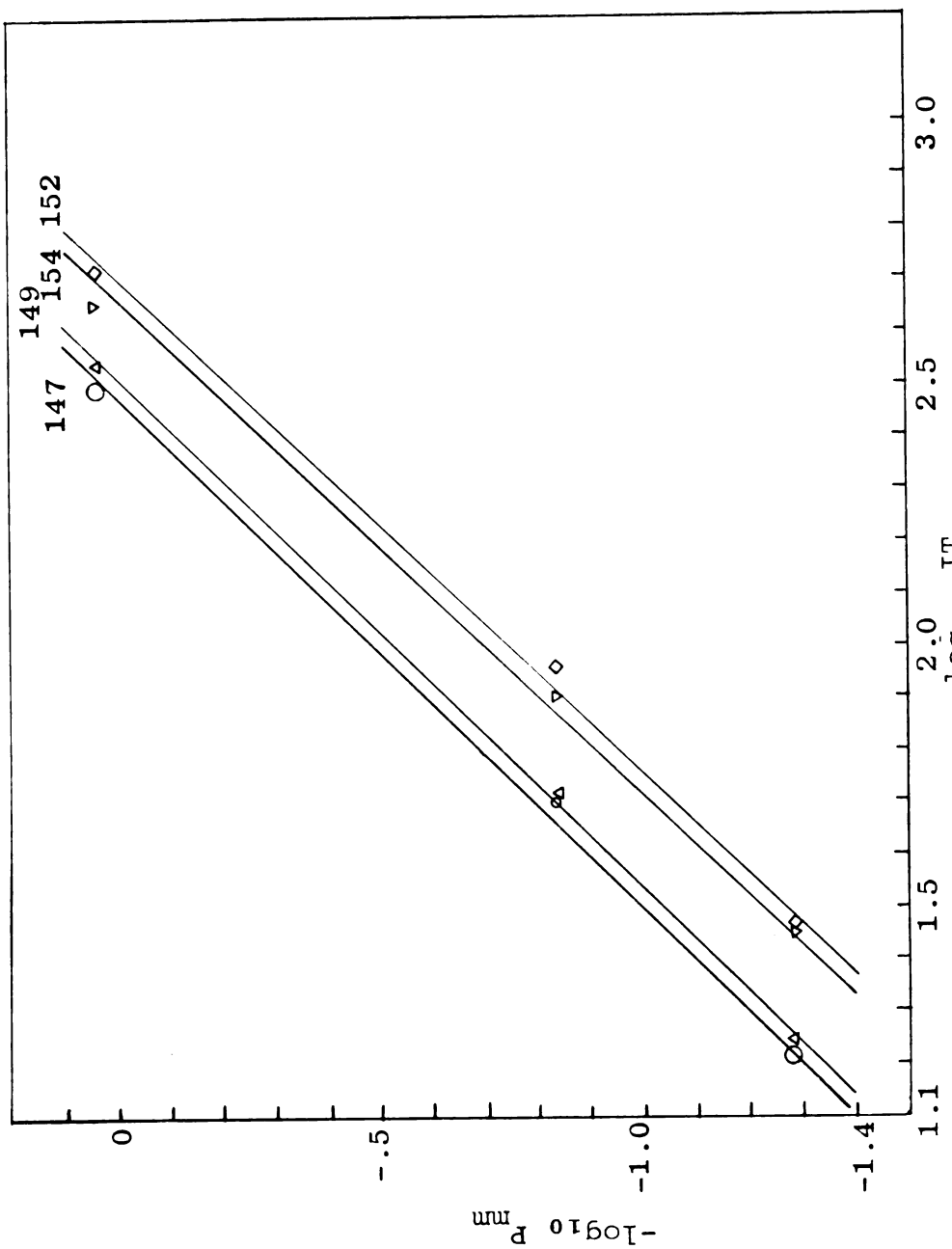

Figure 6. Samarium calibration experiment II62.

Table IV. Vaporization data for samarium dicarbide

Exp. No.	Sm Isotope	ΔH^0_T (kcal/gfw)	$R\sigma_b$ (kcal/gfw)	No. of Pts	a	σ_a	Range ^0K	Md Pt Temp, ^0K	Type Cell
II27	147	55.8	2.4	14	20.11	0.67	1563-	1830	Mo-C
	152	58.7	2.5	15	21.03	0.71	2043		
	154	56.8	3.2	15	20.62	0.89			
II34	147	58.3	1.1	21	21.32	0.29	1561-	1796	Mo-C
	149	62.2	1.7	22	22.15	0.47	2030		
	152	57.9	1.1	22	20.73	0.30			
	154	58.6	1.1	22	21.01	0.30			
II41	147	56.8	1.8	15	19.51	0.48	1673-	1871	Mo-C
	149	59.4	2.3	14	20.48	0.62	2058		
	152	57.4	2.5	17	19.54	0.67			
	154	56.9	2.2	17	19.53	0.61			
II43	147	60.2	1.2	23	19.67	0.34	1653-	1839	Mo-C
	149	59.0	1.6	20	19.69	0.43	2024		
	152	58.7	1.2	23	19.08	0.34			
	154	57.6	1.0	23	19.16	0.27			
III06	147	60.5	3.1	10	21.25	0.85	1627-	1810	Mo-C
	148	61.6	3.0	10	21.56	0.82	1992		
	149	59.3	2.8	10	20.93	0.75			
	150	60.1	3.2	9	21.10	0.85			
	152	59.5	3.1	10	20.96	0.85			
	154	59.1	3.1	10	20.83	0.82			

Table IV. (Cont.)

Exp. No.	Sm Isotope	ΔH_T^0 (kcal/gfw)	$R\sigma_b$ (kcal/gfw)	No. of Pts	a	σ_a	Range ^0K	Md Pt Temp, ^0K	Type Cell
III16	152	59.6	3.0	16	18.29	0.81	1685-1911	1798	Mo-C
	154	56.4	2.9	15	18.85	0.80			
III63	WGP	57.0	4.1	10	21.71	1.24	1431-1860	1646	W
III701	WGP	55.5	1.7	11	20.92	0.51	1542-1784	1663	W
III702	WGP	59.7	2.3	10	22.00	0.70	1531-1735	1633	W
III703	WGP	61.1	4.1	13	21.69	1.25	1577-1741	1659	W

Notes:
1. R is gas constant.
2. a, σ_a, are the ordinate intercept and standard deviation of the intercept, respectively of the Clausius-Clapeyron least squares equation.
3. WGP means 360 nanosec gate pulse used to sum the ^{152}Sm and ^{154}Sm current intensities.

Table V. Summary of samarium dicarbide vaporization data

Expt.	Total Pts	ΔH_T^0 (kcal/gfw)	$R\sigma_b$ (kcal/gfw)	ΔS_T^0 eu	$R\sigma_a$ eu	$\Delta H_{298}^0(45)$ (kcal/gfw)	$\Delta S_{298}^0(45)$ eu
II27	44	56.9	2.7	15.7*	1.5	60.8	24.0*
II34	87	59.3	1.2	--	-	63.1	--
II41	63	57.6	2.2	14.3	1.2	61.6	22.6
II43	89	58.9	1.2	13.5	0.7	62.8	21.9
III06	59	60.0	3.0	--	-	63.9	--
III16	31	58.0	2.9	--	-	61.8	--
III63	10	57.0	4.1	12.2	1.2	60.6	20.4
III701	11	55.5	1.7	11.4	0.5	58.9	19.5
III702	10	59.7	2.3	13.8	0.7	63.3	22.0
III703	13	61.1	4.1	14.7	1.2	64.7	22.8

Notes:

1. * Included for comparison; not used to obtain average $\Delta S_{298}^0(45)$.
2. R is the gas constant.
3. a, σ_a, σ_b are the ordinate intercept, standard deviations of the intercept and slope, respectively, of the Clausius-Clapeyron least squares equation.

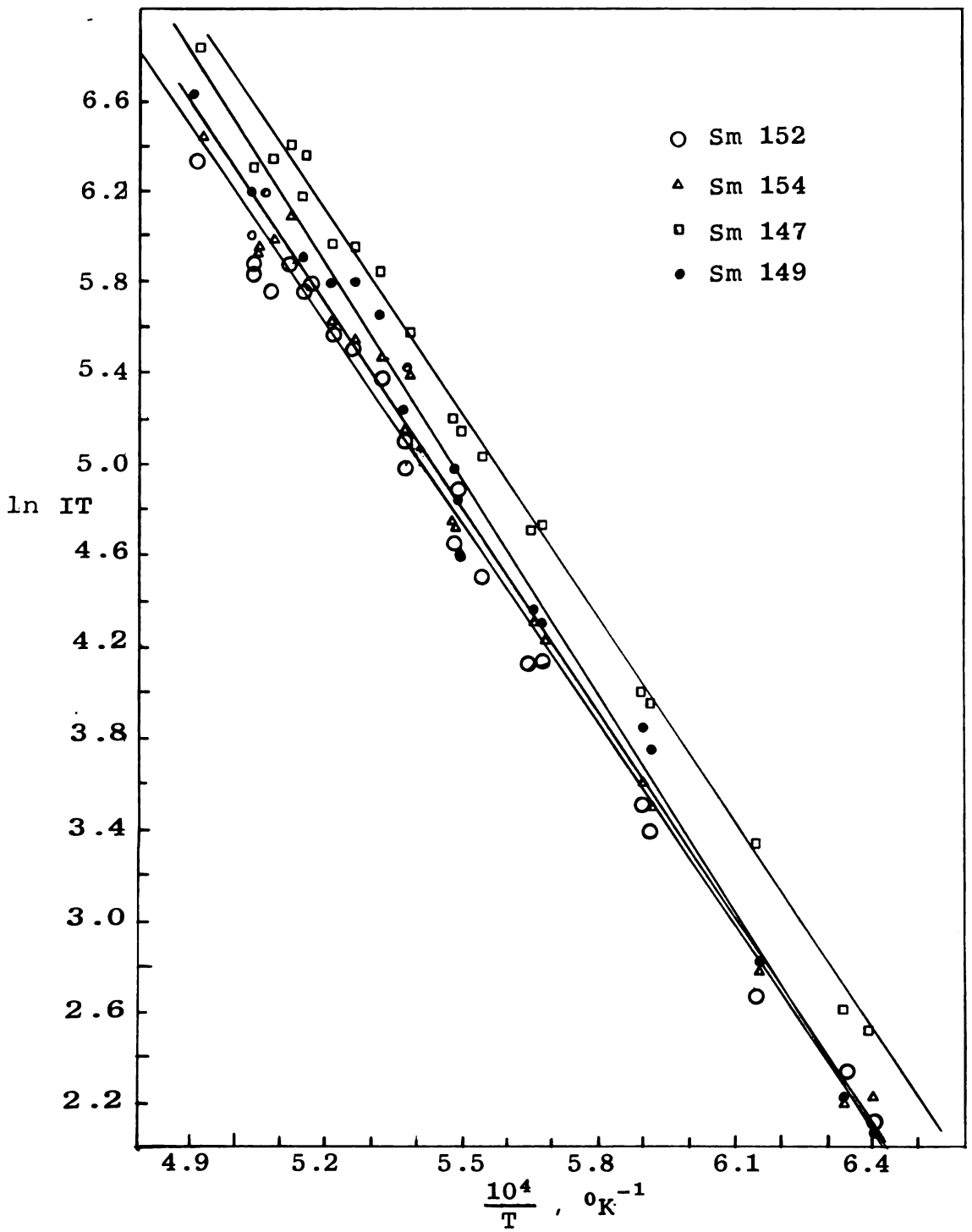

Figure 7. Vapor pressure of Sm^+ from samarium dicarbide Experiment II34.

Calculation of ΔH^0_{298} for reaction (45) using the Third Law method resulted in a value of 66.9 ± 1.7 kcal/gfw, where the uncertainty is the standard deviation among the values. A compilation of the values used to calculate the Third Law ΔH^0_{298} is presented in Appendix A. Values of Δfef were interpolated from Table VI; Figure 8 illustrates Δfef vs T.

6.7.2. Entropy of Reaction

Treatment of the data obtained from six vaporization experiments resulted in a value of ΔS^0_{298} of 22.1 ± 2.3 cal/deg-gfw for reaction (45). The method employed to obtain the expressed uncertainty associated with ΔS^0_{298} will be explained fully since it was not straightforward. The major source of error is in k, the calibration constant and a minor contribution is the error in the literature data used to reduce ΔS^0_T to the 298° standard state. The following logic was used to obtain an estimate of the uncertainty in k. To the ln P vs $\frac{1}{T}$ data (Appendix A), which are shown in Figure 8a, was assigned the identical value of the slope as obtained from the Second Law analysis. From the known value of the slope a value of the standard deviation of the intercept of the absolute pressure data was calculated using the variation equations of Youden (98). The total error in ΔS^0_T using this procedure was found to be 1.8 eu and this value is the product of the gas constant and the standard deviation of the intercept. Additional errors arising from

Table VI. Free energy functions

	Values of -fef in cal/deg-unit shown						-Δfef for Eq(45) eu
T, °K	Sm(g)	2C(gr)	Sm(l)	Ca(l)	CaC_2(s)	SmC_2(s)	
1400	49.279	8.196	23.58	15.83	30.41	38.16	19.31
1500	49.676	8.696	24.29	16.35	31.42	39.36	19.01
1600	50.053	9.182	24.96	16.84	32.39	40.51	18.73
1700	50.409	9.654	25.60	17.30	33.30	41.60	18.47
1800	50.748	10.110	26.21	17.73	34.17	42.65	18.21
1900	51.070	10.552	26.79	18.13	35.00	43.66	17.96
2000	51.376	10.980	27.33	18.50	35.80	44.63	17.73
2100	51.669	11.396	27.86	18.84	36.53	45.55	17.52
Ref.	87	86	88,89	88,89	89,90	88,89,90	

Notes:

1. Equation (45): $SmC_2(s) \longrightarrow Sm(g) + 2C(gr)$

2. $fef(SmC_2(s)) = fef(CaC_2(s)) - fef(Ca(l)) + fef(Sm(l))$

Figure 8. Δfef for $SmC_2(s) \longrightarrow Sm(g) + 2C(gr)$

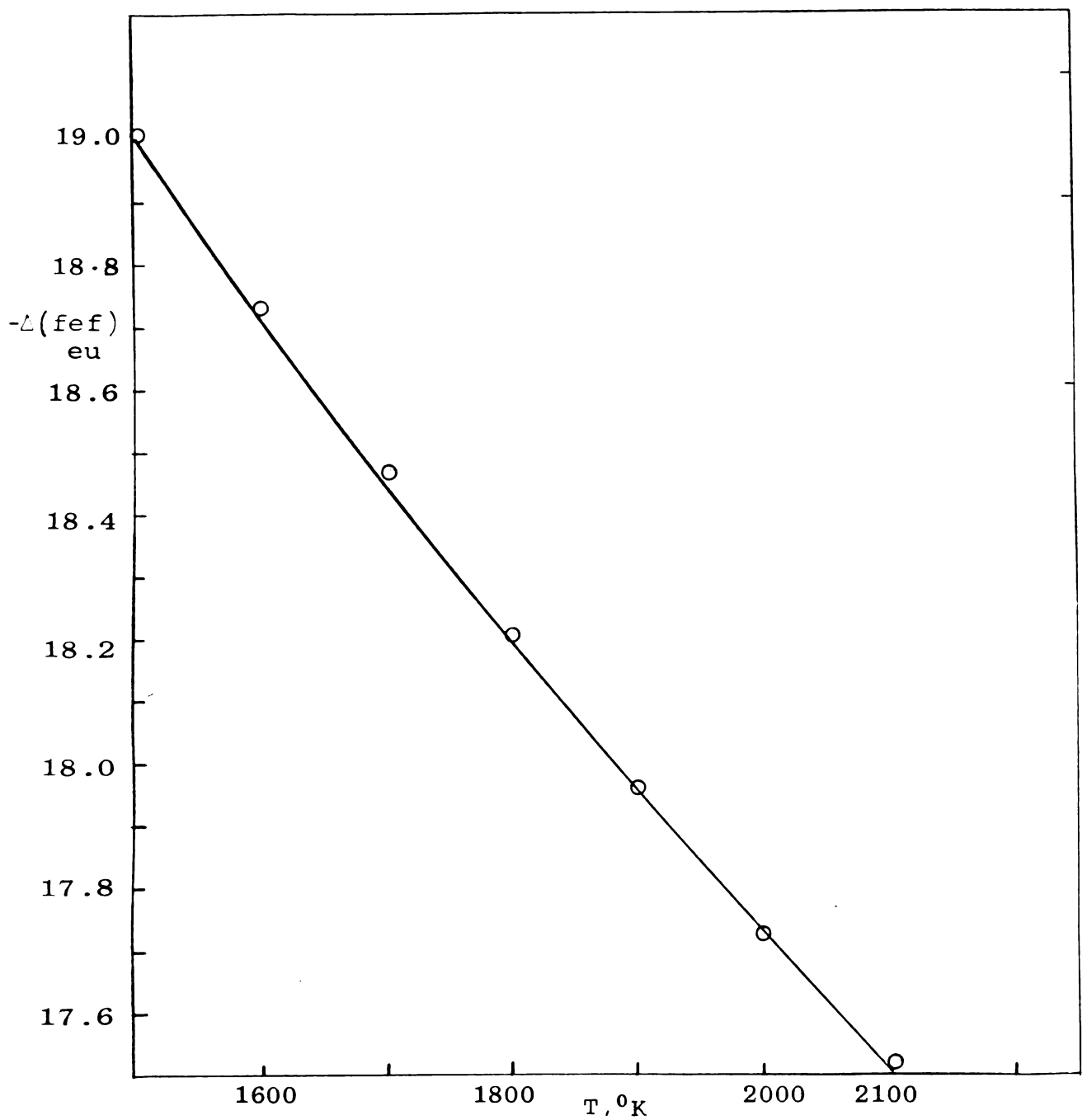

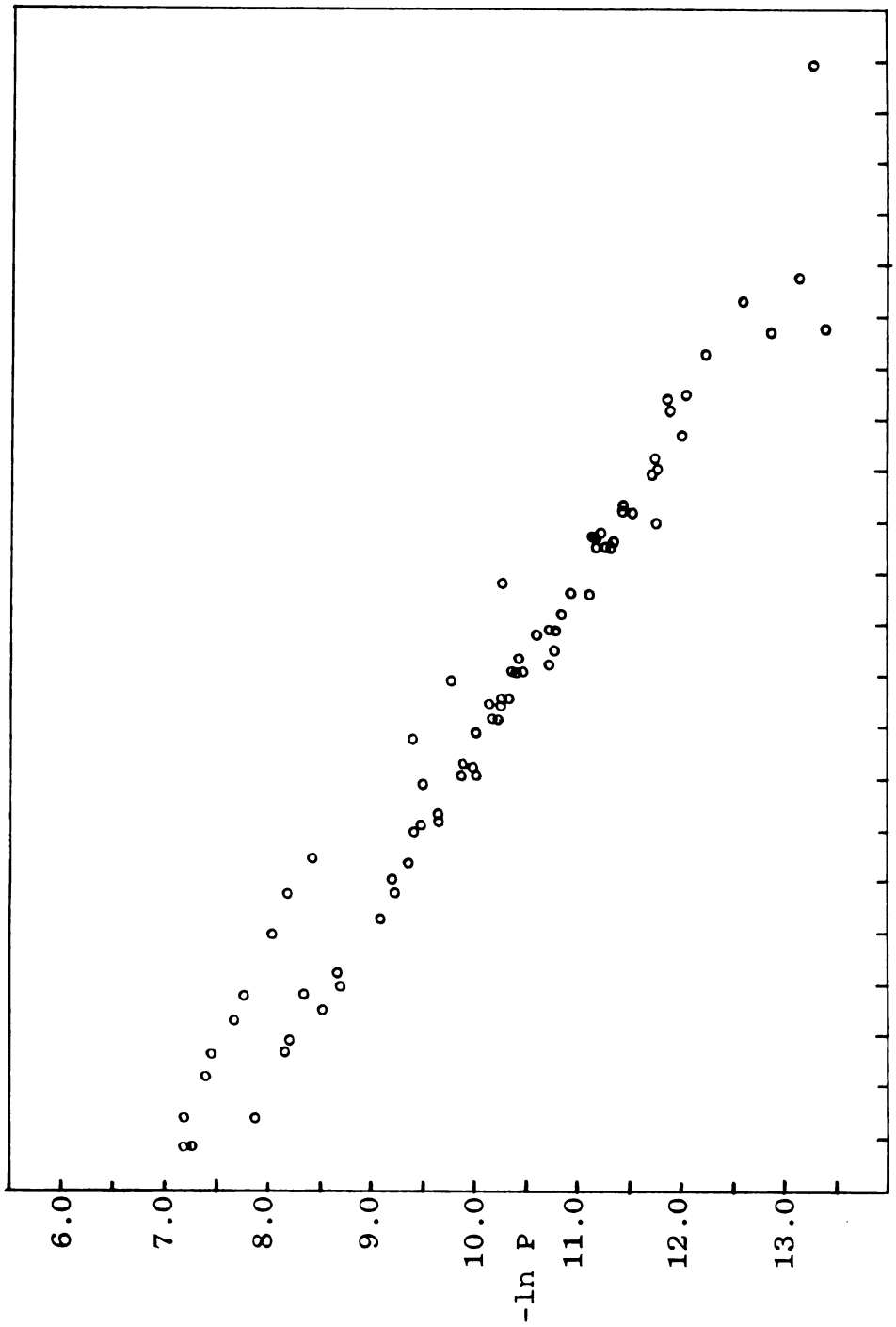

Figure 8a. Absolute P_{Sm} over $SmC_2(s)$.

using literature data to obtain ΔS^{o}_{298} were estimated to be 0.53 cal/deg/gfw (Cf. Section 8.2).

The least squares intercepts used in equation (20) to calculate, ΔS^{0}_{T} for the various experiments are compiled in Table IV (p. 76); the respective calibration constants are found in Table III (p. 73). The values of the entropy of reaction as obtained from the individual experiments are summarized in Table V on page 78.

6.7.3. Formation Energetics

The standard enthalpy and entropy of formation of $SmC_2(s)$ may be obtained by consideration of the reactions

$$SmC_2(s) \longrightarrow Sm(g) + 2C(gr) \qquad (45)$$

$$Sm(s) \longrightarrow Sm(g) \qquad (46)$$

It is apparent that subtraction of equation (45) from (46) gives

$$Sm(s) + 2C(gr) \longrightarrow SmC_2(s) \qquad (47)$$

for which the enthalpy of formation of $SmC_2(s)$ is obtained as

$$\Delta H^{0}_{298,f}(SmC_2(s)) = \Delta H^{0}_{298}(46) - \Delta H^{0}_{298}(45) \qquad (48)$$

Using the average value obtained from the Second and Third Law calculation for reaction (45) and $\Delta H^{0}_{298} = 51.03 \pm 0.24$ kcal/gfw for reaction (46) (from Habermann and Daane (76)) $\Delta H^{0}_{298,f}(SmC_2(s)) = -14.6 \pm 2.3$ kcal/gfw. Similarly the value of the entropy of formation may be obtained analogously using $\Delta S^{0}_{298}(46) = 27.1 \pm 0.5$ eu from Hulgren, et al. (88) as

$$\Delta S^{0}_{298,f}(SmC_2(s)) = 5.0 \pm 2.8 \text{ eu}.$$

6.7.4. Standard Entropy of SmC_2

The standard entropy of SmC_2 is found using the relation

$$\Delta S^0_{298}(45) = S^0_{298}(Sm(g)) + 2S^0_{298}(C(gr)) - S^0_{298}(SmC_2(s)) \quad (49)$$

which results in

$$S^0_{298}(SmC_2(s)) = 24.4 \pm 2.9 \text{ eu.}$$

Values for $S^0_{298}(C(gr))$ and $S^0_{298}(Sm(g))$ were taken from references (86) and (87) respectively.

6.7.5. The Vapor Pressure as a Function of Temperature

The equilibrium vapor pressure of samarium over SmC_2 as a function of temperature over the temperature region of 1431-2058^{0}K is

$$2.303R \log P_{Sm(atm)} = \frac{(-58,600 \pm 2100)}{T} + (13.7_0 \pm 1.8). \quad (50)$$

This equation was obtained by taking a weighted mean of the least squares values of ΔH^0_T and ΔS^0_T. Thus the values are obtained for reaction (45): $\Delta H^0_{1745} = 58.6 \pm 2.1$ kcal/gfw and $\Delta S^0_{1745} = 13.7 \pm 1.8$ eu. The errors expressed are the standard deviations.

6.8. Congruency of Vaporization of Nd_2O_2Te

Analysis of the residue remaining in the effusion cell after vaporization experiments indicates that Nd_2O_2Te vaporizes incongruently with a loss of Nd(g) and Te(g) and with a shift in composition toward that of Nd_2O_3. The results of a series of vaporizations from a molybdenum crucible are

shown in Table H-II of Appendix H. These effusion cells used for the congruency tests were considered free of occluded gases when their weight loss at constant temperature remained invariant. The tungsten cell was observed to be less reducing than the molybdenum cell since the X-ray powder diffraction photograph of the residue from a vaporization experiment in which 48% of the sample was vaporized (0.3142 g sample initially) showed only lines characteristic of Nd_2O_2Te. However, using the same cell and at the same temperature, a vaporization in which 72% of the sample (0.3198 g initially) was vaporized gave an X-ray pattern characteristic of Nd_2O_3.

6.9. Thermodynamics of Vaporization of Nd_2O_2Te

Reliable thermodynamic data on the vaporization of Nd_2O_2Te was thought to be obtainable if the extent of vaporization were kept sufficiently small such that the composition varied insignificantly from the stoichiometric value. With this viewpoint in mind three vaporization experiments were conducted in the mass spectrometer. The data are summarized in Table VII and the individual experimental data points are presented in Appendix I. These results indicated the species observed in the vaporization upon which quantitative calculations are based are the products of several simultaneous equilibria (Cf. Section 7.2).

Table VII. Vaporization of neodymium(III) monotelluro oxide in the mass spectrometer

Expt.	Species Monitored	ΔH_T^0, (kcal/ gfw)	$R\sigma_b$ (kcal/ gfw)	% Vapor-ized	Temp. Range ^0K	No. Pts.	Cell	MdPt T, ^0K
III 46	Nd-142	111.86	8.36	22	2021-2293	10	Mo	2157
III 46	Nd-144	107.60	9.30	22	2021-2293	10	Mo	2157
III 46	NdO-142	130.30	8.84	22	2021-2293	10	Mo	2157
III 46	NdO-144	133.96	8.73	22	2021-2293	10	Mo	2157
III 55	Nd-142,144	78.23	9.31	42	1902-2346	9	W	2124
III 55	NdO-142,144	106.69	8.04	42	1902-2346	9	W	2124
III 55	Te-128,130	103.78	13.84	42	1902-2346	9	W	2124
III 61	Nd-142	83.24	22.96	23	2084-2318	7	W	2201
III 61	Nd-144	89.85	24.37	23	2084-2318	7	W	2201
III 61	NdO-142	106.89	13.35	23	2084-2318	7	W	2201
III 61	NdO-144	113.46	13.38	23	2084-2318	7	W	2201

6.10. Appearance Potentials

The results of the ionization efficiency measurements are presented in Table VIII. Figures 9 and 10 illustrate the shape of these curves. Comparison of both the literature and the corrected appearance potentials of the ion species indicates that all the species vaporizing from Nd_2O_2Te (except for O^+ whose appearance potential was not measured) to be primary species.

6.11. Sensitivity of the Spectrometer with Relative Abundance

During the course of this work a comparison was made of the set of proportionality constants, k, obtained from two different calibration experiments. The parameter k is defined by equation (18) and characterized by equation (34) (cf. Sections 3.2.1 and 3.4.2). The term k is the proportionality constant between the total samarium vapor pressure and the IT product where I is the normalized ion current i.e., it is the ion current (corrected for background) of a specific isotopic species divided by the isotopic abundance of the species. Figure 11 illustrates the results obtained. It is apparent that for each curve k decreases with increasing isotopic abundance of a samarium species. Assuming that ionization cross-sections vary negligibly between the samarium isotopes, the mass spectrometer efficiency is seen to be higher for the more abundant isotopes.

VIII. Appearance potentials of ions from the vaporization of SmC_2 and Nd_2O_2Te

t.	Species	Literature Value(s), eV	Observed eV	Corrected value eV
64	Xe^+	12.12(91), 12.08(94)	10.9	Standard(+1.2)
	Nd^+	5.51(91), 6.3(94)	4.7	5.9
	NdO^+	5.7(41)	3.9	5.1
	Te^+	9.01(91), 8.96(94)	10.0	11.2
II 66	Xe^+	Cf. above	13.4	Standard(-1.3)
	Nd^+	Cf. above	7.1	5.8
	NdO^+	Cf. above	6.8	5.5
	N_2^+	14.53(91), 15.51(94)	17.1	15.8
	H_2O^+	12.59(91), 12.56(94)	14.9	13.6
III 18-1	N_2^+	Cf. above	16.6	Standard(-1.1)
	Xe^+	Cf. above	11.6	10.6
III 18-2	N_2^+	Cf. above	10.2	Standard(+4.3)
	Sm^+	Cf. above	2.3	6.5

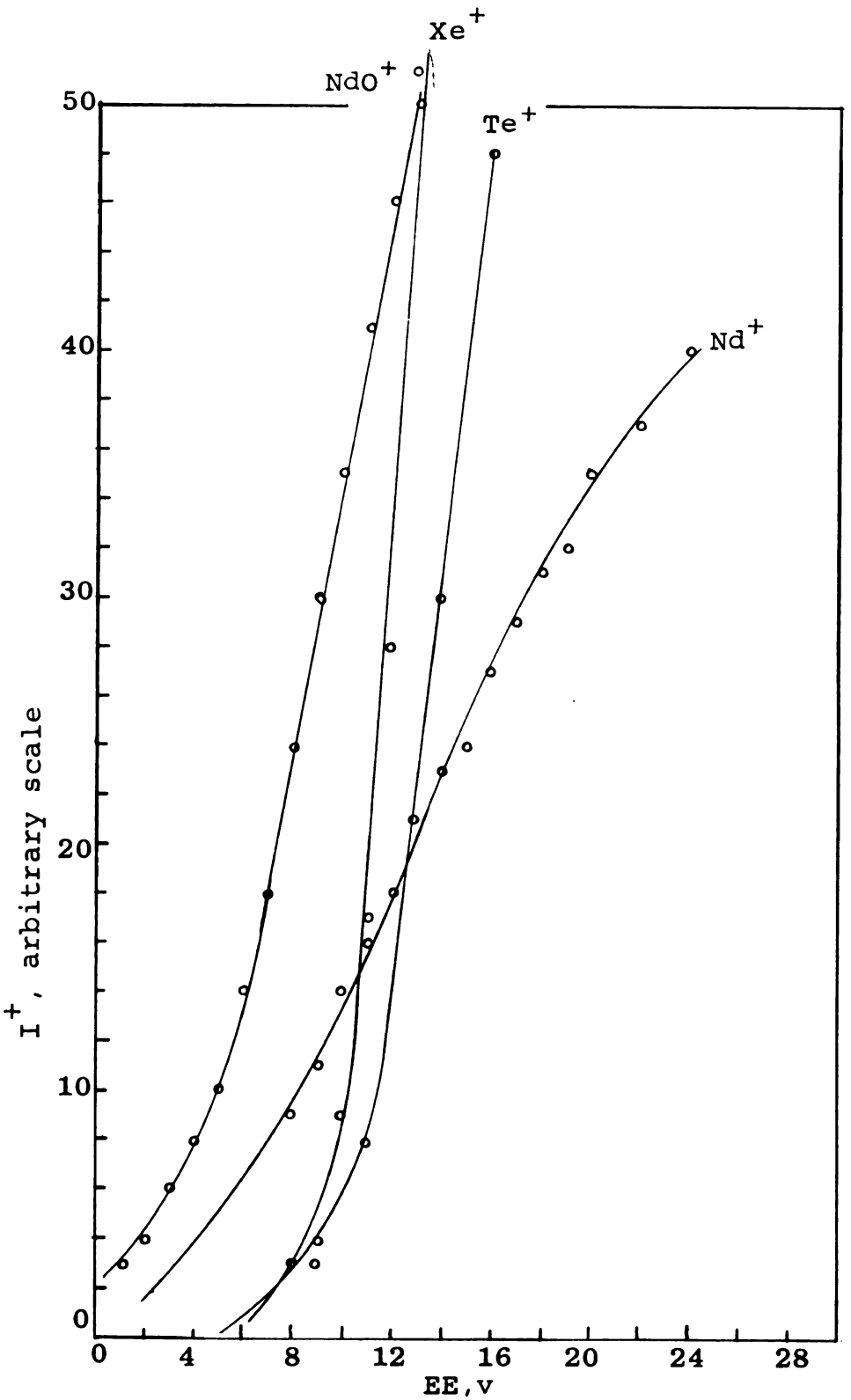

Figure 9. Ionization efficiency curves for Xe^+, Nd^+, NdO^+ and Te^+.

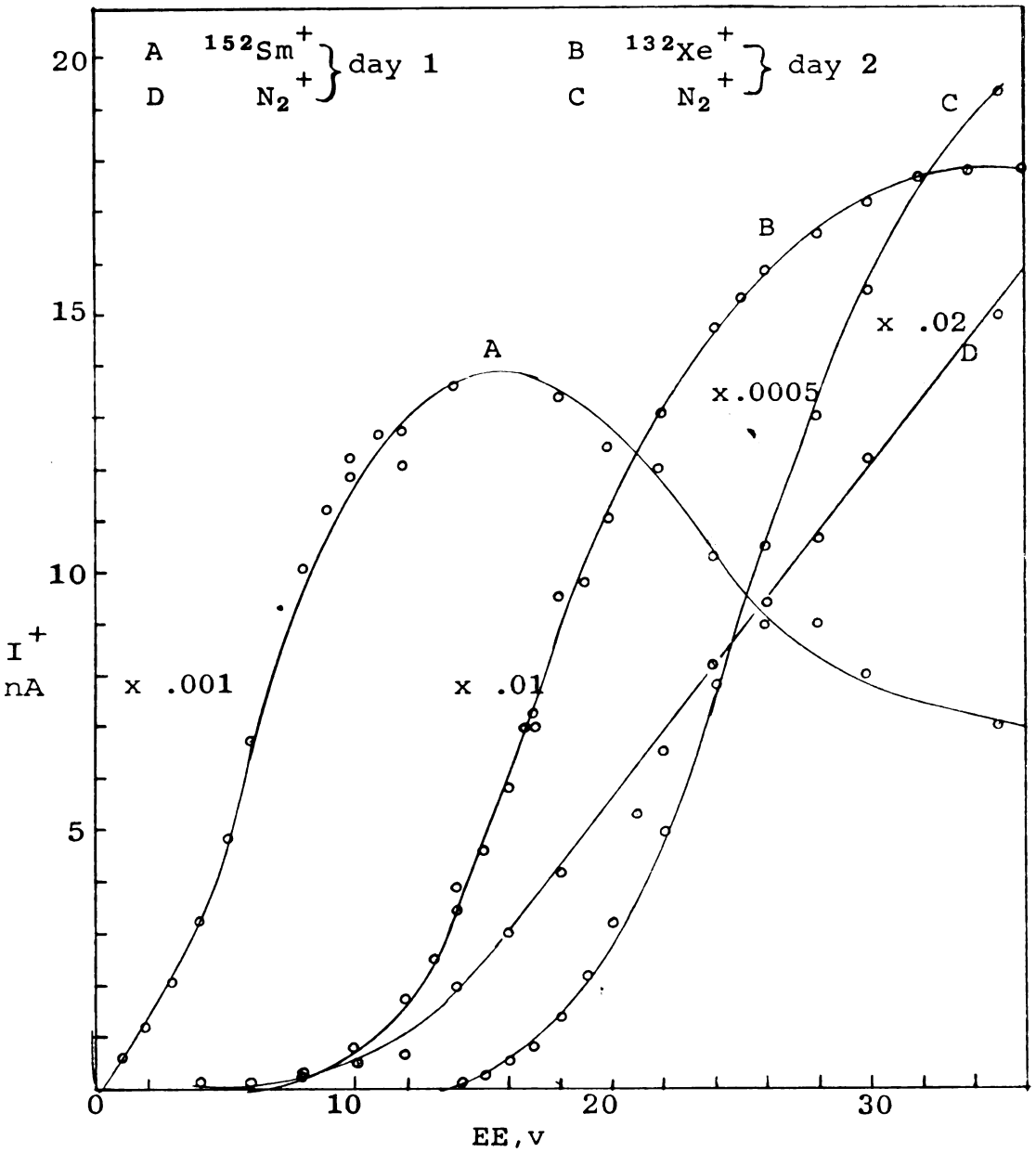

Figure 10. Ionization efficiency curves for Xe^+, N_2^+, and Sm^+.

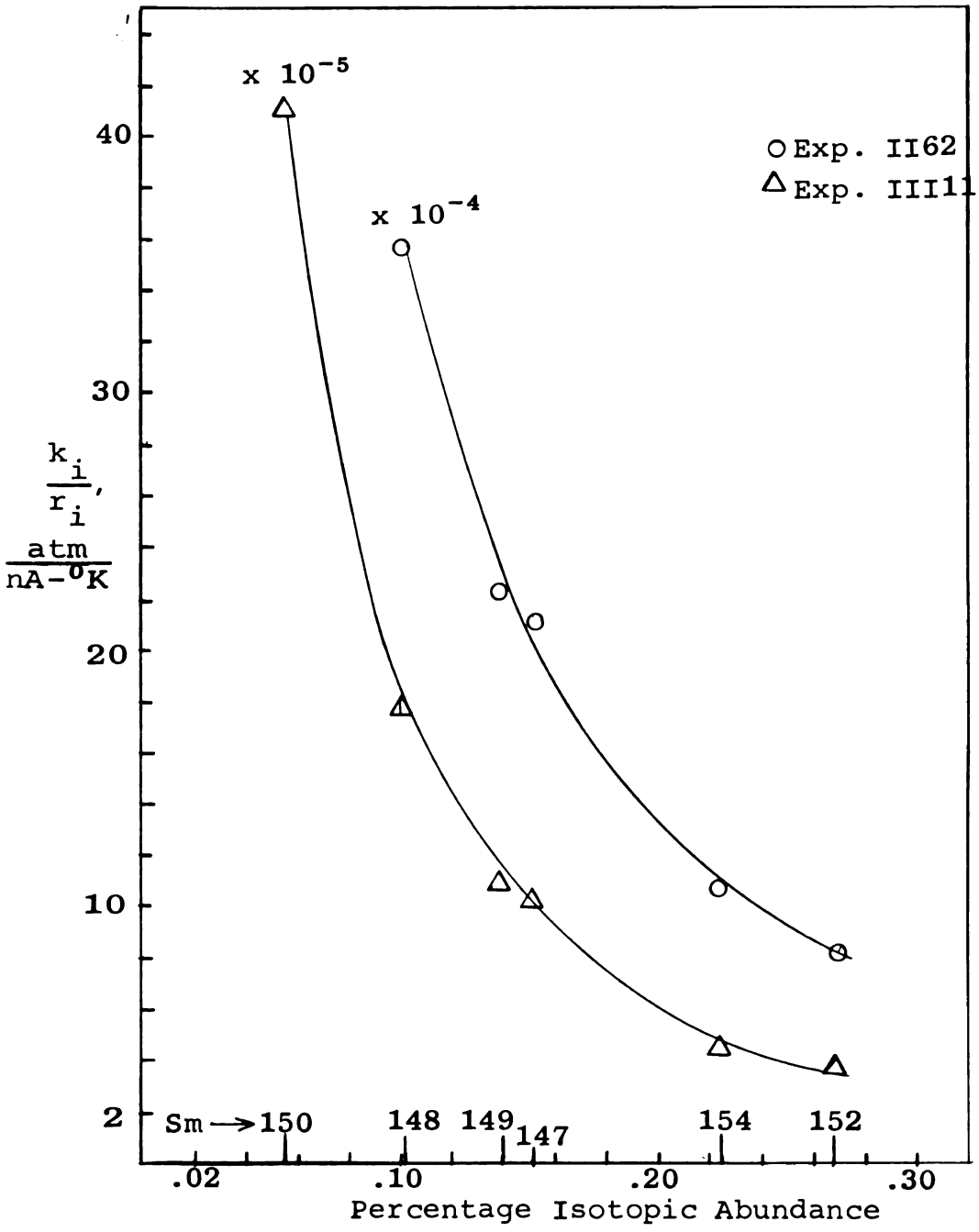

Figure 11. Sensitivity of the multiplier-effects of abundance and machine parameters.

6.12. Free Energy Function of Reaction for Samarium Dicarbide

Utilization of equation (27) implies that the Δfef for the vaporization reaction of samarium dicarbide is known. Unfortunately, the high temperature heat capacity of samarium dicarbide has not been measured. Since samarium dicarbide has been shown to be alkaline earth in its behavior with respect to the oxidation state of samarium in the compound (6) and also similar in its hydrolysis products (10), CaC_2 was used as a basis for comparison in order to obtain an estimate of the fef of samarium dicarbide. This value of fef was obtained as

$$fef(SmC_2(s)) = fef\ (CaC_2(s)) - fef(Ca(l)) + fef(Sm(l)). \quad (51)$$

The values of fef(Ca(l)) and fef(Sm(l)) were chosen to correct the effect of substitution of a samarium atom for a calcium atom in the lattice of calcium dicarbide instead of fef(Ca(s)) and fef(Sm(s)), respectively because at the temperatures employed for the vaporization of samarium dicarbide the values of the fef of both samarium and calcium had to be obtained by extrapolation since neither metal exists as a solid in this range of temperature. It was estimated that the extrapolation error introduced in the fef of either metal was less if extrapolation were made from the liquid state, rather than the solid state, to the temperature needed. Since samarium dicarbide was found to vaporize as (Cf. Section 6.3)

$$SmC_2(s) \longrightarrow Sm(g) + 2C(gr) \qquad (45)$$

then for this reaction

$$\Delta fef = fef(Sm(g)) + 2fef(C(gr)) - fef(SmC_2(s)) \qquad (52)$$

The sources of fef for the substances in this section are found referenced in Table VI.

CHAPTER VII

DISCUSSION

7.1. Comparison of Samarium Dicarbide with other Lanthanon Dicarbides

To the present date seven lanthanon dicarbides have been studied and characterized from a thermodynamic viewpoint. The thermodynamics of vaporization of three alkaline earth dicarbides and of yttrium dicarbide have also been determined. These properties are presented in Table IX, and compared to the thermal properties and vapor pressure of the corresponding metal. Certain explanations on the structure of Table IX are necessary. The choice of $1500^{0}K$ for the temperature at which to tabulate the metal vapor pressures was made since at a higher temperature the vapor pressure of ytterbium rises exceedingly high while at a lower temperature than $1500^{0}K$ the metal vapor pressure of lanthanum becomes extremely small. All thermodynamic quantities listed were reduced to values at the standard temperature at $298^{0}K$ whenever the values found in the reference literature were not given at this temperature. This reduction of data to $298^{0}K$ necessitated using the heat capacity change for the calcium dicarbide vaporization reaction (Cf. Equation (24)) since the heat capacity data of none of the compounds in Table IX has been measured.

Table IX. Thermodynamic comparison of the dicarbides

	Metal				Metal Dicarbide				
Species	$-\log P_{1500}$ (P, atm.)	$\Delta H^0_{298,v}$ (kcal/ g-at)	$\Delta S^0_{296,v}$ (e.u.)	S^0_{298} (e.u.)	$\Delta H^0_{298,v}$ (kcal/ gfw)	$\Delta S^0_{298,v}$ (e.u.)	$-\Delta H^0_{298,f}$ (kcal/ gfw)	$\Delta S^0_{298,f}$ (e.u.)	S^0_{298} (e.u.)
La	8.684[a]	104.06[a]	29.96[b]	13.6[b]	136.0[k]	--	28.2[k]	--	--
Y	7.834[b]	101.52[a,*]	32.24[b]	10.63[b]	125.0[i]	--	27.0[i]	--	13.7[i]
Ho	7.76[g]	98.05[h]	29.12[h]	18.0[b]	117.9[t,h]	21.4[t,h]	19.8[t]	7.8[t]	28.5[m]
Gd	7.430[a]	95.99[a]	30.06[b]	15.77[a]	106.7[j]	--	10.8[j,a]	--	--
Nd	5.658[a]	81.51[a]	28.29[b]	16.95[b]	76.2[l]	--	-5.3[l,a]	--	--
Sm	1.289[a]	48.59[a,*]	27.11[b]	16.61[b]	64.2[n]	22.1[n]	14.6[n]	5.0[n]	24.4[n]
Ba	.935[b]	41.74[c]	24.7[b]	16.0[b]	61.2[q]	22.4[q]	19.5[q]	2.3[q,b]	21.0[q,b]
Ca	.777[b]	42.37[b,*]	27.04[b]	9.95[b]	54.3[r]	22.9[s]	13.5[r]	4.1[s]	16.8[s]
Eu	.708[d]	42.07[d]	25.79[e]	19.31[a]	55.8[p]	27.1[p]	13.8[p,d]	-1.3[p,e]	20.6[u,a]
Sr	.345[b]	39.30[b,*]	26.8[b]	12.5[b]	59.3[q]	25.1[q]	20.2[q]	1.7[q,b]	17.0[q]
Yb	-.284[a]	36.22[a]	27.04[b]	14.31[a]	56.1[o]	27.1[o]	18.0[o]	-0.1[o,f]	17.0[o]

Notes and References:

1) Metal vaporization reaction: $M(s) \longrightarrow M(g)$.

2) Dicarbide vaporization mode: $MC_2(s) \longrightarrow M(g) + 2C(gr)$.

Table IX. (Cont.)

3) All reductions of thermal data to the standard state for the dicarbides were accomplished using equation (24). When no thermal data were available for a dicarbide those of the CaC_2 vaporization were used with data for CaC_2(s), Ca(g) and C(gr) taken from references (89), (89) and (86), respectively.

4) When necessary, graphical extrapolations of the reference data were made to obtain thermal data at higher temperatures.

*Value based on Third Law calculation; otherwise Second Law value used.

[a]Habermann and Daane (76).

[b]Hultgren, et al. (88)

[c]Stull and Sinke (97)

[d]Spedding, et al. (99)

[e]S^0_{298} (Eu(g)) from ref. (88) and S^0_{298} (Eu(s)) from ref. (76).

[f]Obtained analogously as in e.

[g]Calculated from the least squares line of Figure 2 from ref. (76).

[h]Data for Ho(s), Ho(g) from Kelley (89), and Feber and Herrick (87), respectively.

[i]De Maria, et al. (27).

[j]Jackson, et al. (26).

[l]$\Delta H^0_{2050,v}$ calculated from the vapor pressure equation of De Maria (29).

[m]S^0_{298} of Ho(s), C(gr) from ref. (88), (87), respectively.

Table IX. (Cont.)

[n] Present work.

[o] Eick, et al. (100).

[p] Gebelt (22).

[q] Flowers and Rauh (31).

[r] Faircloth, et al. (32).

[s] S^0_{298} of CaC_2, Ca, C from Kelley and King (90), and references (88), (86), respectively.

[t] Wakefield, et al. (25).

[u] Calculated from reference (22) using the empirical formula of $EuC_{1.87}$.

It may be seen from an inspection of Table IX that there is a correlation between the vapor pressure of the metal and $\Delta H^0_{298,v}$ of the corresponding dicarbide--the $\Delta H^0_{298,v}$ of the dicarbide is inversely related to the volatility of the corresponding metal. This is consistent to the conclusion drawn by Wakefield and Daane (25) in which they state that the more volatile elements have the less stable lanthanon dicarbides. Figure 12 presents this trend of $\Delta H^0_{298,v}$ of the dicarbides with metal vapor pressure. The dicarbides seem to be congregate into either of two groups on the graph. The group at the lower left portion of the graph is composed of the dicarbides in which the metals are either known to be in the +2 oxidation state or in which they have a strong tendency to be divalent. The remaining group is composed of metal dicarbides in which the metals exhibit the +3 oxidation state. These two groups of dicarbides also are differentiated by mode of vaporization. Whereas the dicarbides of the predominantly +2 metals vaporize giving the gaseous metal and solid carbon the +3 lanthanon dicarbides vaporize not only in this mode but also vaporize congruently, giving gaseous metal dicarbide molecules, at higher temperatures.

The fact that samarium dicarbide falls in the group of +2 metal dicarbides (in its relation of the samarium vapor pressure and $\Delta H^0_{298,v}$ of the dicarbide) confirms Vikery's conclusion that samarium is in the +2 oxidation state in the dicarbide (6) and is not in the +3 oxidation state as proposed by Jensen and Hoffman (14). This a posteriori

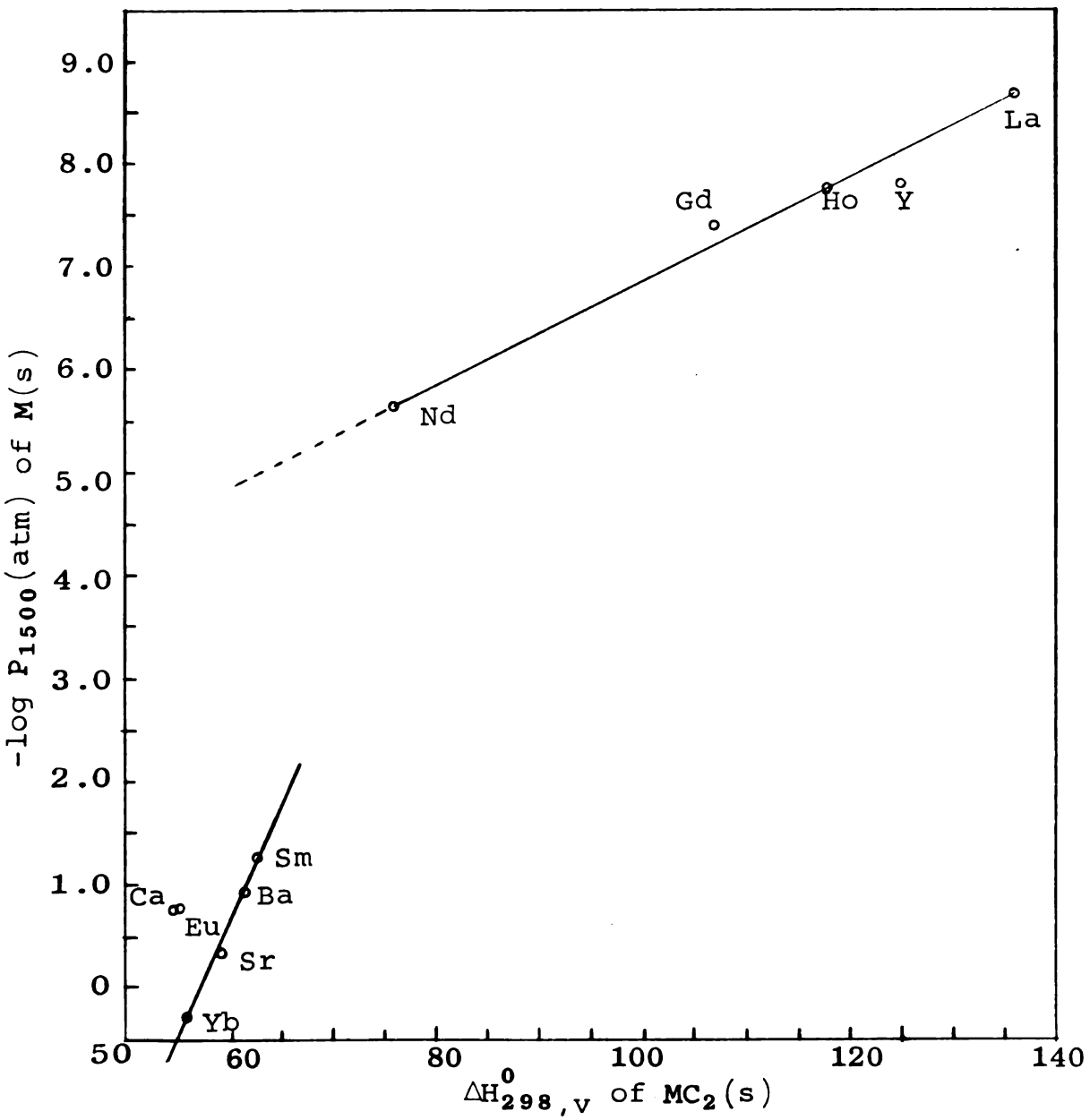

Figure 12. Correlation of $\Delta H^0_{298,V}(MC_2)$ with log $P_{1500}(M)$.

conclusion shows further that the heat capacity of calcium dicarbide may be used as an approximation for the unknown heat capacity of samarium dicarbide in order to obtain thermodynamic data at the standard reference temperature ($298^{0}K$ in this work) from data at temperature.

Using Figure 12 several predictions should be possible on the values of $\Delta H^{0}_{298,v}$ for the lanthanon dicarbides which have not yet been thermodynamically studied. Using the values of the metal vapor pressures the predicted values of $\Delta H^{0}_{298,v}$ for the lanthanon dicarbides whose thermodynamic properties have not been characterized are given in Table X.

Table X. Predicted values of $\Delta H^{0}_{298,v}$ for $MC_2(s)$

Metal	$-\log P_{1500}(M)$ (P, atm)	$\Delta H^{0}_{298,v}(MC_2)$ (kcal/gfw)
Ce	8.11 (88)	125
Lu	8.08 (76)	125
Tb	6.98 (76)	103
Pr	6.24 (88)	88
Er	5.19 (76)	67

The usual difficulty encountered in pressure calibration (uncertainty in the values of the ionization cross-sections) may be overcome using a calibration procedure employing the same species to be calibrated if the vapor pressure of this species is known as a function of temperature. This procedure is relatively straightforward for most metals.

Problems are met, however, when the species is a complex molecule. If another compound whose pressure-temperature curve has been determined, is known this substance may be used in a procedure analogous to that described previously to calibrate the mass spectrometer. This general technique has the disadvantage that one must assume no sensitivity changes occur in the instrument providing all machine parameters are duplicated exactly in both the calibration and the vaporization experiment. What is needed is an *in situ* procedure in which the sensitivity of the mass spectrometer is measured just prior to and immediately after the vaporization experiment. In a T.O.F. mass spectrometer the addition of a movable Faraday cup immediately before the electron multiplier would measure the sensitivity of this component. The measurement of the partial pressure of a particular species in the ion source would result in a known sensitivity for the ionization process performed using a unique set of machine parameters. Effectively, a detector is needed which is sensitive to specific vapor species or some phenomena or property characteristic of the species.

Another technique which may overcome some calibration problems is the use of a double (or multiple) chamber Knudsen effusion cell (108). Using this cell with the calibrating substance (whose vapor pressure is known as a function of temperature) in one compartment will result in a reference point possible at *every* temperature. Ideally it would be desirable to calibrate the sensitivity of the mass

spectrometer with the same species that one wishes to measure the pressure. This may be accomplished by using an isotopically enriched compound or metal. For illustration consider the case of a hypothetical compound having two isotopes A^y and A^{y+n}. The compound AB (the isotopic distribution of A is natural) is placed in one chamber and in the other chamber is placed the metal (or compound) A which is enriched in A^y. For the case of dissociative vaporization of AB, the spectrum in the mass region of A will consist of the sums of the species from A (enriched in A^y) and from AB. The fractional contribution of the standard metal A to the A^y peak may be determined from a comparison of the observed abundance ratios of A^y to A^{y+n} in the spectrum and the natural abundance ratios. Thus a known intensity may be attributed as originating from A and the remainder to AB. In this way the intensity-temperature data of A may be used in conjunction with the known vapor pressure of A to calibrate the sensitivity of the mass spectrometer for <u>every</u> experimental point. Of course, this procedure would correct completely any machine sensitivity fluctuations which may occur from one experimental point to another. One weak point of this technique is that the volatility of the metal must not be significantly higher than that of AB.

A comparison of the results obtained by other workers (105,106,107) with those obtained in the present work is presented in Table XI. From the table the value of ΔS_T^0 and ΔH_T^0 are directly given in column two for which T is the midpoint

Table XI. The vapor pressure of the samarium dicarbide system

Ref.	2.303 R log P(atm)	Range ^0K	$P_{1600} \times 10^5$ atm	$P_{1700} \times 10^5$ atm
105	18.5-65,200/T	1300-2051	1.51	5.01
106	15.5-61,500/T	1400-2000	1.00	3.05
107	16.5-63,300/T	1400-2080	.871	3.89
Present Work				
II27	15.7-56,900/T	1563-2043	2.76	13.5
II41	14.3-57,600/T	1673-2058	1.82	5.50
II43	13.5-58,900/T	1653-2024	.813	2.46
III63	12.2-57,000/T	1431-1860	.776	2.09
III701	11.4-55,500/T	1542-1784	.813	2.34
III702	13.8-59,700/T	1531-1735	.725	2.19
III703	14.7-61,100/T	1577-1741	.741	2.24

value of the temperature range given in column three. Also pressures at 1600^0K and 1700^0K are shown for comparison.

Of the experiments performed in this work experiment II27 was the only one calibrated using silver metal to obtain absolute pressures. Inspection of the pressures listed shows that the pressures obtained in II27 are from a factor of 2 to 6 higher than the others. That the pressure given by this calibration procedure is not in agreement with the other pressures is not surprising if the inherent errors of the calibration procedure using silver metal (ratio of ionization cross-section of silver to samarium, multiplier efficiency differences, etc.) are considered. Experiments III63, III701, III702, and III703 were calibrated by the weight loss method using SmC_2 and show good internal consistency. Experiments II41 and II43 were calibrated using the measured vapor pressure of samarium metal in which the temperature and ion current intensity were monitored and the absolute pressure was found from the literature as a function of temperature. This procedure is explained in detail in Section 3.4. The experimental temperatures were of the order of 800^0 and some difficulty was encountered in measuring the temperature of the orifice since the design of the heating system of the spectrometer caused the orifice to appear darker than the surrounding surface of the effusion cell due to reflected radiation from the heating filament.

The extent of agreement between the predicted pressures as given by the references in Table XI and the present work

are fairly good considering the different methods of estimating absolute pressures from the mass spectrometric intensity data employed. The technique of target collection used by Faircloth, et al. (107) is generally recognized as being a more precise method of measuring absolute partial pressures and it would seem that of the three reports in the literature this is the most accurate. The pressures given by runs III63, III701, III702 and III703, which were calibrated by a weight loss method of SmC_2 agree most closely with those of Faircloth, et al. (107). The higher values of II41 may result from temperature measurement errors.

7.2. Evaluation and Conclusions on the Vaporization of Neodymium(III) Monotelluro Oxide

The vaporization mode occurring for Nd_2O_2Te is not a simple process. The facts upon which this conclusion is based are (1) the vaporization products are Nd(g), NdO(g), Te(g), O(g) and Nd_2O_3(s), and (2) the ratio of partial pressures of NdO(g) to Nd(g) is temperature dependent, changing from less than unity to greater than unity at about 2150^oK.

All of these observations are consistent with the hypothesis that several simultaneous equilibria are occurring in the vaporization of Nd_2O_2Te. The probable reactions are

$$Nd_2O_2Te(s) \longrightarrow \frac{2}{3} Nd_2O_3(s) + \frac{2}{3} Nd(g) + Te(g) \quad (53)$$

$$Nd_2O_2Te(s) + O(g) \longrightarrow Nd_2O_3(s) + Te(g) \quad (54)$$

$$Nd_2O_3(s) \longrightarrow 2NdO(g) + O(g) \quad (55)$$

$$Nd_2O_2Te(s) \longrightarrow 2NdO(g) + Te(g) \quad (56)$$

Reaction (53) is postulated to predominate at lower temperatures while reactions (55) and (56) would become more favorable at higher temperatures. The fact that some O(g) coming from reaction (55) might react with $Nd_2O_2Te(s)$ is accounted for by the side reaction (54). Also since Nd(g) and NdO(g) result from different processes a different slope would be expected in the respective Clausius-Clapeyron log IT vs 1/T plots.

To show the plausibility of the above reactions and also to demonstrate that reactions (55) and (56) are favored over reaction (53) at higher temperatures, the values of the equilibrium constants for all three reactions were calculated at 1800, 2000, and 2200°K. The method used was based on the equation

$$-R \ln K = \Delta fef + \frac{\Delta H^0_{298}}{T}$$

which is obtained from the definition of Δfef for a reaction and the equation $\Delta G^0_T = -RT \ln K$. The fef of $Nd_2O_2Te(s)$ was approximated as

$$fef(Nd_2O_2Te(s)) = fef(Nd_2O_3(s)) - fef(O(g)) + fef(Te(g))$$

and the standard enthalpy of formation as

$$\Delta H^0_{298}(Nd_2O_2Te(s)) = \Delta H^0_{298}(Nd_2O_3(s)) + \Delta H^0_{298}(Te(g)) - \Delta H^0_{298}(O(g)).$$

A compilation of the thermodynamic quantities, the sources of reference and the calculated values of the equilibrium constants are given in Appendix I. The results of these

calculations show that in going from 1800^0K to 2200^0K the equilibrium constant of reaction (53) increases by a factor of $10^{5.1}$, reaction (54) stays practically constant--its equilibrium constant changing by a factor of about $10^{-.57}$, and reactions (55) and (56) increase by a factor of $10^{8.6}$ and $10^{8.3}$, respectively. The magnitude of the changes in the equilibrium constants of reaction (53) compared to those of reactions (55) and (56) with increasing temperature supports the proposed hypothesis, Furthermore, the calculation supports the observed experimental fact that the ratio $\frac{(IT)_{NdO}}{(IT)_{Nd}}$ does invert from less than unity at lower temperature to greater than unity at higher temperatures. It should be mentioned that the substitution of the ratios of the IT product in lieu of partial pressures is a valid approximation since according to Panish (46) the ionization cross-sections of Nd(g) and NdO(g) are approximately the same.

The postulate that reaction (55) is the favored reaction at higher temperature is supported by the work of White, et al. (101) who show that at 2215^0K the vaporization products of this reaction have low but detectable pressures (for mass spectrometric studies)--the partial pressures of NdO(g) and O(g) being 4.951×10^{-6} and 7.900×10^{-7} atmosheres, respectively. These pressures are consistent with ascribing the O(g) as coming from reaction (55) since the measurement that O(g) was coming from the effusion cell was performed at about 2300^0K, a temperature at which reaction (55) has a partial pressure of O(g) of 1.35×10^{-6} atmospheres (101).

CHAPTER VIII

ERROR ANALYSIS

8.1. General Discussion of Errors in High Temperature Mass Spectrometric Measurements

If a set of experiments, each containing many (>10) measured points, are performed independentaly and their average value is used as a measure of the "true" value, this "true" value will have associated with it an uncertainty which will reflect the random statistical fluctuation in each experiment as well as the inter-experimental errors. The intra-experimental error may arise from various uncontrollable factors such as electronic fluctuations in the ion source, electron multiplier or read-out apparatus (analogues, recorder) and from systematic errors such as a slowly drifting electron energy or trap current, or a growing metal coating on the optical window. Systematic errors may be found in the individual experiments and these errors are either eliminated in succeeding measurements or their effect is removed by appropriate correction. The remaining uncertainty is commonly estimated by either of two quantities: (a) an average deviation from the mean or (b) the standard deviation from the mean. In this work the "unbiased" form of the equation used to calculate the standard deviation was

$$\sigma = \left[\frac{\sum_{i=1}^{n} (X_i - \bar{X})^2}{n - 1} \right]^{1/2} \qquad (57)$$

where σ is the standard deviation, X_i is the observed experimental value, $\bar{X}$ is the average value of the X_i's, and n is the number of points in the experiment. The divisor $(n - 1)$ in equation (57) represents the number of degrees of freedom in the set and ensures that the estimate made of the standard deviation using this equation (on small sets) will have the same value as that obtained from an experiment with a very large number of measurements.

The other error associated with an average experimental value obtained from combining a series of experiments is the uncertainty (or amount of difference) between experiments. It is likely that this latter type contributes to the uncertainty in the average value of ΔS_T^0 since it arises from the calibration procedure which assumes identical machine parameters between experiments. The net effect of this inter-experimental error should be a noticeably larger range (or spread) in the values of ΔS_T^0 than in ΔH_T^0. For example, the data for SmC_2 contained in Table V show a 15% variation between the lowest and highest value of ΔS_T^0 (based on the average value of ΔS_T^0 in the set) whereas the same measure of the range in ΔH_T^0 is 9.6%.

Another consideration in the analysis of data is systematic errors. The absence of such an error may be shown in a set of data which is fitted statistically to a straight

line by the method of least squares if all (or most) of the experimental points lie within $\pm\zeta$ where ζ is the uncertainty along either the ordinate or abscissa about the least squares line. The magnitude of ζ is obtained from the combined errors in the experimental measurements and hence the errors produced in ΔH_T^0 should be totally accountable by the statistical fluctuations or inherent limitations of the measurements of temperature and the current ion intensity of the particular isotope. The reproducibility with which temperature may be measured using an optical pyrometer in the range of $1500\text{-}2000^0$ is dependent, to a large measure on the observer's experience but has been quoted to be of the order of $\pm 2^0$ (102). Since each temperature measurement was made in triplicate and the average value used, an uncertainty in the measured temperature was judged to be within $\pm 5^0$. The uncertainty in the calibration of the pyrometer to the 1948 International Temperature Scale (cf. Appendix D) is quoted to be $\pm 4^0$ for the experimental temperature range used. The quantitative reproducibility of the mass spectrometer in measuring the ion current is quoted to be (2-5% (103).

The contribution to the error in the ordinate made by the estimated uncertainty of $\pm 9^0$ in the temperature is the displacement of $\Delta\ 1/T$ along the abscissa.

For an actual calculation a random selected point from the data for Sm-152 of experiment II34 is chosen. This point has a temperature of 1801^0K and an ion current intensity

of 0.0501 nanoamperes. The error contribution of $\pm 9^0$K at 1801^0K on the abscissa of a ln IT *vs* 1/T graph (*cf*. Figure 13) is calculated to be $\pm 0.0555 \times 10^{-4}$ The relation between the uncertainty in the abscissa and the ordinate is

$$\Delta y = \Delta x \cdot \text{slope}$$

where Δy and Δx are the uncertainties in ln IT and 1/T respectively. From the least squares computer program (*cf*. Appendix E) experiment II34 has the slope of -2.91×10^4. Hence the error in ln IT is calculated to be ± 0.30. Examination of Figure 13 reveals that in the vicinity of $10^4/T = 5.55$ (temperature of 1801^0K) most of the points do fall within this error interval about the calculated least squares pressure line, and hence it is concluded that the error in the experimental data is free of errors not reducible to statistical fluctuations in the experimental design.

It should be mentioned that certain types of systematic errors such as having a pyrometer calibration in error by a constant number of degrees will not be revealed by the previous analysis. This type of possible error, however, is checked for by the following method. It is generally the practice in high temperature thermodynamic studies to compare "Second Law" and "Third Law" heats of vaporization. The agreement of the two methods coupled with an examination of the individual values of the enthalpy obtained by the Third Law method is indicative that there are no systematic

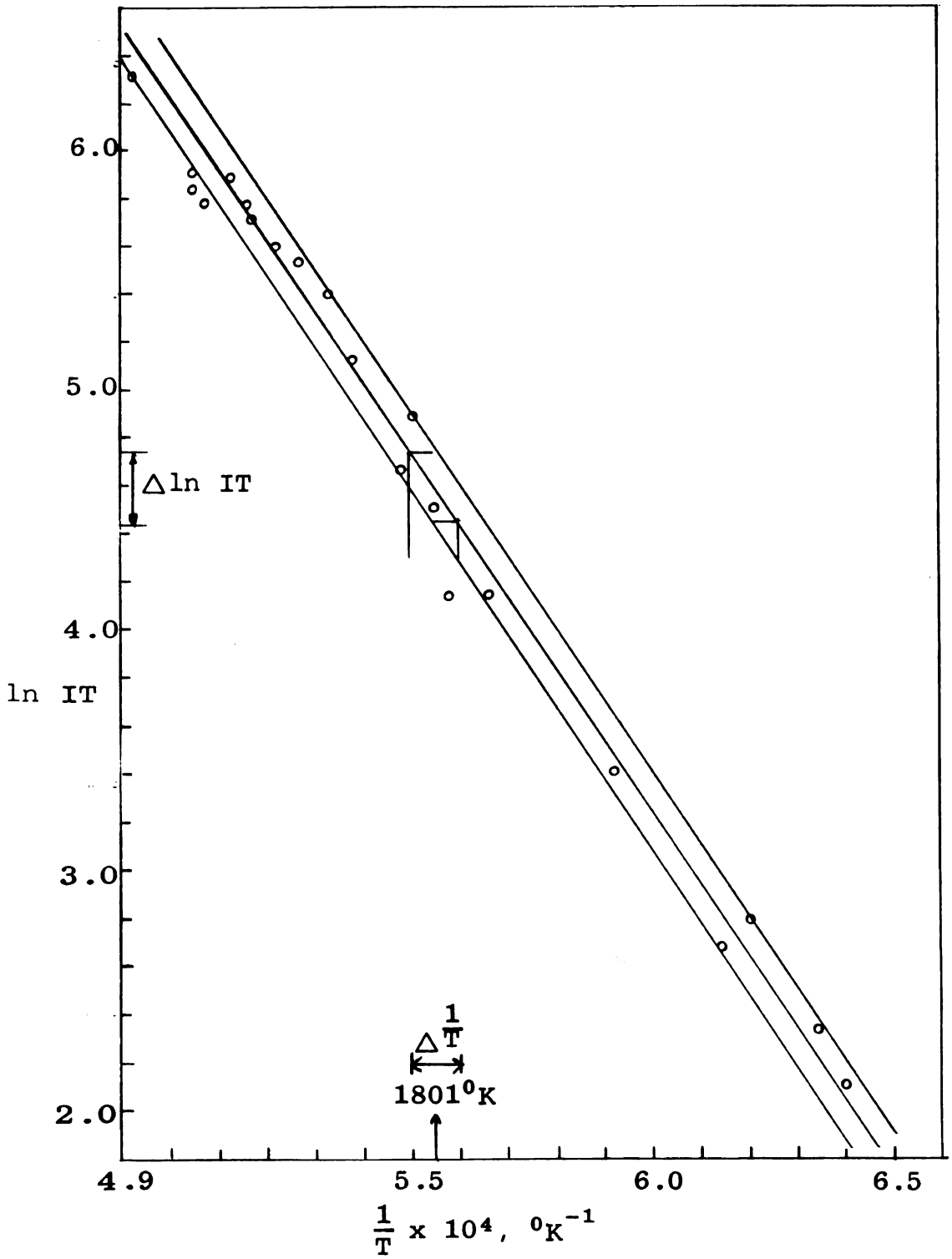

Figure 13. Analysis of error in Sm-152 of Experiment II34.

errors because of temperature measurement, vapor pressure measurement or in the tabular free energy functions used to compute the Third Law enthalpy. A critical statistical evaluation of the random errors and other approximations inherent in the estimation of Second and Third Law enthalpies of sublimation are given by Horton (104) whose conclusions may be paraphrased as:

(1) The better precision usually noted in Third Law heats as compared to Second Law heats is a consequence due to the difference between the two estimators of the precision;

(2) The Second Law heat is generally biased in its calculation;

(3) The Third Law heat is not the minimum variance unbiased estimator of the heat;

(4) The standard deviation obtained from a least squares fitting consistently overestimates the true standard deviation.

These conclusions are not of great practical importance, however, since the magnitude of the effects of the discrepencies is very small. Thus for the Third Law enthalpy of tungsten the difference between the usual method of calculation and the minimum-variance estimator is calculated to be 17 calories per gram-atom or 0.008%, a difference too small to be of significance. Experimentally it was found that there is agreement between the Second and Third Law enthalpies of vaporization of SmC_2 (although this may be fortuitous) and also no observable trend of the Third Law enthalpy with temperature was observed (Cf. Appendix A).

8.2. Error in the Enthalpy and Entropy of Vaporization of Samarium Dicarbide

The total uncertainty in the standard enthalpy of vaporization of SmC_2 may be considered to arise from the statistical fluctuations inherent in the measurement technique and from the errors associated with the literature values of the quantities necessary to reduce the enthalpy to a standard temperature. Table IV contains the enthalpy of vaporization as well as the associated error for the various experiments. The following equation, which is a variation of equation (24), was used to obtain the Second Law enthalpy at 298^0K

$$\Delta H^0_{298} = \Delta H^0_T - [(H^0_T - H^0_{298})Ca(g) + 2(H^0_T - H^0_{298})C(gr) - (H^0_T - H^0_{298})CaC_2(s)] \quad (24a).$$

The sources used and the errors associated with each quantity of equation (24a) are given in Table XII. Combining the individual error contributions, the sum of the errors in $(H^0_T - H^0_{298})$ at 1900^0K for vaporization of one mole of $CaC_2(s)$ is found to be 503 calories. The statistical uncertainty in the average value of ΔH^0_{298} is 2.11 kcal/gfw. Therefore the value of the Second Law enthalpy and its total associated uncertainty for the vaporization of SmC_2 is $\Delta H^0_{298} = 64.2 \pm 2.6$ kcal/gfw. Similarly, the error associated with the literature values used to compute ΔS^0_{298} of vaporization for SmC_2 results to be 0.53 cal/deg/gfw. This error, combined with the statistical variation in the average value (1.8 eu), results in a ΔS^0_{298} for the vaporization of SmC_2 of 22.1 ± 2.3 eu.

Table XII. Uncertainty in calcium dicarbide vaporization quantities for T = 1900°K

Species	Uncertainty in $(H_T^0-H_{298}^0)$	Uncertainty in $(S_T^0-S_{298}^0)$
$CaC_2(s)$	0.1%; ±29 cal/mole	0.1%; ±0.034 cal/mole/deg
Ca(g)	0.1%; ± 8 cal/mole	0.1%; ±0.009 cal/mole/deg
C(gr)	3.0%; ±238 cal/mole	3.0%; ±0.243 cal/mole/deg

Data taken from Kelley (89).

8.3. Error in Other Thermodynamic Values

The uncertainty associated with the enthalpy (entropy) of formation of SmC_2 may be determined by inspection of the errors in the quantities of equation (48) (and an analogous one for the entropy). The enthalpy and entropy of sublimation of samarium at the reference temperature of 298°K are given as 48.59 ± 0.22 kcal/gfw by Habermann and Daane (80) and 27.11 ± 0.50 eu by Hultgren, et al. (88), respectively. Combining the errors of the quantities in equation (48) results in a standard enthalpy of formation for $SmC_2(s)$ of -14.6 ± 2.8 kcal/gfw. The standard entropy of formation for $SmC_2(s)$ and its total calculated uncertainty is 5.0 ± 2.8 eu.

The error associated with $S_{298}^0(SmC_2(s))$ may be determined by combining the errors of the absolute entropies found in equation (49). The absolute entropy of samarium gas is given by Kelley and King (90) as 43.75 ± 0.01 eu and that of 2 gram-atoms of graphite is 2.71 ± 0.04 eu (90). Combining these values results in $S_{298}^0(SmC_2(s)) = 24.1 \pm 2.9$ eu.

REFERENCES

1. Thermodynamics, Vol. I, International Atomic Energy Agency, Vienna, 1966, p. 245.

2. J. DeVillelume, Compt.Rend., 232, 235 (1951); Ann. Chim. (Paris), 7, 265 (1952).

3. W. A. Chupka, J. Berkowitz, C. F. Giese, M. G. Inghram, J. Phys. Chem., 62, 611 (1958).

4. F. H. Spedding, K. Gschneidner, Jr., A. H. Daane, J. Am. Chem. Soc., 80, 4499 (1958).

5. R. C. Vikery, R. Sedlacek, A. Ruben, J. Chem. Soc., (1959) 498.

6. Ibid., 503.

7. Ibid., 505.

8. F. H. Pollard, G. Nickless, S. Evered, J. Chromatog., 15, 211 (1964).

9. G. J. Palenik, J. Wolf, Inorg. Chem., 1, 345 (1962).

10. H. J. Svec, J. Cappelen, F. E. Saalfeld, J. Inorg. Nucl. Chem., 26, 721 (1964).

11. N. N. Greenwood, A. J. Osborn, J. Chem. Soc., (1961) 1775.

12. M. Atojii, K. Gschneidner, Jr., A. H. Daane, R. E. Rundle, F. H. Spedding, J. Am. Chem. Soc., 80, 1804 (1958).

13. K. Gschneidner, Ph.D. Thesis, Iowa State University, 1957.

14. N. L. Jensen, C. J. Hoffman, Fourth Rare Earth Conference, Phoenix, Arizona, April (1964).

15. R. E. Gebelt, H. A. Eick, Inorg. Chem., 3, 335 (1964).

16. M. Atojii, J. Chem. Phys., 35, 1950 (1961).

17. M. Atojii, D. E. Williams, loc. cit., 1960.

18. M. Atojii, J. Chem. Phys., 46, 1891 (1967).

19. A. L. Bowman, N. H. Krikorian, G. P. Arnold, T. C. Wallace, N. G. Nereson, Sixth Rare Earth Conference, Gatlinburg, Tenn., May (1967).

20. I. Binder, J. Am. Ceram. Soc., 43, 287 (1960).

21. F. Gaume-Mahn, Bull. Soc. Chim. France, (1956) 1862.

22. R. E. Gebelt, Ph.D. Thesis, Michigan State University (1964).

23. D. D. Jackson, R. G. Bedford, G. W. Barton, Jr., University of California Radiation Laboratory Report UCRL-7362T(1963).

24. L. Brewer, J. S. Kane, J. Phys. Chem., 59, 105 (1955).

25. G. F. Wakefield, A. H. Daane, F. H. Spedding, Fourth Rare Earth Conference, Phoenix, Arizona, April (1964).

26. D. D. Jackson, G. W. Barton, Jr., O. H. Krikorian, R. S. Newbury, University of California Radiation Laboratory Report UCRL-6701 (1962).

27. G. DeMaria, M. Guido, L. Malaspina, B. Pesce, J. Chem. Phys., 43, 4449 (1965).

28. G. Balducci, A. Capalbi, G. DeMaria, M. Guido, loc. cit., 2136.

29. G. DeMaria, G. Balducci, A Capalbi, M. Guido, Meeting on Thermodynamics of Ceramic Systems, London, April (1966).

30. R. E. Gebelt, H. A. Eick, J. Chem. Phys., 44, 2872 (1966).

31. R. H. Flowers, E. G. Rauh, J. Inorg. Nucl. Chem., 28, 1355 (1966).

32. R. L. Faircloth, R. H. Flowers, F. C. W. Pummery, Atomic Energy Research Establishment Report AERE-M1771 (1966).

33. M. Hoch, P. E. Blackburn, D. P. Dingledy, H. L. Johnson, J. Phys. Chem., 59, 97 (1955).

34. W. A. Chupka, M. G. Inghram, loc. cit., 100.

35. W. H. Zachariasen, Acta. Cryst., 2, 60 (1949).

36. H. A. Eick, J. Am. Chem. Soc., 80, 43 (1958).

37. H. A. Eick, Acta Cryst., 13, 161 (1960).

38. R. A. Kent, H. A. Eick, Inorg. Chem., 1, 956 (1962).

39. P. M. Raccah, J. M. Longo, H. A. Eick, Inorg. Chem., In Press.

40. P. Khodadad, T. Tek, J. Flahaut, L. Domange, Compt. Rend., 260, 2235 (1965).

41. R. M. Jacobs, M. S. Thesis, Michigan State University (1965).

42. P. W. Gilles, University of Kansas, Private Communication.

43. D. White, P. N. Walsh, L. L. Ames, H. W. Goldstein, Thermodynamics of Nuclear Materials, International Atomic Energy Agency, Vienna, Austria, 1962.

44. D. White, P. N. Walsh, H. W. Goldstein, D. F. Dever, J. Phys. Chem., 65, 1400 (1961).

45. M. B. Panish, J. Chem. Phys., 34, 2197 (1961).

46. Ibid., 1079.

47. G. R. Belton, R. J. Fruehan, J. Phys. Chem., 71, 1403 (1967).

48. D. Cubicciotti, ibid., 70, 2410 (1966).

49. M. Knudsen, Ann. Physik, 28, 75 (1909). Translated into English at the Argonne National Laboratory by L. Venters (1958).

50. Ibid., 999(1909). Translated into English at Argonne National Laboratory by K. D. Carlson and E. D. Cater (1958).

51. Ibid., 29, 179 (1909).

52. K. D. Carlson, Argonne National Laboratory Report ANL-6156 (1960).

53. J. W. Ward, Los Alamos Scientific Laboratory Report LA-3509 (1966).

54. P. Clausing, Physica, 9, 65 (1929).

55. S. Dushman, Scientific Foundations of Vacuum Technique, John Wiley and Sons, Inc., New York, 1949.

56. J. G. Edwards, P. W. Gilles, J. Chem. Phys., 44, 4426 (1966).

57. R. D. Freeman, J. W. Edwards, Technical Documentary Report ASD-TDR-63-754 (1963).

58. R. J. Ackermann, R. J. Thorn, G. H. Winslow, Argonne National Laboratory Report ANL-6663 (1962).

59. R. J. Thorn, G. H. Winslow, J. Chem. Phys., 26, 186 (1955).

60. J. H. McFee, P. M. Marcus, I. Estermann, Rev. Sci. Instr., 31, 1013 (1960).

61. G. M. Rosenblatt, J. Phys. Chem., 71, 1327 (1967).

62. M. G. Inghram, J. Drowart, "Mass Spectrometry Applied to High Temperature Chemistry," in High Temperature Technology, McGraw-Hill Book Co., Inc., New York, 1960.

63. L. Presnykov, J. Expt. and Theor. Phys., 20, 760 (1965). Translated into English by the American Institute of Physics.

64. L. Vries, Physics, 31, 385 (1965).

65. H. Bethe, Ann. Physik, 5, 352 (1930).

66. N. F. Mott, H. S. W. Massey, The Theory of Atomic Collisions, Oxford University Press, London, 1949.

67. F. E. Stafford, J. Chem. Phys., 45, 859 (1966).

68. J. B. Mann, ibid., 46, 1646 (1967).

69. J. W. Otvos, D. P. Stevenson, J. Am. Chem. Soc., 78, 546 (1956).

70. H. S. W. Massey, E. A. S. Burhop, Electronic and Ionic Impact Phenomena, Oxford University Press, Oxford, 1952.

71. F. W. Lampe, J. W. Franklin, F. H. Field, J. Am. Chem. Soc., 79, 6129 (1957).

72. A. P. Lyubimov, S. I. Pavlov, V. I. Rakhovskii, N. G. Zaitseva, Bulletin of the Academy of Sciences of the USSR, Physical Sections, 27, 1033 (1963). Translated into English by Columbia Technical Translations, White Plains, New York.

73. J. L. Cooper, G. A. Pressley, Jr., F. E. Stafford, J. Chem. Phys., 44, 3946 (1966).

74. E. D. Cater, R. J. Thorn, J. Chem. Phys., 44, 1342 (1966).

75. R. Colin, P. Goldfinger, M. Jeunehomme, Nature, 187, 408 (1960).

76. C. E. Habermann, A. H. Daane, J. Chem. Phys., 41, 2188 (1964).

77. M. G. Inghram, W. A. Chupka, R. F. Porter, ibid., 23, 2159 (1955).

78. W. C. Wiley, I. H. McLaren, Rev. Sci. Instr., 26, 1150 (1955); W. C. Wiley, Science, 124, 217 (1956).

79. Instruction Manual for Models 1003 and 1005 (Basic Model 12) Bendix Time-of-Flight Mass Spectrometer, The Bendix Corporation, Cincinnati Division, 1963.

80. E. G. Rauh, R. C. Sadler, R. J. Thorn, Argonne National Laboratory Report ANL-6536 (1962).

81. R. A. Kent, Ph.D. Dissertation, Michigan State University, 1963.

82. A. D. Butherus, Ph.D. Dissertation, Michigan State University, 1967.

83. R. E. Vogel, C. E. Kempter, Los Alamos Scientific Laboratory Report LA-2317 (1959); Acta. Cryst., 14, 1130 (1961). Re-written for the CDC 3600 computer by H. A. Eick, 1967.

84. E. G. Rauh, Argonne National Laboratory, Private Communication.

85. O. H. Krikorian, University of California Radiation Laboratory Report UCRL-6132 (1960).

86. JANAF Thermochemical Tables, The Dow Chemical Company Midland, Michigan, 1963

87. R. C. Feber, C. C. Herrick, Los Alamos Scientific Laboratory Report LA-3184 (1965).

88. R. Hultgren, R. L. Orr, P. D. Anderson, K. K. Kelley, Selected Values of Thermodynamic Properties of Metals and Alloys, John Wiley and Sons, Inc., 1963.

89. K. K. Kelley, Contributions to the Data on Theoretical Metallurgy XIII, Bureau of Mines Bulletin 584, 1960.

90. K. K. Kelley, E. G. King, Contributions to the Data on Theoretical Metallurgy XIV, Bureau of Mines Bulletin 592, 1961.

91. R. W. Kiser, Introduction to Mass Spectrometry and Its Applications, Prentice-Hall, Inc., Englewood Cliffs, N. J., 1965.

92. F. E. Grubbs, Ann. Math. Stat., 21, 27 (1950).

93. W. R. Savage, D. E. Hudson, F. H. Spedding, J. Chem. Phys., 30, 211 (1959).

94. Handbook of Chemistry and Physics, 45th Edition, Chemical Rubber Publishing Co., Cleveland, Ohio, 1964-65.

95. Physiochemical Measurements at High Temperatures, J. O'M. Bockris, ed., Chapter 2, Butterworths Scientific Publications, London, 1959.

96. D. F. Avery, J. Cuthbert, N. J. D. Prosser, C. Silk, J. Sci. Instr., 43, 436 (1966).

97. D. R. Stull, G. C. Sinke, Thermodynamic Properties of the Elements, American Chemical Society, Washington, D.C., 1956

98. W. J. Youden, Statistical Methods for Chemists, John Wiley and Sons, Inc., New York, 1951.

99. F. H. Spedding, J. J. Hanak, A. H. Daane, Trans. AIME 212, 379 (1958).

100. H. A. Eick, J. M. Haschke, P. A. Pilato, Paper presented at the Thermodynamics Symposium, International Union of Pure and Applied Chemistry, Heidelberg, Germany, Sept. 12-14, 1967.

101. P. N. Walsh, H. W. Goldstein, D. White, J. Am. Ceram. Soc., 43, 229 (1960).

102. D. R. Lovejoy, Can. J. Phys., 36, 1397 (1958).

103. C. N. Reilley, Advances in Analytical Chemistry and Instrumentation, Vol. 4, page 371, John Wiley and Sons, Inc., New York, 1964.

104. W. S. Horton, J. Research of NBS, 70A, 533 (1966).

105. D. F. Avery, J. Cuthbert, C. Silk, Brit. J. Appl. Phys., 18, 1133 (1967).

106. J. Cuthbert, R. L. Faircloth, R. H. Flowers and F. C. W. Pummery, Proc. Brit. Ceram. Soc., 8, June (1967).

107. R. L. Faircloth, R. H. Flowers, F. C. W. Pummery, Atomic Energy Research Establishment Report AERE-R5480, Harwell, England (1967).

108. J. V. Hackworth, Ph.D. Dissertation, University of Cincinnati, 1967.

109. Chem. Eng. News, 39, No. 47 (1961).

110. H. W. Goldstein, E. F. Neilson, P. N. Walsh, D. White, J. Phys. Chem., 63, 1445 (1959).

111. C. E. Wicks, F. E. Block, Thermodynamic Properties of 65 Elements - Their Oxides, Halides, Carbides and Nitrides, Bureau of Mines Bulletin 605, 1963.

APPENDICES

APPENDIX A

Third Law ΔH^0_{298}: $SmC_2(s) \longrightarrow Sm(g) + 2C(gr)$

The values of ΔH^0_{298} contained in this table were based on a calculation using the fef of $CaC_2(s)$ (corrected for the effect of substitution of a samarium atom for calcium in the lattice) as was described in Section 6.12. The numbers "2-4" under the heading "Isotope" mean that the intensity measured was the sum of Sm-152 and Sm-154 intensities. This addition was effected using a 360 nsec wide gate pulse obtained with a PIC #841 pulse transformer in lieu of the PIC #811 (~60 nsec wide) component in the gate pulse circuit of the analogues. "Ave" under the "Isotope" column means that the average total intensity (as obtained by the average of the normalized isotopic ion currents measured) was used. A graph of ln P vs $1/T$ of this data is presented in Figure 8a on page 83.

Expt.	Isotope	T, ^{0}K	ln IT	-ln k	$-\Delta$fef e.u.	ΔH^0_{298} kcal/gfw	$\frac{10^4}{T}$	-ln P
III63	2-4	1431	2.304	15.56	20.15	66.19	6.988	13.26
III63	2-4	1519	2.398	15.56	18.96	68.51	6.583	13.16
III702	2-4	1532	2.409	15.04	18.92	67.43	65.27	12.63
III701	2-4	1542	2.813	15.21	18.89	67.12	6.485	13.40
III63	2-4	1546	2.687	15.56	18.88	68.75	6.468	12.87
III702	2-4	1556	2.795	15.04	18.432	67.39	6.427	12.25
III63	2-4	1575	3.499	15.56	18.80	67.35	6.349	12.06
III703	2-4	1577	2.421	14.30	18.80	66.87	6.341	11.88
III701	2-4	1582	3.315	15.21	18.78	67.10	6.321	11.90
III702	2-4	1595	3.074	15.04	18.74	67.81	6.270	11.97
III701	2-4	1607	3.460	15.21	18.71	67.59	6.222	11.75
III703	2-4	1614	2.548	14.30	18.70	67.87	6.196	11.75
III702	2-4	1616	3.299	15.04	18.69	67.89	6.188	11.74
III702	2-4	1631	3.575	15.04	18.81	67.84	6.131	11.47
III701	2-4	1634	3.763	15.21	18.64	67.62	6.120	11.45
III703	2-4	1634	2.767	14.30	19.42	67.90	6.120	11.53
III63	2-4	1634	4.080	15.56	18.64	67.72	6.120	11.48
II41	ave	1639	1.874	12.65	18.63	65.64	6.101	10.78
III701	2-4	1645	3.973	15.21	18.45	67.75	6.079	11.24
III703	2-4	1648	3.057	14.30	18.60	67.49	6.068	11.24
II43	ave	1648	1.431	12.59	18.60	67.20	6.068	11.16
III703	2-4	1650	2.960	14.30	18.60	67.89	6.061	11.34
II43	ave	1653	1.479	12.65	18.59	67.43	6.050	11.17
III703	2-4	1653	2.954	14.30	18.59	68.02	6.050	11.35
III703	2-4	1653	2.974	14.30	18.59	67.96	6.050	11.33
II41	ave	1673	2.331	12.59	18.54	65.13	5.977	10.26
III703	2-4	1678	3.212	14.30	18.53	68.06	5.959	11.09
III702	2-4	1679	4.091	15.04	18.52	67.62	5.956	10.95
III701	2-4	1688	4.376	15.21	18.50	67.57	5.924	10.83
III703	2-4	1698	3.594	14.30	18.73	67.94	5.889	10.71
II43	ave	1698	1.893	12.65	18.47	67.67	5.889	10.76
III63	2-4	1700	4.954	15.56	18.47	67.22	5.882	10.61
III702	2-4	1701	4.411	15.04	18.47	67.32	5.879	10.63
II43	ave	1710	1.885	12.65	18.44	68.11	5.848	10.77
III702	2-4	1714	4.321	15.04	18.43	68.08	5.834	10.72
III703	2-4	1715	3.867	14.30	18.43	67.17	5.831	10.43
III702	2-4	1720	4.575	15.04	18.42	67.42	5.814	10.47
III701	2-4	1721	4.765	15.21	18.41	67.42	5.811	10.45
III703	2-4	1722	2.890	14.30	18.41	67.34	5.807	10.41
II41	ave	1726	2.833	12.59	18.40	65.23	5.794	9.76
III702	2-4	1735	4.780	15.04	18.38	67.25	5.764	10.26
II43	ave	1737	2.307	12.59	18.37	67.40	5.757	10.28
II43	ave	1739	2.439	12.59	18.37	67.03	5.750	10.15
III703	2-4	1741	4.046	14.30	18.36	67.45	5.744	10.25
III701	2-4	1747	5.031	15.21	18.34	67.41	5.724	10.18
III701	2-4	1747	4.991	15.21	18.34	67.54	5.724	10.22
II43	ave	1758	2.579	12.59	18.32	67.32	5.688	10.01
II41	ave	1760	3.186	12.59	18.31	65.11	5.682	9.40
II43	ave	1776	2.695	12.59	18.27	67.33	5.631	9.90
II43	ave	1781	2.659	12.59	18.26	67.66	5.615	9.93

Expt.	Isotope	T, ^{0}K	ln It	-ln k	-Δfef e.u.	ΔH^0_{298} $\frac{kcal}{gfw}$	$\frac{10^4}{T}$	-ln P
III63	2-4	1781	5.577	15.56	18.26	67.85	5.615	9.98
III63	2-4	1783	5.695	15.56	18.25	67.50	5.609	9.87
III701	2-4	1784	5.122	15.21	18.25	68.33	5.605	10.09
II41	ave	1789	3.642	12.59	18.24	64.18	5.590	8.95
II43	ave	1807	2.968	12.59	18.19	67.40	5.534	9.62
II41	ave	1812	3.944	12.59	18.18	64.07	5.519	9.65
III63	2-4	1815	6.089	15.56	18.17	67.15	5.510	9.47
II43	ave	1817	3.179	12.59	18.17	66.99	5.504	9.41
II41	ave	1836	4.172	12.59	18.12	63.97	5.447	8.42
II43	ave	1840	3.237	12.59	18.11	67.53	5.435	9.35
II43	ave	1852	3.389	12.59	18.08	67.33	5.400	9.20
II41	ave	1859	4.421	12.59	18.06	63.76	5.379	8.17
III63	2-4	1860	6.338	15.56	18.06	67.67	5.376	9.22
II43	ave	1876	3.530	12.59	18.02	67.57	5.330	9.06
II41	ave	1886	4.555	12.59	18.00	64.06	5.302	8.04
II43	ave	1916	3.920	12.59	17.93	67.34	5.219	8.67
II43	ave	1922	3.902	12.59	17.91	67.60	5.203	8.69
II41	ave	1932	4.829	12.59	17.89	64.34	5.176	7.76
II43	ave	1932	4.263	12.59	17.89	66.52	5.176	8.33
II43	ave	1941	4062	12.59	17.87	67.58	5.152	8.53
II41	ave	1949	4.923	12.59	17.85	64.48	5.131	7.67
II43	ave	1963	4.394	12.59	17.81	66.94	5.094	8.20
II43	ave	1971	4.426	12.59	17.80	67.04	5.074	8.16
II41	ave	1971	5.154	12.59	17.79	64.30	5.074	7.44
II41	ave	1988	5.202	12.59	17.76	64.47	5.030	7.39
II43	ave	2024	4.717	12.59	17.68	67.45	4.941	7.87
II41	ave	2025	5.397	12.59	17.67	64.74	4.938	7.19
II41	ave	2045	5.310	12.59	17.63	65.42	4.890	7.28
II41	ave	2047	5.402	12.59	17.60	65.40	4.885	7.19

APPENDIX B

The Mass Spectrometric Vaporization of Copper

As a check on the reliability of obtaining absolute pressures a sample of copper was vaporized in the mass spectrometer and its pressure was measured as a function of temperature. Both copper isotopes were used to obtain log IT vs $\frac{1}{T}$ graphs. The value of k for copper was obtained from that measured for silver by using the ionization cross-sections of Mann(68) in equation (39) and had a value of 3.14×10^{-6} atmospheres deg^{-1} $nanoampere^{-1}$. The results obtained are presented in Table B-1, in which ΔS^0_{1747} was obtained using equation (20).

Table B-1. Copper vaporization.

Isotope	ΔH^0_{1747} $\frac{kcal}{g\text{-}at}$	σ*	a**	-ln k	ΔS^0_{1747} e.u.
Cu-63	78.9	1.8	27.8	12.7	30.0
Cu-65	75.9	1.8	26.9	12.7	28.2

*σ is the standard deviation in the least squares slope.

**a is the intercept of the least squares line.

Using Kelley (89), the values of ΔH^0_{1747} and ΔS^0_{1747} obtained as the average from the two isotopes resulted in $\Delta H^0_{298} = 83.3 \pm 1.8$ kcal|g-at and $\Delta S^0_{298} = 34.3 \pm 1.0$ e.u. (the uncertainties are the standard deviations). Values of ΔH^0_{298} calculated from the Third Law method were obtained using the free energy function of copper from Hültgren et al.(88)

in equation (27) and are presented in Table B-2. The average value for ΔH^0_{298} thus obtained (with its standard deviation) is 78.4 ± 1.1 kcal/g-at which may be compared to 80.86 kcal/g-at given by Hultgren and to the mass spectrometric measured values of 81.88 and 82.39 kcal/g-at obtained by Avery et al.(96) using the Second and Third Law methods, respectively. If the value of ΔS^0_{1656} obtained by Avery, et al. (96) for the vaporization of copper is reduced to ΔS^0_{298} using reference (88) a value of 31.5 e.u. is obtained.

The Third Law ΔH^0_{298} shows a detectible temperature trend. This decrease of ΔH^0_{298} with increasing temperature may have been due to an insufficient correction for the lowering of the observed temperature from a copper coating which developed on the optical window. Thus, the temperatures used in the calculation are probably lower than the "true" temperatures and thus resulted in lower ΔH^0_{298} values at higher temperatures.

Table B-2. Third Law ΔH^0_{298} for copper vaporization.

Isotope	T, ^{0}K	ln IT	-Δfef e.u.	ΔH^0_{298} kcal/g-at
63	1542	1.832	30.37	80.0
65	1542	2.249	30.37	78.8
63	1609	3.355	30.22	78.4
65	1609	3.109	30.22	79.2
63	1715	4.799	30.01	78.3
65	1715	4.694	30.01	78.6
63	1789	5.574	29.86	78.7
65	1789	5.572	29.86	78.7
63	1852	6.454	29.75	78.0
65	1852	6.439	29.75	78.0
63	1881	6.319	29.69	79.6
65	1881	6.218	29.69	80.0
63	1883	6.794	29.69	77.9
65	1883	6.735	29.69	78.1
63	1916	7.133	29.63	77.8
65	1916	7.135	29.63	77.8
63	1953	7.687	29.57	77.1
65	1953	7.7601	29.57	76.1

Notes:

1. Data is experiment II26.

2. ln k for the table is -12.67.

APPENDIX C

Mass Spectometric Vaporization of Samarium

In the course of using samarium as a calibration substance for the mass spectrometer partial pressures, the energetics of its vaporization were obtained. In the temperature range 1145 to 1218°K the current intensities of Sm-152 and Sm-154 were measured. The average value obtained from the least squares analysis for the isotopes gave a Second Law ΔH^0_{1181} = 47.0 ± 1.9 kcal|g-at which compares favorably with Kelley's value of 47.7 kcal|g-at (89). By plotting P vs T for samarium, where the value of P was taken as a function of the experimental "true" temperature using the vapor pressure data of Stull and Sinke for samarium (97), the values of k_{152} and k_{154} were obtained from the slopes. Using equation (20), and reduction of the ΔS^0_{1181} by Kelley's data a ΔS^0_{298} of 24.9 ± 1.5 e.u. was obtained as the average value from the two isotopes, which may be compared to 27.5 ± 1.0 e.u. obtained by Kelley and King (90). The Third Law ΔH^0_{298} was calculated using reference (88) for the free energy function of samarium and equation (27). The values calculated are presented in Table C-1, and the average ΔH^0_{298} derived is 48.9 ± 0.6 kcal|g-at (the error is the standard deviation). The total error in ΔH^0_{298} is estimated to be about Rσ or about 1.3 kcal|g-at. A comparison of the ΔH^0_{298} obtained for the vaporization of samarium may be seen to compare favorably

with the value of 49.56 measured by Savage et al. (93).

Table C-1. Experiment III31-The vaporization of samarium

Isotope	T, ^{0}K	ln IT	-ln k	-Δfef e.u.	ΔH^{0}_{298} kcal g-at
152	1145.0	2.7699	11.116	26.252	49.05
154	1145.0	2.7933	11.120	26.252	49.01
152	1152.6	3.4140	11.116	26.242	47.89
154	1152.6	3.3595	11.120	26.242	48.02
152	1161.5	2.8368	11.116	26.230	49.58
154	1161.5	2.7758	11.120	26.230	49.73
152	1182.5	3.5350	11.116	26.203	48.80
154	1182.5	3.4869	11.120	26.203	48.92
152	1192.2	3.6061	11.116	26.190	49.02
154	1192.2	3.5875	11.120	26.190	49.07
152	1212.0	4.1717	11.116	26.155	48.43
154	1212.0	4.1552	11.120	26.155	48.47
152	1214.4	4.2548	11.116	26.150	48.31
154	1214.4	4.1739	11.120	26.150	48.52
152	1217.5	3.6392	11.116	26.143	49.92
154	1217.5	3.6231	11.120	26.143	49.97
152	1237.2	4.5247	11.116	26.102	48.50
154	1237.2	4.5525	11.120	26.102	48.44

APPENDIX D

Temperature Corrections

1. The NBS Calibration Data for L & N Pyrometer #1619073.

Table D-1 presents the calibration table for the pyrometer with its internal tungsten lamp, XY85. The pyrometer was calibrated on April 19, 1963 and was reported to have the maximum uncertainty of $\pm 4^0$ at 800^0 to about $\pm 3^0$ at 1063^0 and increasing to about $\pm 5^0$ at 2800^0. "True" temperatures are those based on the 1948 International Temperature Scale.

Table D-1. NBS calibration data.

L Range		H Range		XH Range	
Actual	True	Actual	True	Actual	True
800^0C	796^0C	1100^0C	1092^0C	1500	1485
850	845	1200	1189	1600	1581
900	893	1300	1289	1700	1678
950	943	1400	1391	1800	1777
1000	994	1500	1494	1900	1876
1050	1045	1600	1598	2000	1977
1100	1097	1700	1702	2200	2183
1150	1149	1750	1753	2400	2390
1200	1201	--	--	2600	2597
1225	1226	--	--	2800	2804

2. Transmissivity Correction

A black body radiator emits electromagnetic energy according to Plank's Law of Radiation

$$J_\lambda = \frac{C_1}{\lambda^5 (e^{C_2/\lambda T} - 1)}$$

where J_λ is the rate of energy radiation per unit area, λ is the wavelength and C_1, C_2 are the first and second radiation constants, respectively. Plank's equation may be considerably simplified at low values of λT to

$$J_\lambda = C_1 \lambda^{-5} e^{-C_2/\lambda T}$$

which is known as Wien's equation. Margrave (95) states that for λT less than 0.3 cm^0K, Wien's equation fits the observed spectral distribution within 1%. The transmissivity correction follows from Wien's Law and is given for any material as

$$K = \frac{1}{T_0} - \frac{1}{T}$$

where K is the transmissivity correction, T_0 is the temperature of the object viewed through the material and T is the true temperature of the object (Cf. Section 3.5 for a more detailed description).

APPENDIX E

Computer Program for Clausius-Clapeyron Plot

The following computer program was used to obtain the least squares line of ln IT vs 1/T. The equations of the least squares analysis were obtained from Youden (98). All analyses were performed on a Control Data Corporation 3600 computer.

```
      PROGRAM LSTSQR
C K1=NUM OF CARDS IN KWORD··· KWORD=HEADING CARDS WITH INFO ABOUT RUN DATA···
C NP IS NUM OF ENTRIES IN THE PYROM TABLE···PT IS PYROM TABLE TEMP,DEG CENTIG
C PC IS PYROM TABLE CORRECTION, DEG CENT···NT IS NUM OF EXP POINTS IN A SET···
C TL,TC,TD ARE TEMP OF W LAMP READ WITH PYROM ALONE, WITH CLEAN PRISM AND WINDOW
C THROUGH DIRTY WINDOW AND PRISM··· CF IS WINDOW AND PRISM COR PER DEG CENT
C YI,YB,YC ARE THE CURRENT INTENSITYUNCOR, BACKGROUND, CORRECTED, RESPECTIVELY
C A,TTC ARE EXP TEMP IN DEG KEL CORR FOR PYROM,AND PYROM, WINDOW AND PRISM, RESP
C SA,SB ARE STD DEV IN SLOPE, INTERCEPT···W IS WEIGHT OF AN EXP POINT
C AF IS THE ISOTOPIC ABUNDANCE FACTOR···IT IS PYROM SCALE USED
C INPUT DIRECTIONS···CARD ONE, COL 1-5 VALUE OF NP···CARDS 2-5,
C COLS (1-10,11-20),(21-30,31-40), (41-50,51-60),(61-70,71-80) VALUES OF (PT,PC)
C FOR L PYROM SCALE...CARDS 6-10, REPEAT AS IN CARDS 2-5 FOR PYROM SCALE H...
C CARDS 11-15, REPEAT AS IN CARDS 2-5 FOR PYROM SCALE XH...CARD 16, COL 1-5
C VALUE OF K1...CARD 17, PUNCH 1 IN COL 1, COL 2-80 PUNCH TITLED INFORMATION...
C CARD 18, COL 1-5 VALUE OF NT, COL 6-15 VALUE OF TL, COL 16-25 VALUE OF TC,
C COL 26-35 VALUE OF TD, COL 36-45 VALUE OF AF (IF AF BLANK THEN VALUE GIVEN IS
C ONE)...CARD 19, COL1-5 VALUE OF IT, COL 6-15 VALUE OF XT, COL 16-25 VALUE OF
C YI, COL 26-35 VALUE OF YB, COL 36-45 VALUE OF W (IF W BLANK THEN VALUE GIVEN
C IS ONE)...CARDS 20-ON ARE DATA CARDS WHICH SAME FORMAT AS CARD 19...FOR
C ANOTHER SET OF DATA FOLLOWING FIRST SET REPEAT DIRECTIONS FROM CARD 16 TO CARD
C 20...PROGRAN IS TERMINATED WITH A BLANK CARD.
      DIMENSION X(50), Y(50), YCALC(50), T(50), KWORD(50), W(50)
      COMMON PT(3,16), PC(3,16), NP(3)
    1 FORMAT (8F10.2)
    3 FORMAT (15,5F10.5,F5.3, F6.3)
    7 FORMAT (//, I10, E20.10, F7.4, 41X, * NT CF AF*)
    8 FORMAT (3F20.10,20X,*TL  TC  TD*)
    9 FORMAT (3E20.10,20X,*T1  T2  T3*)
   16 FORMAT (4E20.10,2X,F5.3)
   17 FORMAT (4E20.10)
   26 FORMAT(//,5E18.8,1X,F5.2,2X,*SUMWX SUMWY SUMWXY SUMWX2 SUMWY2 SUMW 1*)
   61 FORMAT (//,*INTERCEPT=*E18.10,15X,*SLOPE=*E18.10,15X,
     1*ENTHALPY-*E18.10,/)
   70 FORMAT (1HO, *STD DEV OF SINGLE Y-*,E17.10,10X,*STD DEV OF SLOPE=*
     1,E17.10,/,*STD DEV OF INTERCEPT=*,E17.10,14X,*3(STD DEV)=*,E17.10)
```

```
  200 FORMAT(1HO,2X,14HREJECTED POINT,5X,E20.10)
  667 FORMAT (//,*          XT  YI                A  YB                TTC
     1YC            X(I)  Y(I)       W*)
  771 FORMAT (1HO,*ERROR-NEG OR ZERO VALUE FOR YC IN THIS SET=*,
     1315,3E15.5,10X,*I NT NLEFT YI YC YB*)
  902 FORMAT(//,*           X(I)                Y(I)              YCALC(
     1I)              T(I)*)
  998 FORMAT (17A8)
  999 FORMAT (10A8)
 3333 FORMAT(*WEIGHTED KELVIN TEMP=*E14.6,15X,*ERROR IN ENTHALPY=*E14.6)
C
      DO 5 I=1,3
      READ 3, NP(I)
      M=NP(I)
    5 READ 1, (PT(I,L), PC(I,L), L=1,M)
 1111 READ 3, K1
      IF(K1)1020,1020,889
  889 K2=10*K1
      READ 999, (KWORD(I), I=1, K2)
      PRINT 998, (KWORD(I), I=1, K2)
      READ 3, NT,TL,TC,TD,AF
   10 M=2
      NLEFT=NT
      CALL PYROM(TL, M, X)
      T1=TL+X + 273.2
      CALL PYROM(TC, M,X)
      T2=TC + X+273.2
      CALL PYROM(TD, M, X)
      T3= TD + X + 273.2
      CF=2./(T2+T3)-1./T1
      IF(AF)1020,11,112
   11 AF=1.0
  112 CONTINUE
      KT=0
      PRINT 7, NT,CF,AF
```

```
      PRINT 8, TL, TC, TD
      PRINT 9, T1, T2, T3
      SUMTTC=0.
      KY=0
      DO 12 I=1, NT
  522 READ 3, IT, XT, YI, YB, W(I)
      IF (W(I)) 1111,523,524
  523 W(I)=1.
  524 NLEFT=NLEFT-1
      YC=(YI-YB)/AF
      IF (YC)770,770,776
  770 PRINT 771, I,NT,NLEFT,YI,YC,YB
      IF (NLEFT) 1111,1111,475
  475 NT=NT-1
       GO TO 522
  776 CALL PYROM(XT, IT, XC)
      A=XT+XC+273.2
      TTC=A/(1.-A*CF)
      SUMTTC=SUMTTC+TTC
      X(I)=1./TTC
      Y(I)=LOGF(YC*TTC)
      KY=KY+I
      IF (KY-1) 1020,666, 777
  666 PRINT 667
  777 PRINT 16, XT, A, TTC, X(I),W(I)
   12 PRINT 16, YI, YB, YC, Y(I),W(I)
      N=NT
   20 KT=KT+1
      SUMW=0.
      SUMWX=0.0
      SUMWY=0.0
      SUMWXY=0.0
      SUMWX2=0.0
      SUMWY2=0.0
      DO 25 I=1,N
```

```
      SUMW=SUMW+W(I)
      SUMWX=SUMWX+W(I)*X(I)
      SUMWY=SUMWY+W(I)*Y(I)
      SUMWXY=SUMWXY+W(I)*X(I)*Y(I)
      SUMWX2=SUMWX2+W(I)*X(I)**2
   25 SUMWY2=SUMWY2+W(I)*Y(I)**2
      PRINT 26, SUMWX,SUMWY,SUMWXY,SUMWX2,SUMWY2,SUMW
      AVETTC=SUMTTC/SUMW
      DENOM=SUMW*SUMWX2-SUMWX**2
      A=(SUMW*SUMWXY-SUMWX*SUMWY)/DENOM
      B=(SUMWY*SUMWX2-SUMWX*SUMWXY)/DENOM
      ENTALPY=-1.987173*A
      PRINT 61, B, A, ENTALPY
      S2=(SUMY2-SUMWY**2/SUMW-(SUMWXY-SUMWX*SUMWY/SUMW)**2/(SUMWX2-SUMW
     1X**2/SUMW))/(SUMW-2)
      S=SQRTF(S2)
      SA2=S2*SUMW/DENOM
      SA=SQRTF(SA2)
      SIGMAH=1.987174*SA
      PRINT 3333,AVETTC, SIGMAH
      SB2=S2*SUMWX2/DENOM
      SB=SQRTF(SB2)
      S3=3.0*S
      PRINT70,S,SA,SB,S3
      DO90I=1,N
      YCALC(I)=A*X(I)+B
   90 T(I)=Y(I)-YCALC(I)
      PRINT 902
      PRINT 17, (X(I), Y(I), YCALC(I), T(I), I=1,N)
      IF(KT-1)1020,125,1111
  125 VMAX=T(1)
      DO 89 I=2,N
      TEST = VMAX - T(I)
      IF (TEST) 82,89,89
   82 VMAX = T(I)
      JAM = I
```

```
 89 CONTINUE
    DEV = T(JAM) - 3.0*S
    IF(DEV)  115,100,100
100 PRINT 200, Y(JAM)
    DO 110 I = JAM,N
    X(I) = X(I+1)
    YCALC(I)=YCALC(I+1)
    T(I)=T(I+1)
110 Y(I) = Y(I + 1)
    N = N - 1
    IF(N.LT.1)1111,125
115 IF (N-NT) 20, 1111, 1111
1020 END
    SUBROUTINE PYROM(TO,K,TC)
    COMMON PT(3,16), PC(3,16), NP(3)
    L=NP(K)
    DO 10 I=2,L
    IF (TO-PT(K,I)) 20, 20, 10
 10 CONTINUE
 20 J=I-1
    S=(PC(K,I)-PC(K,J))/(PT(K,I)-PT(K,J))
    TC=S*(TO-PT(K,I)) + PC(K,I)
    RETURN
    END
```

APPENDIX F

Selected Physical Constants

R = 1.98726 cal/deg mole

π = 3.14156

1 atm = 1013250 dyne/cm^2

Masses: Basis is ^{12}C = 12.000 amu (109)

Sm = 150.35	Ag = 107.870
Nd = 144.24	Te = 127.60
Cu = 63.54	

Isotopic Abundances: Basis is reference (91)

Sm-147 = .1509	Te-128 = .3179
Sm-148 = .1135	Te-130 = .3448
Sm-149 = .1396	Ag-107 = .51817
Sm-150 = .0747	Ag-109 = .48183
Sm-152 = .2655	Cu-63 = .691
Sm-154 = .2243	Cu-65 = .309
Nd-142 = .2711	
Nd-144 = .2385	

APPENDIX G

Second Law Data for SmC_2 Vaporization

The following is a compilation of a portion of the Clausius-Clapeyron data for the vaporization of SmC_2. The remaining part of the data is not tabulated here since it is presented (in a different form) in Appendix A.

Table G-1. Experiment III06

T, °K	- ln IT			
	Sm-147	Sm-149	Sm-152	Sm-154
1784	4.416	4.376	4.385	4.378
1896	5.448	5.411	5.415	--
1982	6.059	6.057	6.074	6.064
1627	2.398	2.524	2.428	2.476
1706	3.433	3.366	3.404	3.361
1839	4.689	4.723	4.685	4.667
1932	5.533	5.509	5.374	5.702
1981	5.766	5.786	5.678	5.743
1976	5.639	--	5.631	5.635
1934	5.321	5.323	5.343	5.281
1992	--	5.734	--	5.732

Table G-2. Experiment II34

T, ^{o}K	ln IT			
	Sm-147	Sm-149	Sm-152	Sm-154
2030	6.818	5.618	6.342	6.453
1578	2.609	2.211	2.342	2.213
1689	3.952	3.741	3.408	3.500
1766	4.711	4.355	4.151	4.315
1819	5.153	4.605	4.882	4.736
1878	5.846	5.648	5.387	5.482
1937	6.174	5.898	5.767	5.801
1950	6.403	6.302	5.881	6.096
1979	6.307	6.004	5.899	5.927
1981	6.302	6.194	5.832	5.928
1966	6.335	6.181	5.772	5.918
1933	6.355	6.264	5.701	5.785
1898	5.940	5.797	5.531	5.656
1859	--	5.244	5.116	5.162
1823	5.189	4.977	4.661	4.748
1762	4.730	4.285	4.144	4.236
1696	3.988	3.842	3.522	3.633
1627	3.334	2.802	2.689	2.793
1801	5.029	4.849	4.502	4.632
1917	5.966	5.793	5.585	5.639
1855	5.563	5.412	4.998	5.199
1562	2.519	2.067	2.108	2.241

Table G-3. Experiment III16

T, ^{0}K	ln IT	
	Sm-152	Sm-154
1854	3.363	3.329
1873	3.534	3.496
1873	3.682	--
1887	3.848	3.678
1911	4.100	3.888
1909	4.095	--
1904	4.068	4.168
1904	--	3.905
1911	4.208	4.038
1863	3.895	3.747
1844	3.724	3.541
1810	3.417	3.329
1775	3.009	2.984
1740	2.592	2.500
1686	1.919	1.910
1740	2.541	2.474
1685	1.981	2.053

APPENDIX H

Congruency Data for Neodymium(III) Monotelluro Oxide

Table H-1. Outgassing Data

Run	Average Temp., ^{0}C	Final Wt. (g)	Wt. Loss (mg)	Time Heated (min.)	Rate Loss (mg/min. x 10^2)
A.	Tungsten effusion cell:	Initial starting weight: 96.2479g			
1-5	2000	96.1637	80.6	1440	5.60
6	2180	96.1528	14.5	*	*
7	2200	96.1379	14.9	500	2.98
8	2200	96.1225	15.4	759	2.03
9	2200	96.1126	9.9	500	1.98
10	2200	96.1026	10.0	600	1.67
11	2200	96.0961	6.5	372	1.75
12	2200	96.0881	8.0	556	1.44
13	2200	96.0740	14.1	1107	1.27
14	2200	96.0644	9.6	642	1.33
15	2500	96.0211	43.3	223	19.4
16	2200	96.0164	4.7	327	1.44
17	2200	96.0105	5.9	575	1.03
18	2500	95.9552	55.3	374	14.8
19	2500	95.8422	113.0	*	*
20	2500	95.7475	94.7	537	17.6
21	2500	95.6354	112.1	512	21.9
22	2500	95.3875	247.9	1025	24.1
B.	Molybdenum effusion cell:	Initial weight: 18.3287g			
1	2200	27.3850	943.7	292	3.232
2	2200	26.9119	473.1	208	2.275
3	2200	26.2209	691.0	320	2.159
4	2200	24.8521	1368.8	635	2.156

*Not available since furnace shut off during run.

Table H-2. Vaporization of neodymium(III) monotelluro oxide from molybdenum cell

Run No.	Initial Sample Wt. g	Single Run Loss %	Time Heated min.	Av. T °C	Wt. Loss for X-Ray g	Sum X-Ray Loss g	N g	D g	100N/D %	X-Ray Residue
V-1	.0169	19	105	1505	--*	--*	--	--	--	Nd_2O_2Te
V-2	.0138	96	60	1848	--*	--*	--	--	--	Nd_2O_3
V-3A	.3127	7	90	1610	.0436	.0436	.0211	.3127	7	Nd_2O_2Te Nd_2O_3
V-3B	.2480	16	120	1715	.0262	.0698	.0606	.2691	23	Nd_2O_2Te Nd_2O_3
V-3C	.1823	18	120	1780	.0088	.0786	.0936	.2429	39	Nd_2O_2Te Nd_2O_3
V-3D	.1405	51	150	1835	.0049	.0835	.1653	.2341	71	Nd_2O_3
V-3E	.0639	32	80	1820	--*		.1856	.2292	81	Nd_2O_3
V-4A	.0660	28	85	1700	--**	--**	.0187	.0660	28	--
V-4B	.0473	30	120	1700	--**	--**	.0327	.0660	50	--
V-4C	.0333	44	180	1700	--**	--**	.0473	.0660	72	--
V-4D	.0117	12	45	1700	*	*	.0487	.0660	74	Nd_2O_3

Note: N = combined wt. loss due to evaporation.

D = total amount of sample which may be evaporated in any one run.

= the initial sample wt. - amount removed as X-ray sample.

Thus, for series V-3C run:

$$D_i = .3127 - \sum_{n=1}^{i-1} (\Delta g_{x\text{-}ray})_n$$

$\frac{N}{D} \times 100$ = % total evaporated of the possible amount.

*Does not apply since (1) the x-ray sample was removed after the weight loss was calculated, and (2) no subsequent vaporization experiment was made on the remaining sample.

**The sample was only weighed; none of it was removed.

Table H-3. Vaporization of neodymium(III) monotelluro oxide from tungsten cell

Run	Initial Sample Wt. g.	% Loss	Av. T °C	Time Heated min.	X-Ray Residue
III28	0.3142	48	2000	120	Nd_2O_2Te
III32	0.3466	>89	2190	60	Nd_2O_3
III36	0.3722	72	2000	231	Nd_2O_3

APPENDIX I

I. Calculation of Equilibrium Constants

The equilibrium constants of reactions (53), (54) and (55) were calculated (Cf. Section 7.2) from the data contained in Tables I-1 and I-2 and are presented in Table I-3 below.

Table I-1. Free energy functions

T, ^{0}K	$-(G^0 - H^0_{298})/T$, cal/mole-deg					
	Nd_2O_3 (s)	Te (g)	O (g)	NdO (g)	Nd (g)	Nd_2O_2Te
1800	63.74	48.47	43.37	68.5	51.18	68.64
2000	67.28	48.93	43.81	69.4	51.77	72.40
2200	70.14	49.35	44.22	70.1	52.31	75.27
Ref.	(110)	(97)	(97)	(43)	(97)	calc'd

Table I-2. Standard enthalpies of formation

Species	O (g)	Nd_2O_3 (s)	Te (g)	NdO (g)	Nd (g)	Nd_2O_2Te (s)
ΔH^0_{298}, $\frac{cal}{mole}$	59,550	-432,150	46,500	-36,000	76,800	-419.1
Ref.	(97)	(111)	(97)	(43)	(97)	calc'd

Table I-3. Calculation of equilibrium constants using H-1 and H-2.

T, °K	$-\left(\frac{\Delta G - \Delta H^{o}_{298}}{T}\right)$, cal/mole-deg				$\frac{\Delta H^{o}_{298,f}}{T}$, cal/mole-deg				log K			
	Rx (53)	Rx (54)	Rx (55)	Rx (56)	Rx (53)	Rx (54)	Rx (55)	Rx (56)	Rx (53)	Rx (54)	Rx (55)	Rx (56)
1800	56.24	20.40	116.6	137	127	-14.6	233	219	-15.5	7.65	-25.4	-17.9
2000	55.90	20.48	115.3	136	114	-13.1	210	197	-12.7	7.33	-20.7	-13.3
2200	55.71	20.52	114.3	135	104	-11.9	191	179	-10.6	7.08	-16.8	- 9.6

II. The Mass Spectrometer Data for Neodymium(III) Monotelluro Oxide:

Table I-4. Experiment III46

T, °K	ln IT					$\frac{(IT)_{NdO}}{(IT)_{Nd}}$
	Nd-142	Nd-144	142-NdO	144-NdO	Te-130	
2293	5.025	5.036	5.330	5.407	5.938	1.403
2267	4.583	4.603	4.963	4.980	5.531	1.460
2183	3.568	3.673	3.988	4.014	4.132	1.461
2227	4.398	4.362	4.574	4.650	4.497	1.262
2264	4.464	4.425	4.824	4.897	5.376	1.517
2194	3.891	3.968	4.030	4.067	4.460	1.126
2153	3.024	3.033	3.302	3.360	3.648	1.354
2181	3.393	3.392	3.352	3.422	4.096	0.995
2021	1.721	1.836	1.498	1.444	3.479	0.734
2188	4.005	4.103	4.216	4.296	4.088	1.223

Table I-5. Experiment III55

T, °K	ln IT			$\frac{(IT)_{NdO}}{(IT)_{Nd}}$
	$Nd-\frac{142}{144}$	$\frac{142}{144}-NdO$	$Te-\frac{128}{130}$	
2333	5.074	5.414	5.760	1.405
2346	4.864	5.254	5.350	1.477
2305	4.696	4.984	4.650	1.333
2222	3.380	3.908	3.243	1.696
2203	2.844	3.779	3.291	2.547
2173	2.551	3.261	2.711	2.034
2085	1.800	2.158	1.690	1.430
2038	1.420	1.477	0.894	1.059
1978	0.721	0.905	--	1.202

Table I-6. Experiment III61

T, ^{o}K	ln IT				$\frac{(IT)_{NdO}}{(IT)_{Nd}}$
	Nd-142	Nd-144	142-NdO	144-NdO	
2318	2.322	2.432	2.641	2.805	1.416
2293	2.284	2.398	2.449	2.610	1.209
2257	1.984	2.058	2.173	2.323	1.279
2195	1.726	1.753	1.802	1.873	1.104
2166	1.161	1.665	1.520	1.561	0.867
2123	1.171	1.185	0.857	0.884	0.735
2084	0.240	0.207	-0.133	-.0867	0.786